

RD-RL90 677

CAVITATION INCEPTION IN RECTANGULAR TWO-DIMENSIONAL
SLOTS (U) PENNSYLVANIA STATE UNIV UNIVERSITY PARK

1/2

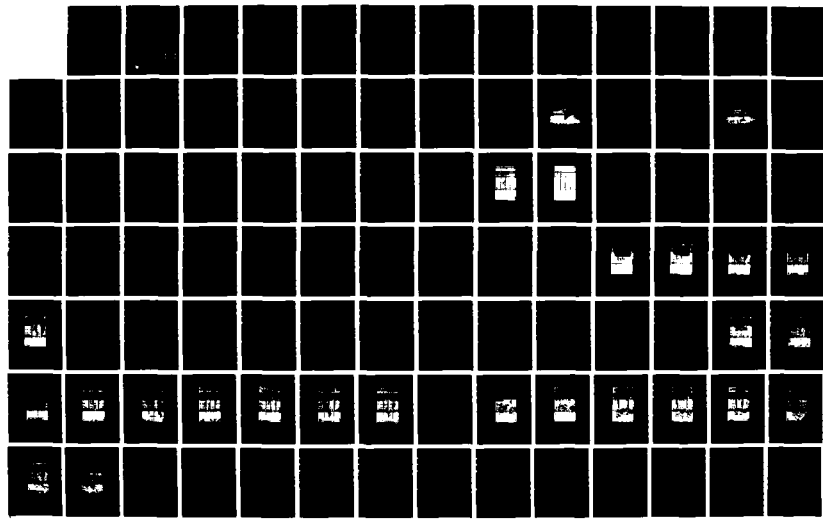
UNCLASSIFIED

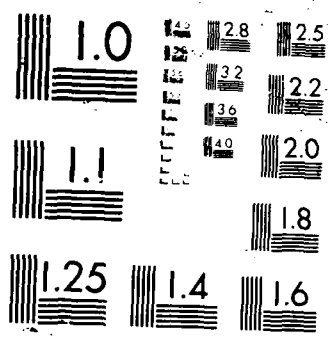
APPLIED RESEARCH LAB H G BLAIR ET AL. DEC 87

ARL/PSU/TR-87-813 N00024-85-C-6841

F/G 28/4

NL





Applied Research Laboratory

AMERICAN
MICROFILE COPY

AD-A190 677

Technical Report

CAVITATION INCEPTION IN RECTANGULAR
TWO-DIMENSIONAL SLOTS

by

W. G. Blair, J. M. Cimbala

Ac

DTIC
ELECTED
FEB 04 1988
S O D
H

PENNSTATE



DISTRIBUTION STATEMENT A

Approved for public release;
Distribution Unlimited

4

The Pennsylvania State University
APPLIED RESEARCH LABORATORY
P. O. Box 30
State College, PA 16804

CAVITATION INCEPTION IN RECTANGULAR
TWO-DIMENSIONAL SLOTS

by

W. G. Blair, J. M. Cimbala

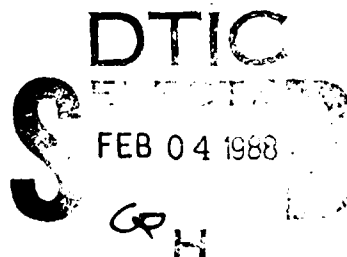


Technical Report No. TR 87-013
December 1987

Accession For	
NTIS GRA&I	<input checked="" type="checkbox"/>
DTIC TAB	<input type="checkbox"/>
Unlimited	<input type="checkbox"/>
Justification	
By	
Distribution	
Availability Codes	
Dist	Avail and/or Special
A-1	

Supported by:
Naval Sea Systems Command

L. R. Hettche, Director
Applied Research Laboratory



Approved for public release; distribution unlimited

88 1 29 026

Unclassified

SECURITY CLASSIFICATION OF THIS PAGE

REPORT DOCUMENTATION PAGE

1a. REPORT SECURITY CLASSIFICATION Unclassified		1b. RESTRICTIVE MARKINGS													
2a. SECURITY CLASSIFICATION AUTHORITY		3. DISTRIBUTION/AVAILABILITY OF REPORT (A) Unlimited													
2b. DECLASSIFICATION/DOWNGRADING SCHEDULE															
4 PERFORMING ORGANIZATION REPORT NUMBER(S) TR 87-013		5. MONITORING ORGANIZATION REPORT NUMBER(S)													
6a. NAME OF PERFORMING ORGANIZATION Applied Research Laboratory The Penna. State University	6b. OFFICE SYMBOL (If applicable) ARL	7a. NAME OF MONITORING ORGANIZATION Naval Sea Systems Command Department of the Navy													
6c. ADDRESS (City, State, and ZIP Code) P. O. Box 30 State College, PA 16804		7b. ADDRESS (City, State, and ZIP Code) Washington, DC 20362													
8a. NAME OF FUNDING/SPONSORING ORGANIZATION Naval Sea Systems Command	8b. OFFICE SYMBOL (If applicable) NAVSEA	9. PROCUREMENT INSTRUMENT IDENTIFICATION NUMBER N-00024-85-C-6041													
8c. ADDRESS (City, State, and ZIP Code) Department of the Navy Washington, DC 20362		10. SOURCE OF FUNDING NUMBERS PROGRAM ELEMENT NO. PROJECT NO. TASK NO. WORK UNIT ACCESSION NO.													
11. TITLE (Include Security Classification) Cavitation Inception in Rectangular Two-Dimensional Slots															
12. PERSONAL AUTHOR(S) W. C. Blair and J. M. Cimbala															
13a. TYPE OF REPORT M.S. Thesis	13b. TIME COVERED FROM _____ TO _____	14. DATE OF REPORT (Year, Month, Day) December 1987	15. PAGE COUNT 138												
16. SUPPLEMENTARY NOTATION															
17. COSATI CODES <table border="1"><tr><th>FIELD</th><th>GROUP</th><th>SUB-GROUP</th></tr><tr><td></td><td></td><td></td></tr><tr><td></td><td></td><td></td></tr><tr><td></td><td></td><td></td></tr></table>		FIELD	GROUP	SUB-GROUP										18. SUBJECT TERMS (Continue on reverse if necessary and identify by block number) Cavitation, Boundary Layer Flow, Flow Visualization, Fluid Flow, Vortex Structures	
FIELD	GROUP	SUB-GROUP													
19. ABSTRACT (Continue on reverse if necessary and identify by block number) <p>The two-dimensional fluid mechanics of flow over a rectangular slot along a flat wall were studied in air. A thick (greater than slot width) turbulent boundary layer was established at the slot entrance location. The flow field within and at the slot entrance was studied as the slot geometry was varied for depth-to-width ratios (aspects ratios) ranging from 0.5 to 3.0.</p>															
20. DISTRIBUTION/AVAILABILITY OF ABSTRACT <input checked="" type="checkbox"/> UNCLASSIFIED/UNLIMITED <input type="checkbox"/> SAME AS RPT <input type="checkbox"/> DTIC USERS		21. ABSTRACT SECURITY CLASSIFICATION Unclassified													
22a. NAME OF RESPONSIBLE INDIVIDUAL		22b. TELEPHONE (Include Area Code) 814/355-6344	22c. OFFICE SYMBOL ARL/PSU												

Unclassified

SECURITY CLASSIFICATION OF THIS PAGE

Flow visualization inside the slot describes the internal flow field of the slot and reveals the highly unsteady nature of the vortex-like structure(s) that develop. Flow visualization of the slot region entrance shows that mass is transferred into the slot from the wall boundary layer; however, this mass does not appear to be drawn into the center of the slot primary vortex located near the entrance. Flow visualization as well as direct pressure measurements inside the slot document vortex location as a function of aspect ratio. The minimum pressure in the slot, found at the primary vortex center, is also documented as a function of aspect ratio.

The measured pressure coefficients inside the slot are an order of magnitude lower than those of which cavitation has been observed in previous water tunnel experiments. These measurements therefore lead to question the interpretation of the previous water tunnel slot cavitation experiments. Specifically, it is likely that the previously reported cavitation was partially gaseous rather than purely vaporous cavitation, as had been assumed.

Unclassified

SECURITY CLASSIFICATION OF THIS PAGE

ABSTRACT

The two-dimensional fluid mechanics of flow over a rectangular slot along a flat wall were studied in air. A thick (greater than slot width) turbulent boundary layer was established at the slot entrance location. The flow field within and at the slot entrance was studied as the slot geometry was varied for depth-to-width ratios (aspects ratios) ranging from 0.5 to 3.0.

Flow visualization inside the slot describes the internal flow field of the slot and reveals the highly unsteady nature of the vortex-like structure(s) that develop. Flow visualization of the slot region entrance shows that mass is transferred into the slot from the wall boundary layer; however, this mass does not appear to be drawn into the center of the slot primary vortex located near the entrance. Flow visualization as well as direct pressure measurements inside the slot document vortex location as a function of aspect ratio. The minimum pressure in the slot, found at the primary vortex center, is also documented as a function of aspect ratio.

The measured pressure coefficients inside the slot are an order of magnitude lower than those of which cavitation has been observed in previous water tunnel experiments. These measurements therefore lead to question the interpretation of the previous water tunnel slot cavitation experiments. Specifically, it is likely that the previously reported cavitation was partially gaseous rather than purely vaporous cavitation, as had been assumed.

TABLE OF CONTENTS

	<u>Page</u>
ABSTRACT.....	iii
LIST OF FIGURES.....	v
NOMENCLATURE.....	vii
ACKNOWLEDGMENTS.....	viii
 <u>Chapter</u>	
1 INTRODUCTION.....	1
1.1 Previous Work.....	2
1.2 Objectives.....	6
2 FACILITIES AND EQUIPMENT.....	7
2.1 Flow Visualization Model.....	10
2.2 Pressure Measurement Model.....	13
3 PROCEDURE AND RESULTS.....	17
3.1 Boundary Layer.....	17
3.2 Flow Visualization.....	22
3.2.1 Internal Cavity Visualization.....	23
3.2.2 External Cavity Visualization.....	29
3.3 Pressure Measurement.....	32
4 DISCUSSION AND CONCLUSIONS.....	48
4.1 Summary of Conculsions.....	52
BIBLIOGRAPHY.....	54
 <u>Appendix</u>	
A INTERNAL PHOTOGRAPHS.....	56
B EXTERNAL PHOTOGRAPHS.....	66
C PRESSURE COEFFICIENT PROFILES.....	75
D PROGRAMS.....	87

LIST OF FIGURES

<u>Figure</u>		<u>Page</u>
1	Wind Tunnel Sketch.....	8
2	Two-Dimensional View of Rectangular Model.....	11
3	Photograph of 38-Inch Flow Visualization Model.....	12
4	Pressure Model Sketch.....	14
5	Pressure Model Photograph.....	15
6	Boundary Layer Profile.....	20
7	Span Photograph - 38-Inch (AR=3.0).....	25
8	Span Photograph - 8-Inch (AR=3.0).....	26
9	Primary Vortex Vertical Position - Visualization Data (nondimensionalized by width).....	30
10	Primary Vortex Vertical Position - Visualization Data (nondimensionalized by depth).....	31
11	Primary Vortex Horizontal Position.....	37
12	Primary Vortex Vertical Position - Pressure Data (nondimensionalized by width).....	38
13	Primary Vortex Vertical Position - Pressure Data (nondimensionalized by depth).....	39
14	Pressure Probe Visualization AR=0.5 (downstream probe).....	41
15	Pressure Probe Visualization AR=0.5 (upstream probe).....	42
16	Pressure Probe Visualization AR=1.0 (downstream probe).....	43

LIST OF FIGURES (continued)

<u>Figure</u>		<u>Page</u>
17	Pressure Probe Visualization AR=1.0 (upstream probe).....	44
18	Pressure Probe Visualization AR=2.0 (downstream probe).....	45
19	Vortex Strength Data.....	46
20	Pressured Coefficient Data to World's Cavitation to World's Cavitation Index Data of 1973.....	51

NOMENCLATURE

AR	Aspect Ratio (D/B)
B	Model Width
C_f	Skin Friction Coefficient
C_p	Pressure Coefficient
D	Model Depth
P_c	Local Cavity Static Pressure
P_v	Vapor Pressure of Water
P_∞	Freestream Static Pressure
R_e	Reynolds number based on Momentum Thickness
S	Model Span
u	Local Time Averaged Velocity
u^+	Nondimensionalized Mean Velocity - $u^+ = u/u_\infty$
u_∞	Freestream Velocity
v^*	Wall-Friction Velocity
y	Vertical Distance
y^+	Nondimensionalized Distance - $y^+ = y v^*/v$
δ	Boundary Layer Thickness based on 99% of The Freestream Velocity
θ	Momentum Thickness
ν	Viscosity of Air
ρ	Density of Air
σ	Cavitation Index

ACKNOWLEDGMENTS

The research described herein was funded by the Applied Research Laboratory and the work was performed in the Subsonic Wind Tunnel Facility of the Department of Mechanical Engineering at The Pennsylvania State University.

The author's gratitude and appreciation extends to his fellow students working at the same facility. Thanks are also due to Professor J. William Hell and Dr. Michael L. Billet at the Applied Research Laboratory for their advice. Particular appreciation is due to Dr. John M. Cimbala, Assistant Professor in Mechanical Engineering at The Pennsylvania State University, under whose guidance and supervision this research was performed.

Chapter 1

INTRODUCTION

The inception of cavitation is caused by a reduction of local pressure that leads to the formation of bubbles in a liquid. The occurrence of cavitation is usually inevitable on underwater bodies moving at high speeds, and designers are constantly challenged to limit and suppress its inception. Two-dimensional slots along a wall are, at times, unavoidable in the designing process. Low pressure regions inside the slot can lead to cavitation. Specifically, cavitation usually occurs in the center of the vortex found inside a two-dimensional rectangular slot. The fluid mechanics of flow in a two-dimensional slot must be understood before further progress can be made toward predicting the inception of cavitation that occurs within the slot.

The purpose of the research presented here is to study the fluid mechanics of flow over a rectangular slot on a flat plate and to document the magnitude and location of the internal vortex with changes in slot geometry. The parameters of critical importance to the flow include the ratio of boundary layer thickness (based on 99% of the freestream velocity) and slot width (δ/B), the slot span/width (S/B), and the depth/width (D/B) ratios. Of interest were cases where the boundary layer was thicker than the slot width (i.e., δ/B was greater than unity). In order to study the fluid mechanics inside the slot without cavitation actually occurring, air rather than water was chosen as the fluid medium.

During the tests the ratio of boundary layer thickness (δ) to slot width was fixed, while S/B and D/B (from now on referred to as the aspect ratio, AR=D/B) were varied.

1.1 Previous Work

Much of the previous research on flow in two-dimensional slots was found to be inapplicable to the present work. However, the problem of slot cavitation seemed to be the incentive for the first research done. Bennett (1949) studied the applied problem concerning the downstream effects of a clearance slot around the top hatch of the water tunnel test section at the Ordnance Research Laboratory at The Pennsylvania State University. He generalized the problem to include the fluid mechanics past a slot used to guide the gates of dams. His research on slot fluid mechanics was performed in a wind tunnel. Boundary layer thickness, freestream velocity, model width, model depth and the downstream corner radius were the variables in his study. Bennett's emphasis was the fluid mechanics of the slot entrance and the downstream corner, not the flow field contained within the slot. This follows since his concern was to suppress cavitation at the downstream corner which would disturb the flow within the water tunnel test section. It seems that the cavitation that probably occurred inside the slot was not of concern or not yet observed since one of his conclusions was that "depth had very little effect" (Bennett, p. 65, 1949) on the minimum pressure found at the downstream corner.

A large amount of the research performed on the two-dimensional slot was aimed at the slot's effect on the passing flow. This includes the effects of low subsonic oscillations due to shallow slots (Sarohia 1977). Sarohia seemed particularly concerned with the effect of the shear layer across the slot entrance on the resulting oscillations. Similar work was performed in a water channel by Rockwell and Knisely (1979) but they investigated the effect of the downstream edge on the unsteadiness of the flow. Both of these investigations had a laminar boundary layer at the upstream corner of their respective slots.

Military applications found a need for research on high subsonic and low supersonic flow across shallow rectangular slots. Clark and Kauffman (1980) presented research on this type of flow for Mach numbers of 0.6 to 3.0. Their emphasis was on the aerodynamic and aero-acoustic effects due to a slot. However, they conclude that more work would be required to estimate the pressure distributions in the slot (Clark and Kauffman 1980).

Several investigations have examined the three-dimensionality of the flow inside a rectangular slot. Maull and East (1963) stated that the flow in a rectangular slot was not two-dimensional anywhere inside. They showed that a regular three-dimensional flow developed in the rectangular slot. The regular three-dimensional type of flow is reenforced by the research of Hiwoda, Mabuchi and Masaya (1985). However, their description of this flow is quite different and more complex than that of Maull and East. This could be due, in part, to the fact that

Maull and East had a laminar boundary layer at the upstream corner of their slot while Hiwada, Mabuchi and Masaya had a small (less than their slot width) turbulent boundary layer at the same location. It is worth noting that Hiwada, Mabuchi and Masaya concluded that "the three-dimensional flow behavior is independent of the span length" (p. 89, 1985). This does not infer that the flow is two-dimensional; rather, their emphasis is on a cell type structure that repeats down the model span.

A mainstay of most of the above work was that performed by Roshko (1955). His wind tunnel experiments showed the unsteady nature of the vortex inside of the two-dimensional slot. He addressed many of the issues of the two-dimensional slot including the internal vortices, induced drag and transport of mass into the slot. However, his boundary layer thickness, located 1.5 inches (38.1 mm) upstream of the slot entrance, was measured to be a third of the slot width.

The experiments most pertinent to the present research came from Ward (1973), and Holl and Billet (1986). Both investigations were performed with turbulent boundary layer thicknesses equal to or greater than the slot width. Holl and Billet performed laser-Doppler velocimeter tests in a wind tunnel and obtained velocity profiles of the internal slot flow field. A minimum pressure coefficient of the slot was obtained by integrating the measured velocity profile assuming a classical vortex structure. This pressure coefficient (C_p) defined as

$$C_p = \frac{P_c - P_\infty}{\frac{1}{2} \rho u_\infty^2}$$

yielded a very low minimum pressure coefficient. This is in contrast to their internal slot vortex cavitation index data from water tunnel tests, which gave very high indices of cavitation; where cavitation index is defined as

$$\sigma = \frac{P_c - P_\infty}{\frac{1}{2} \rho u_\infty^2} .$$

If the cavitation observed during the water tunnel test was purely vaporous then the cavitation index data would be equal to the analogous negative pressure coefficient values obtained from wind tunnel tests. Ward also documented cavitation index values of the same order as Holl and Billet. Both also noted that peak cavitation occurs at an aspect ratio of approximately 1.0. The large difference between the water tunnel cavitation index data and the wind tunnel negative pressure coefficients led Holl and Billet to question whether the observed cavitation is purely vaporous or partially gaseous. Ultimately, Holl and Billet concluded that "the determination of an incipient cavitation scaling relationship for slots remains an unsolved problem because it is very difficult to separate the effects of gaseous cavitation inception from the minimum pressure coefficient . . ." (Holl and Billet, p. 11, 1986).

1.2 Objectives

The primary objective of the present research was the direct pressure measurement of the pressure field inside a two-dimensional slot, with a large turbulent boundary layer at the slot entrance. All measurements were to be conducted with a non-cavitating slot, for the purpose of investigating the fluid mechanics associated with cavitation inception in slots. Toward this end, the following specific objectives are listed:

1. Find a repeatable and consistent means of generating a turbulent boundary layer along the wall upstream of the slot such that its thickness is larger than the slot width.
2. Determine the effect of model span on the two-dimensionality of the flow field by means of flow visualization.
3. Collect, by means of flow visualization, qualitative information on the internal fluid mechanics of a rectangular slot and the mass transfer across the slot entrance as a function of slot aspect ratio.
4. Collect location and strength data on the internal slot vortices as a function of aspect ratio by means of direct pressure measurement.
5. Investigate the reliability of the direct pressure measurements by means of flow visualization. Namely, determine if the pressure probe utilized for direct pressure measurement alters the internal slot fluid mechanics.

Chapter 2

FACILITIES AND EQUIPMENT

The experiments reported here were conducted at The Pennsylvania State University Mechanical Engineering Subsonic Wind Tunnel Facility. The tests were performed on a suction-type wind tunnel with a test section of dimensions 96 inches (2.44 m) in length, 38 inch (0.97 m) width, and 12 inches (0.31 m) in height. The top of the wind tunnel was partitioned in several 8 inch (0.20 m) sections spanning the tunnel width which could be lifted from the top. It was in this way that access was gained to the inside of the test section and also how models were mounted (see Figure 1). The tunnel had a speed range of zero to 50 ft/s (15.2 m/s). Wind tunnel speed was controlled by a frequency controller (Parametrics, Model 6075) feeding power to the wind tunnel motor which also shielded the motor from external electrical interference.

The equipment used in the lab includes a differential pressure transducer (MKS Baratron, Model 398HD) and a pressure signal conditioner (MKS, Model 270B) with a combined accuracy of $\pm 0.08\%$ of the display and an available resolution of 10^{-6} mm Hg. This unit had a wide enough range for use in all pressure measurements including the dynamic head and local pressures in the slot. A x-y traverse system (Maxwell Electronics, Model SMC-102A) with a serial port for computer control was used for the boundary layer hot wire placement. This traversing equipment offered positioning accuracy down

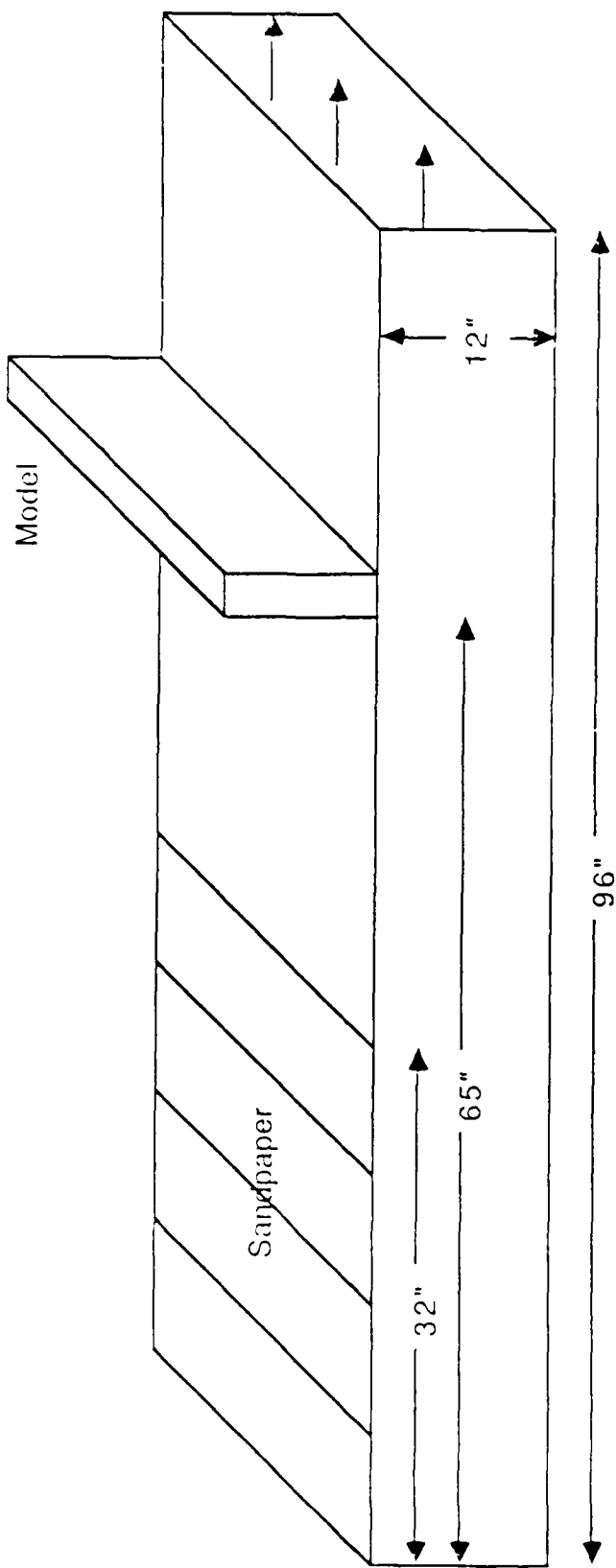


Figure 1. Wind Tunnel Sketch (not to scale).

to 1/4000 of an inch (6.3 μm). The hot wire implemented a common Wheatstone bridge circuit and a low pass filter (Sathianathan 1986). The hot wire sensing area size was 0.00015 inch (4 μm) in diameter and 0.050 inch (1.27 mm) long (TSI, Model 1261A-T1.5). A personal computer (AT&T, Model 6300) with hard disk was used. This computer was equipped with a I/O parallel port used for the traverse control and a 16 channel 12 bit data acquisition board (Metra Byte, Model Dash16F). The data acquisition board was configured to measure voltages from zero to five volts; any signals below or above this range are cut off and interpreted as zero or five volts, respectively. The software accompanying the data acquisition board and its configuration offered some restrictions. For example, only 12 bits were available for analog to digital conversion, which means the measured voltages were stored in integer form from 0 to 4095. This limited the resolution of the stored data and in the 0 to 5 volt configuration this translated to 1.22 millivolt resolution.

The smoke wire technique (Corke et al. 1977) was employed for visualization of the flow. A 0.005 inch (0.13 mm) diameter nichrome wire was used. The equipment included a 50 volt DC power supply (Heathkit, Model IP-20) and strobotach (General Radio Company, Model 1531). A customized timing/synchronization controller unit, built for the wind tunnel laboratory, allowed for precise millisecond timing and control of the smoke and strobe (Sathianathan 1985). The smoke was photographed

with a 35 mm camera (Nikon with 50 mm lens) using black and white, 400 speed film (Kodak Tri-X pan, 24 exposure, 400).

2.1 Flow Visualization Model

The slot models were constructed out of half-inch plexiglass to allow for easy construction and transparency so that photos could be taken of the two-dimensional plane of interest. The internal width of the model was set by the boundary layer measurement at 1.5 inches (38.1 mm). This investigation includes aspect ratios up to three, so the model was made accordingly deep enough, and this can be seen in the sketch in Figure 2. To maintain easy control of the aspect ratio a movable base was used in all of the models and could be adjusted from the outside by means of two 1/4-inch threaded rods.

Only one model was used in the flow visualization. However, the model was later modified with two dividers to take the reduced span photographs. These dividers were set to reduce the span from 38 inches (0.97 m) down to 8 inches (0.20 m) centered around the plane of interest.

To prevent glare and increase the quality of the pictures, the inside of the model was covered with flat black paper on four of the five sides. The fifth side was kept clear for the camera. To get light into the two-dimensional plane where smoke was placed, a half-inch portion of the paper was removed from the upstream and downstream sides of the model. This half-inch slice can be seen in the photograph of the model (Figure 3).

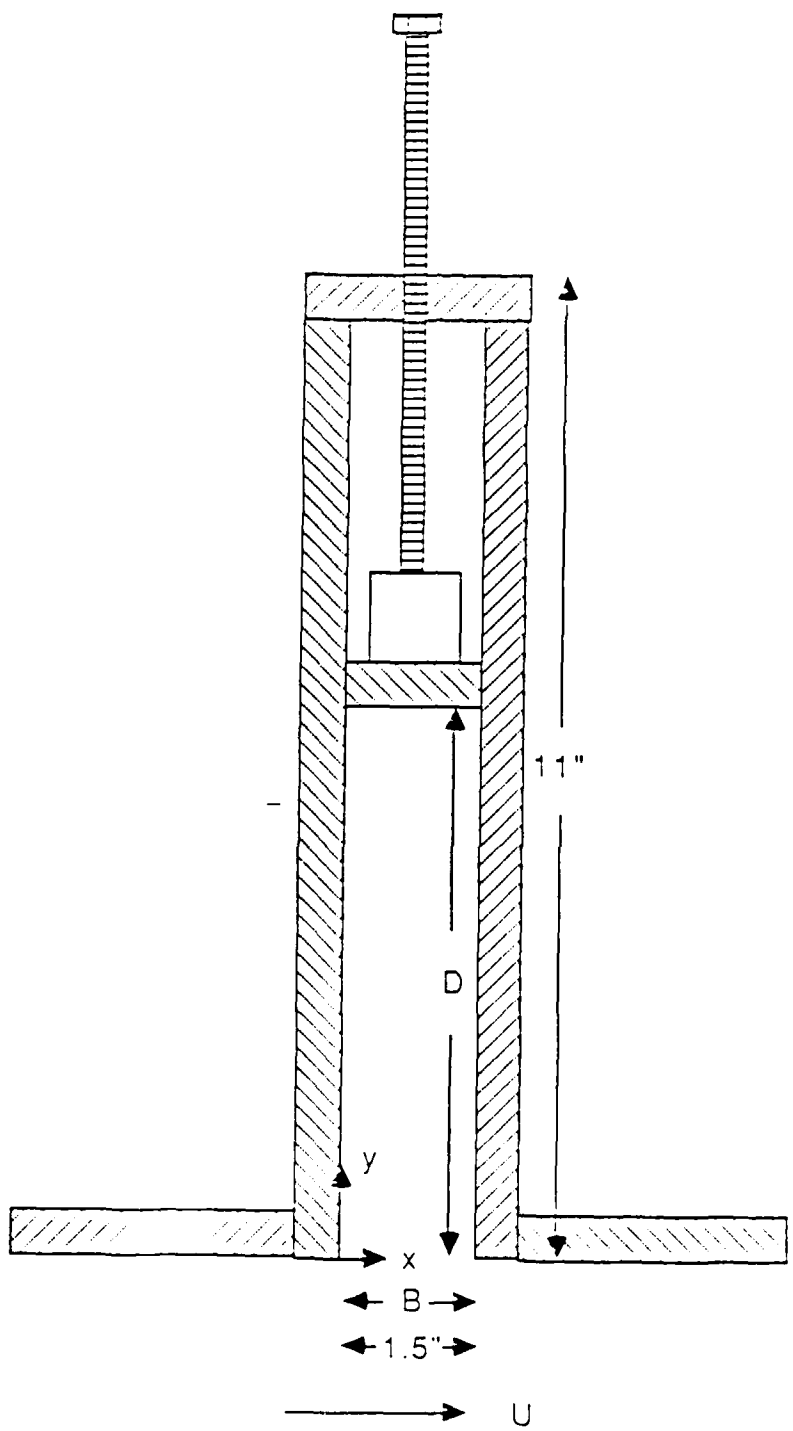


Figure 2. Two-Dimensional View of Rectangular Model (not to scale).

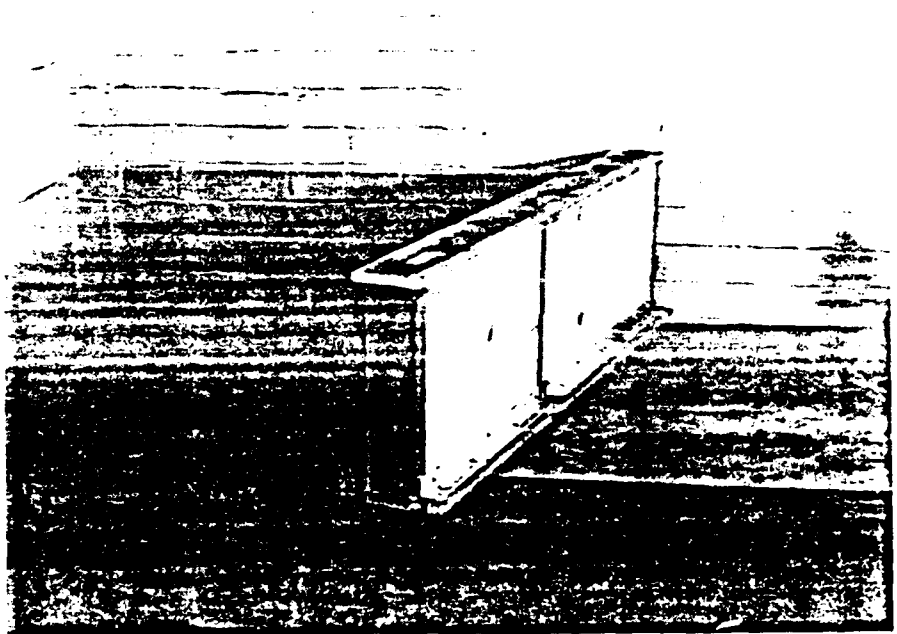


Figure 3. Photograph of 38-Inch Flow Visualization Model.

2.2 Pressure Measurement Model

Based on the results of the flow visualization, the span of the original model could be reduced, without significant affect on the flow, to 8 inches (0.20 m) centered around the two-dimensional plane of interest. A new model was then constructed for pressure measurements. Half-inch plexiglass was again used as the model material and the pressure measurement model had the same internal dimensions as in Figure 2. The differences in this model can best be seen in the sketch and photograph of the pressure model found in Figures 4 and 5. To pass the pressure probe down the span the two end plates were machined with a slot coming up from the bottom. Two manual x-y traverses (Daedal, Model 4526) were mounted to each face as seen in the photograph. The two traverses allowed for placement of the pressure probe perpendicular to the two-dimensional plane and offered movement in the x-y directions. Prior to mounting in the wind tunnel the probe was manually centered in the field through which the traverses could travel. This was done with a pair of verniers and the absolute dimensions of the probe relative to the origin in Figure 2 were recorded for future use.

The pressure probe was made from stainless steel hypodermic needle tubing with a 1/16 inch (1.6 mm) O.D. and 0.009 inch (0.23 mm) wall thickness. The shorter model span was necessary to prevent bowing of the probe in the middle of the span. The probe diameter represents 4.2% of the model width. The probe could not be moved any closer than 0.3 inches (7.6 mm) from the slot entrance and interference of

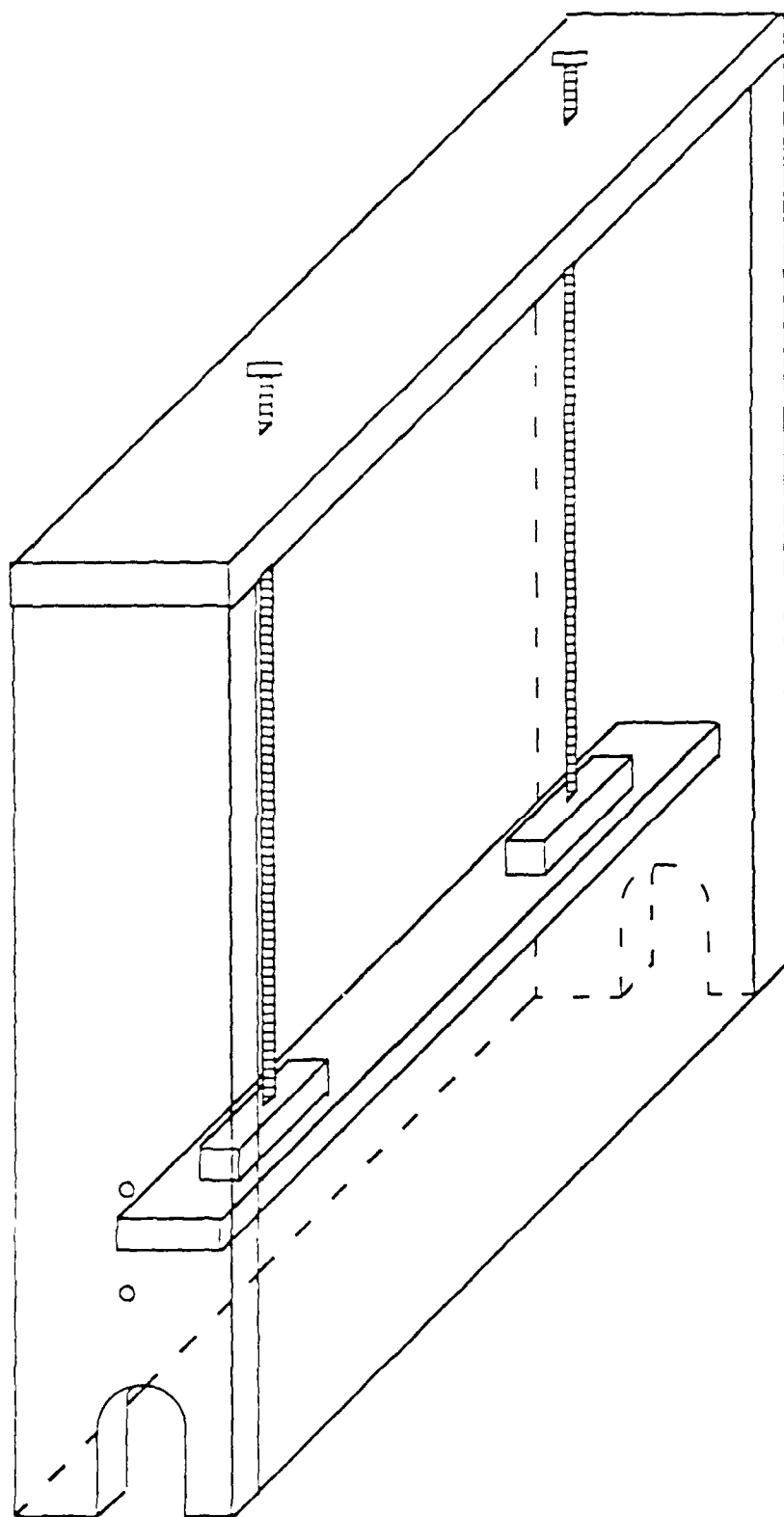


Figure 4. Pressure Model Sketch (not to scale).

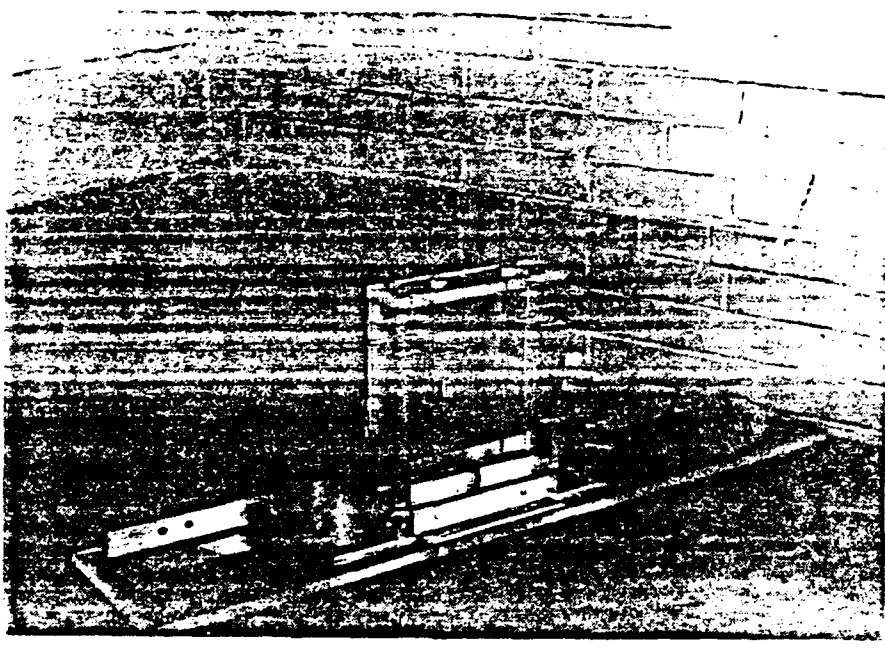


Figure 5. Pressure Model Photograph

the model base plate and the traverse field occurred for aspect ratios less than 0.5. As a result no measurements were possible below AR=0.5. The probe had four holes drilled through the walls and distributed evenly around the circumference near the model midspan. The holes were placed on the probe in this fashion so that the local static pressure could be measured. It was assumed that the average of the four pressure taps would approximate the local static pressure.

The model was sealed at its seams with tape; however, the groove through which the pressure probe passed could not be sealed as easily. A common plastic wrap was used for this purpose. Rubber bands were used around the tube itself while a thin stiff plastic plate was screwed down to the end plates to pinch the plastic wrap against the model. By supplying enough slack in between the probe and pinch points the probe was free to move without restriction in the traverse field while maintaining the seal.

Chapter 3

PROCEDURE AND RESULTS

3.1 Boundary Layer

A thick boundary layer was desired along the wind tunnel wall upstream of the slot. Thus, the first task involved in the project was to find a means of tripping the boundary layer to a consistent thickness (δ). The most flexible means of boundary layer control was found to be rough grain sandpaper. Specifically, our purposes were served by 32 inches (0.81 m) of number 12 grain sandpaper. That is, the first 32 inches (0.81 m) of the wind tunnel test section were covered with sandpaper to trip the boundary layer. During the boundary layer measurement more or less sandpaper could be added or removed in 8 inch (0.20 m) sections from 40 inches (1.02 m) down to 8 inches (0.20 m). This is illustrated in Figure 1. Note that for these boundary layer surveys the slot was not installed in the wind tunnel.

The boundary layer was measured by means of hot wire anemometry. The procedure was entirely computer controlled and the software which was written exclusively for boundary layer measurement can be found in Appendix D. The procedure involved a calibration of the hot wire, measurement of the profile velocities, then a second calibration. For the calibration, the free stream velocity was measured by means of a pitot-static probe. The hot wire and pressure measurements were conditioned to analog voltages which were measured and recorded by

computer. To avoid aliasing, the hot wire voltage signal was passed through a low pass filter set at 50 Hz. During data acquisition the computer would sample at 100 Hz for 10 seconds for each point. This was done for both calibrations as well as for the profile measurements.

The computer was configured to measure voltages from zero to five volts and stored the data in a binary file. The data was later converted to real numbers with each record containing 1000 readings. The hot wire voltage and velocity pairs from the calibration runs and the hot wire voltages at each position in the boundary layer were averaged. The calibration files were then used to find a fifth order least-square fit of velocity versus voltage. The two calibration curves were time weighted when the profile voltages were matched with these curves. This was done to avoid problems caused by room temperature changes over the period of time required for each test. A typical profile test lasted 15 minutes, where the temperature could change by as much as 1° F (0.6° C). This software can also be found in Appendix D.

For each run, temperature and pressure were recorded by the operator. These measurements were recorded at the beginning of each of the two calibration runs. This information was also used for later nondimensionalization of the boundary layer profiles (e.g., to obtain a value for viscosity).

The goal here was to meet the given criterion set in the project proposal (i.e. the boundary layer thickness-to-model width ratio (δ/B) was to be greater than unity). The boundary layer thickness based on 99% of

the freestream velocity to be 1.8 inches (45.7 mm), measured along the top of the test section at the location of the upstream corner of the slot (i.e. 65 inches (1.65 m) downstream of the tunnel entrance) with 32 inches (0.81 m) of number 12 sandpaper at the front and a freestream velocity of 15.75 ft/s (4.8 m/s). The model width was then set at 1.5 inches (38.1 mm) which yielded $\delta/B = 1.2$. For the remainder of the tests this same configuration of sandpaper was installed, and the boundary layer thickness just upstream of the slot was therefore fixed.

The measured boundary layer profile can be seen in nondimensionalized form in Figure 6. The procedure used to get the wall-friction velocity v^* was as follows: First the momentum thickness (θ) was calculated using the definition

$$\theta = \int_0^{\infty} \frac{\bar{u}}{u_{\infty}} \left(1 - \frac{\bar{u}}{u_{\infty}} \right) dy .$$

This was done numerically and the computer code can be found in Appendix D. Next the Reynolds number based on momentum thickness was calculated

$$Re = \frac{u_{\infty} \theta}{v} .$$

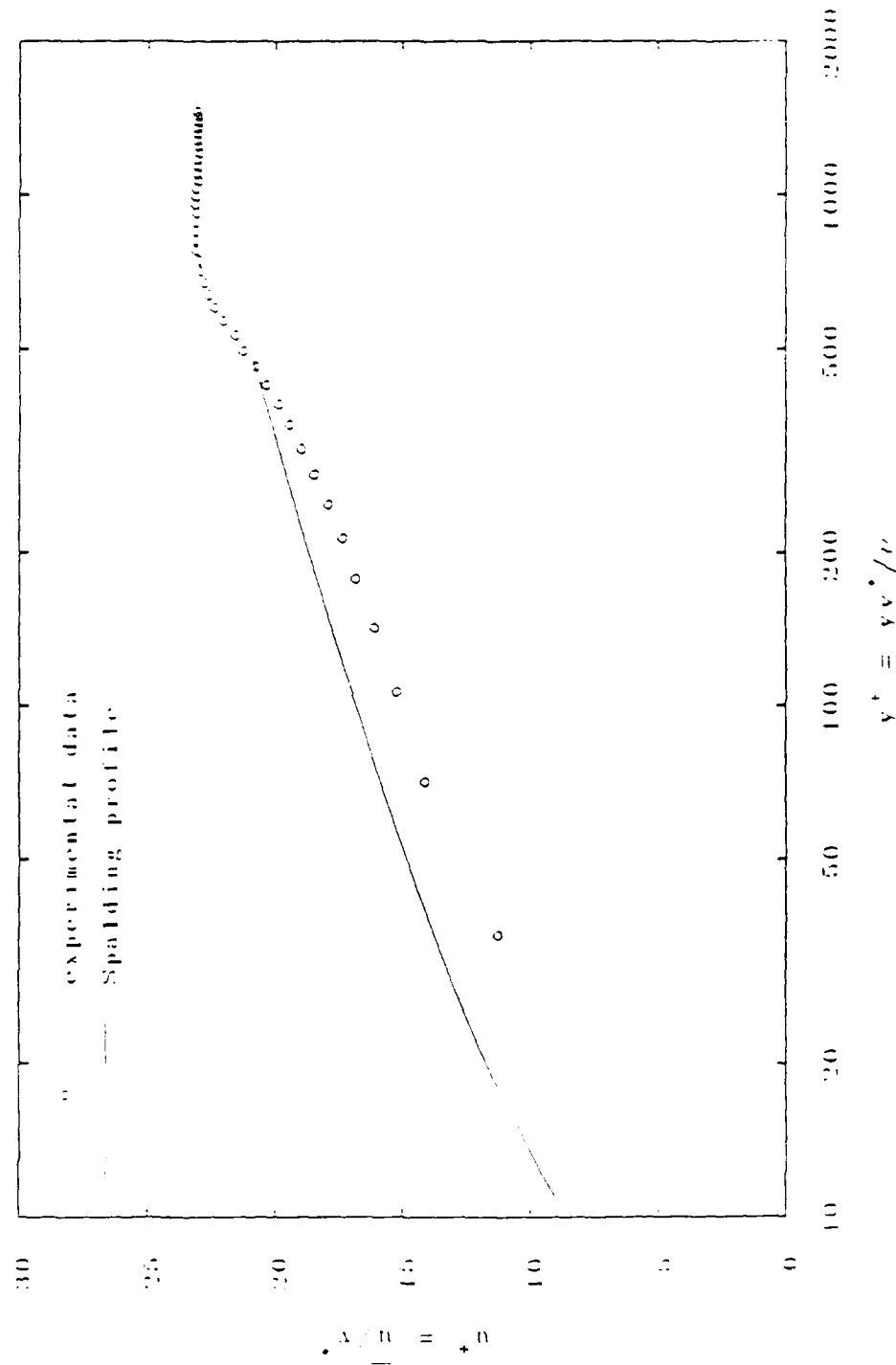


Figure 6. Boundary Layer Profile (32 in. of sandpaper, 15.75 ft/s).

The skin friction coefficient was then calculated according to Kays and Crawford (1980) as

$$\frac{C_f}{2} = .0125 (Re)^{-0.25}$$

Finally the velocity scale was then calculated to be

$$v^* = u_\infty \left(\frac{C_f}{2} \right)^{\frac{1}{2}}$$

The boundary layer was then plotted in traditional fashion as seen in Figure 6. Note that in this case the positive y direction is downward from the top inside of the wind tunnel test section into the freestream.

The solid line on the plot was obtained from Spalding's law-of-the-wall equation,

$$y^+ = u^+ + e^{-kB} \left[e^{ku^+} - 1 - ku^+ - \frac{(ku^+)^2}{2} - \frac{(ku^+)^3}{6} \right]$$

where $k=0.4$ and $B=5.5$ (White 1974). This curve was included for comparison and is said to be one of the simplest and most comprehensive equations of turbulent boundary layers.

Comparison of the experimental data with the Spalding profile shows a right-hand shift of the experimental profile. Overall, the experimentally determined profile is a typical response of a turbulent boundary layer to a

wall disturbance (Clauser 1956). However, the reason for the shift is still of some concern. The most likely reason is a lack of recovery time for the flow from the end of the sandpaper until the model location. The obvious correction for this discrepancy would be to move the model farther downstream in the wind tunnel test section. However, the wind tunnel freestream is not very uniform in the last third of the test section, so the model could not be moved downstream without sacrificing flow quality.

3.2 Flow Visualization

The flow visualization portion of the project had many different goals. The first was to collect some qualitative information on the flow structure inside of the cavity as a function of the aspect ratio $AR = D/B$. The second was to determine if the two-dimensional slot flow structure was altered by shortening the span from the full model span of 38 inches (0.97 m) to some shorter value that would be more conducive to pressure measurement inside the slot. The third goal was to see how the primary vortex center moved as a function of the aspect ratio. The primary vortex was defined as the strongest and closest vortex to the slot entrance. These visualizations also served as a guide for the design of the additional model needed for the pressure measurements. Finally an investigation of the slot entrance region was to be carried out with the smoke wire flow visualization technique. Namely, the goal was to

investigate the mechanism that maintains the vortex in the cavity and to see the extent of mass transfer, if any, across the slot entrance.

3.2.1 Internal Cavity Visualization

The method used to visualize the flow is called the smoke wire method (Corke et al. 1977). The source of smoke comes from a thin nichrome wire passed down through the center of the slot. This wire is weighted at the bottom and kept taut with a spring from the top. To induce smoke in the cavity a mineral oil is dripped down the wire leaving small droplets behind on the wire. A high DC voltage is then placed across the wire which heats up and burns the oil. The smoke created by this process is then carried with the flow and the resulting set of streaklines can be followed.

Creating the smoke in the cavity was not difficult. The difficulties came in trying to synchronize the smoke and strobe flash in order to photograph the process. Fortunately, a timing/synchronization controller was available which provided millisecond control of the smoke wire and the strobe. The strobe was set up at the half-inch ports on the sides of the model to provide an instantaneous flash of light after some desired time delay. The procedure was: coat the wire with oil, turn out the room lights, open the camera shutter, switch on the timing controller, then close the shutter immediately after the strobe flashed. The timing/ synchronization controller would be preset to delay the strobe flash so that the smoke had time to be drawn into the vortex. The delay time between charging

the smoke wire and triggering the flash was varied to provide a variety of smoke wire pictures. The above procedure was followed for aspect ratios of 0.5, 0.75, 1.0, 1.25, 1.5, 1.75, 2.0, 2.5 and 3.0. One entire roll of film was taken for each aspect ratio in order to examine the unsteadiness of the flow.

As will be discussed later, the pressure measurements inside the slot required a slot of significantly shorter span than the flow visualization model which spanned the entire 38 inches (0.97 m) of the wind tunnel test section. Thus, it was necessary to determine if a reduced span would affect the two-dimensionality of the flow. It was reasoned that if changes in the two-dimensionality of the flow take place with changes in the span this would be most visible in the deepest aspect ratio case (i.e. AR=3.0). The flow was first photographed with a span of 38 inches (0.97 m) which when nondimensionalized by model width is equivalent to a span aspect ratio of 25.3. Next the flow visualization was repeated for a reduced span of 8.0 inches (0.20 m), equivalent to a 5.33 span aspect ratio. When compared, no difference was found in the primary vortex location, see, for example, Figures 7 and 8. Based on the y-coordinate of the primary vortex center relative to an origin at the upstream entrance of the slot (see Figure 3), the 38-inch (0.97 m) span model had an average of 0.99 inches (25.2 mm) for the primary vortex depth; while the 8-inch (0.20 m) model offered an average vortex center depth of 1.02 inches (25.9 mm). The difference is only about 3% which is surprisingly small considering the large amount of scatter due to

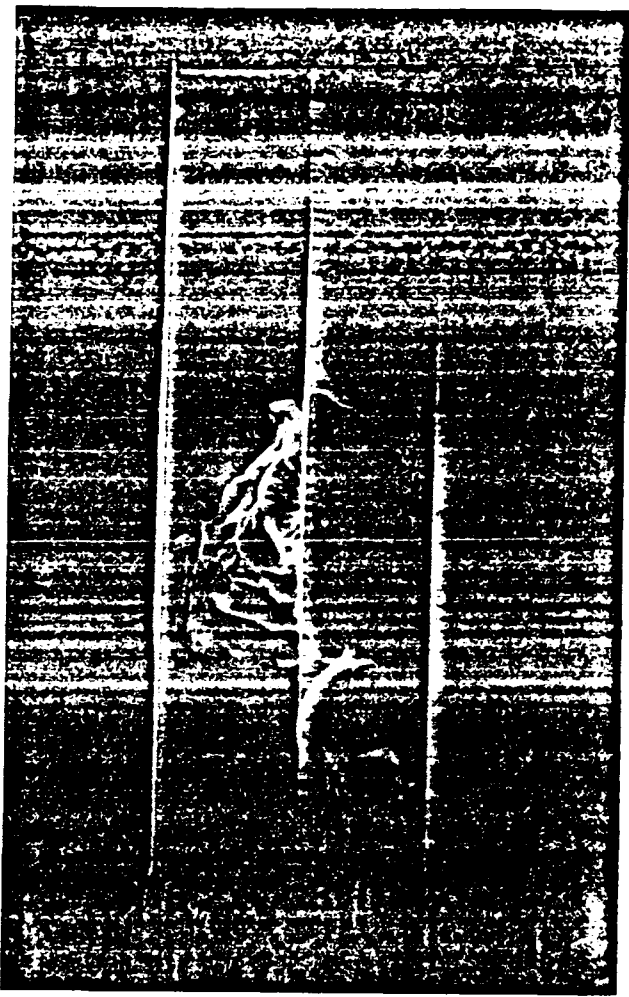


Figure 7. Span Photograph - 38-Inch (AR=3.0).

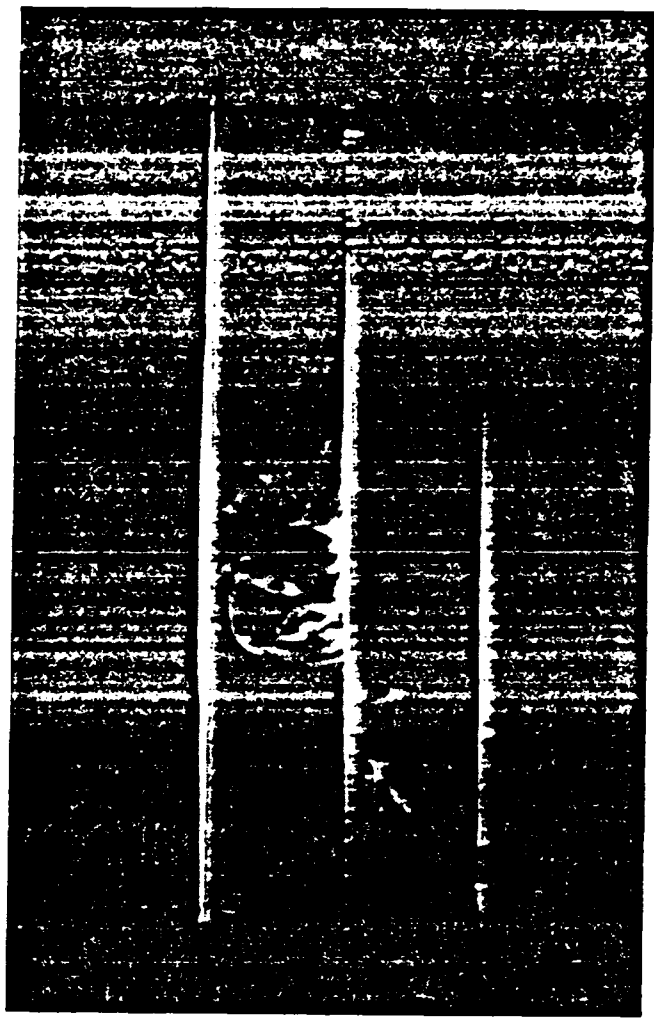


Figure 8. Span Photograph - 8-Inch (AR=3.0).

unsteadiness in both sets of smoke wire pictures. These measurements come from the average of approximately 20 pictures for each set and both sets had a scatter of approximately ± 0.28 inch (7.1 mm). An additional error of ± 0.1 inch (2.5 mm) from measuring, by hand, the vortex center location from the photographs makes the total possible error of vortex vertical location ± 0.38 inch (9.6 mm). This scatter was characteristic of all of the photographs and is most likely due to the unsteadiness of the flow. Since the span change had no apparent effect on the flow the rest of the photographs were taken with the 8-inch (0.20 m) model for convenience. The pressure measurement model was then designed for a span of 8 inches (0.20 m) as well.

The slot flow field was visualized for the aspect ratios previously mentioned. The photographs were taken using the aforementioned flow visualization procedure and can be found in Appendix A for all of the aspect ratios. The pictures in Appendix A were chosen based on their clarity and for their ability to show the flow structure with a well defined primary vortex center. When examining the photos it is advisable to keep some of the inherent problems of the smoke wire method in mind. Specifically, low velocities found at the higher aspect ratios did not allow for distinct streaklines. This may be due to the diffusion process of the smoke or possibly three-dimensional effects on the smoke in the cavity. Note that as the smoke moved out of the plane of interest the smoke also moved out of the focused area of the camera. This can be seen in the higher aspect ratios of 2.0 and 3.0 where the smoke appears to have

folded over itself. These higher aspect ratios with inherently lower cavity velocities required a larger delay between the closing of the smoke wire circuit and the strobe flash. This brings the additional possibility that the relatively hot smoke may have risen in the cavity due to buoyancy effects. These effects could lead to misrepresentation of the vortex center and distortion of the smoke image from the actual vortex structure. Fortunately, this is not observed in the photographs. If buoyancy of the smoke was a factor, the photographs with longer strobe delays would have indicated progressively higher vortex centers; but this was not observed.

This method adequately showed the overall flow structure in the slots. One notable observation from the photographs was that the higher aspect ratios had more than one vortex in the slot. The secondary vortices were found deep in the slot and were weaker than the primary vortices. This was seen by the lack of smoke in the secondary vortex relative to the primary. The indication was that the velocities were lower deeper into the slot. The low aspect ratios (less than 2.0) did not develop the secondary vortex but the intermediate aspect ratios of 1.75 and 1.5 seemed to have a relatively calm region deep in the slot.

The quantitative result data obtained from these photos is the approximate location of the primary vortex center as a function of aspect ratio. It is at the vortex center that the lowest pressures are to be found in the cavity, and that is where cavitation would most likely have occurred if these test had been performed in water rather than air. The smoke wire

photographs were viewed on a 1:1 scale with the model so that the vortex centers could be measured easily. They showed that the vortex center relative to an origin at the upstream entrance of the model (see Figure 2) primarily moves in the y-direction with changes in the aspect ratio. From these photos it was too difficult to tell if the vortex moves upstream or downstream in the x-coordinate. The vertical center location was plotted in two nondimensionalized forms (by width and by depth) in Figures 9 and 10. The first figure with y nondimensionalized by width also showed the error involved. This error included the approximation of ± 0.1 inch (2.54 mm) resulting from measurements off of the frequently fuzzy photographs. The majority of the error came from the scatter found in the twenty or more pictures measured for each aspect ratio. The point plotted is the averaged value found for each case and the error bars indicate the range of the vertical vortex position. Despite the growing scatter with increasing aspect ratio, the y-location increases steadily up to AR of about 2.0 and then levels off. It is significant that the secondary vortex also first appeared deep in the slot at an aspect ratio of about 2.0.

3.2.2 External Cavity Visualization

The exact mechanism of sustaining the vortex in the slot is not completely understood. Specifically, is the vortex maintained solely by the shear from the flow passing over the entrance or is there a more involved interaction with mass being transferred through the slot entrance? This question was addressed by moving the smoke wire out

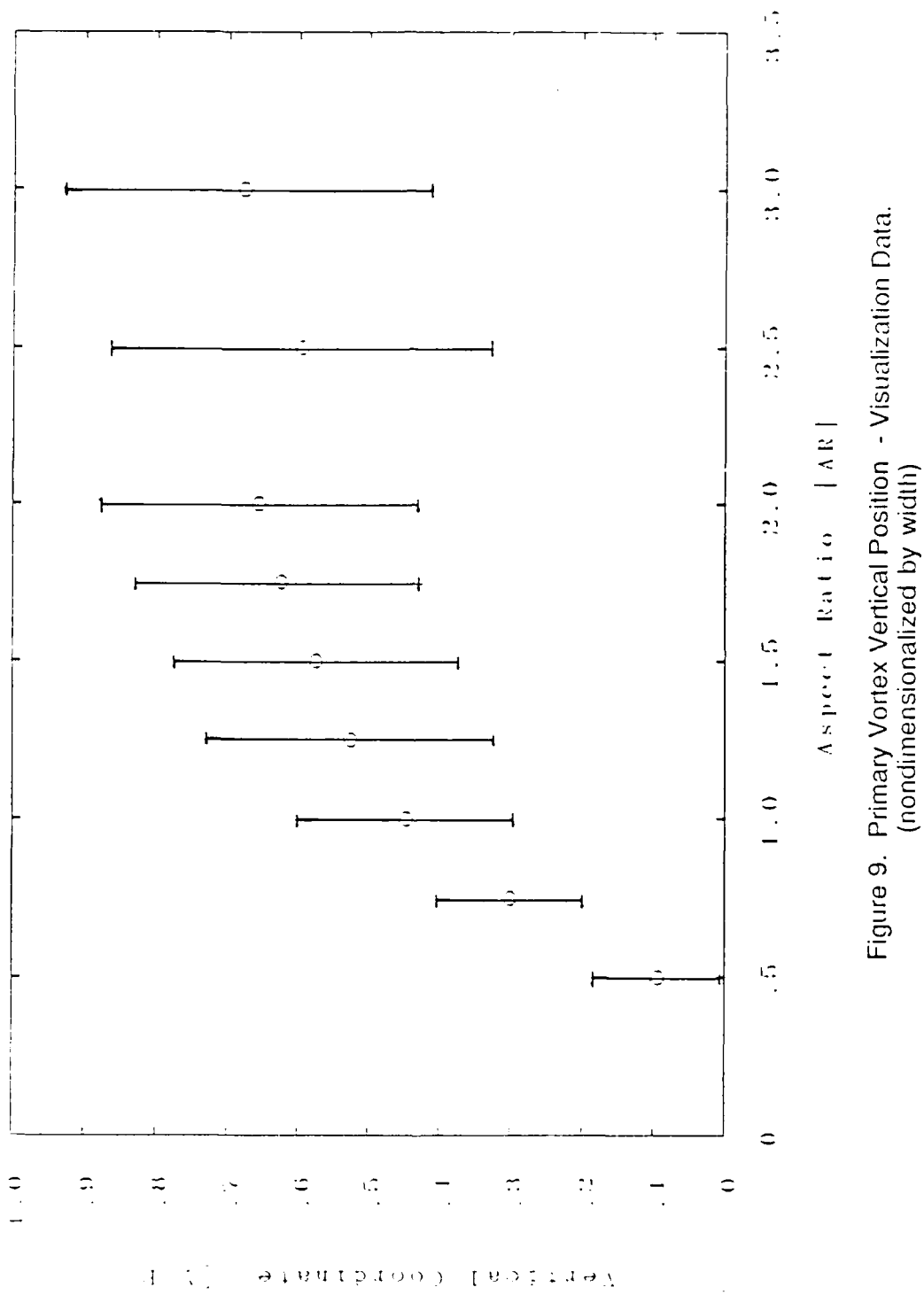


Figure 9. Primary Vortex Vertical Position - Visualization Data.
(nondimensionalized by width)

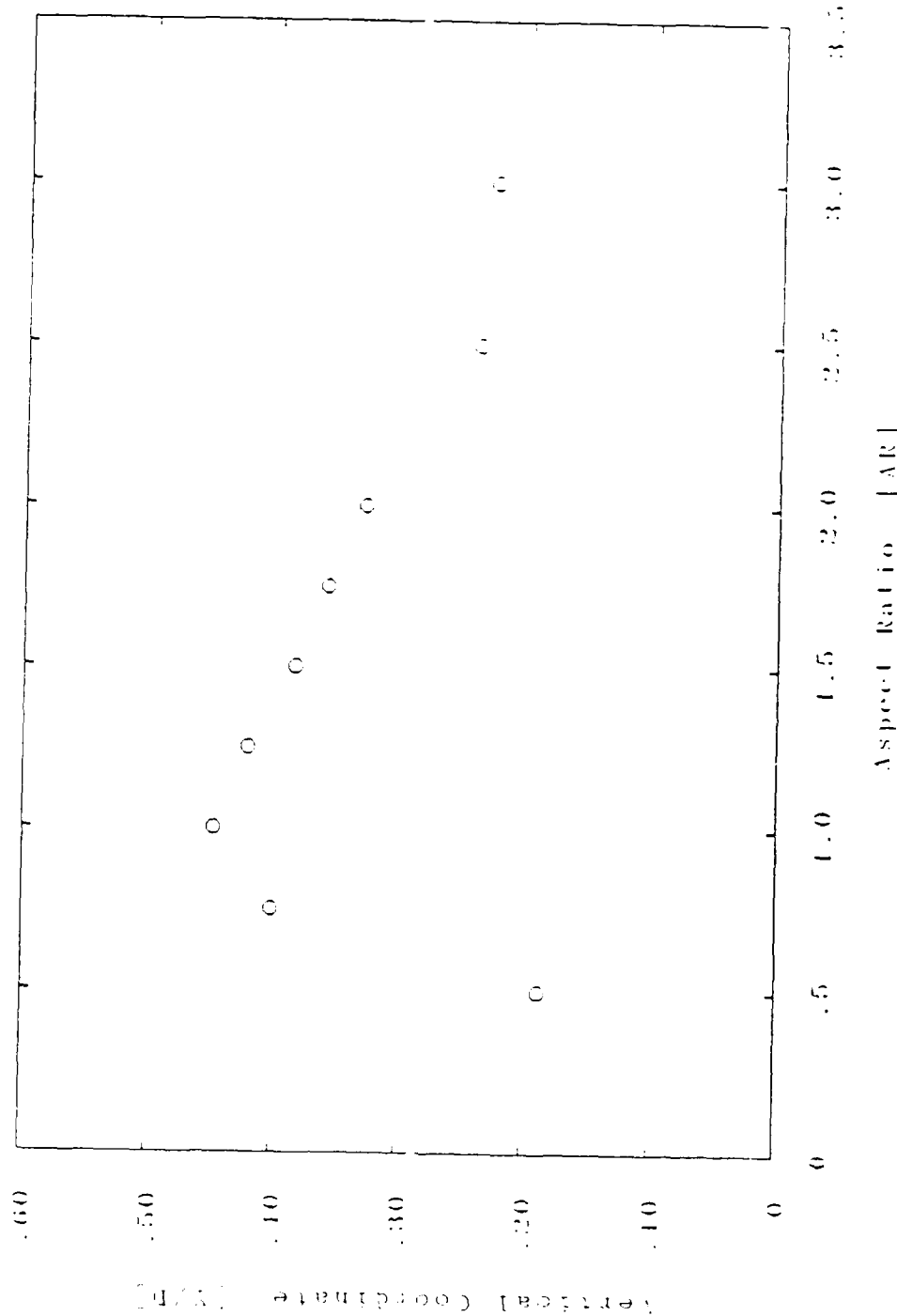


Figure 10. Primary Vortex Vertical Position - Visualization Data.
(nondimensionalized by depth)

of the slot and placing it just in front of the entrance while photographing the slot interior. The procedure for taking the photographs was the same as for the internal flow visualization. Four different aspect ratios were chosen, namely $AR = 1.0, 1.5, 2.0$ and 3.0 . Examples of the flow at each aspect ratio are found in Appendix B. The pictures presented were chosen to demonstrate the contrast between the times when smoke was and was not seen in the slot. An overall examination of the photographs shows that about three out of four pictures had smoke in the slot. This would indicate that some mass transfer is indeed taking place, and that shear at the slot entrance is not the sole cause of vortex motion. The other interesting observation is that smoke was never seen near the center of the primary vortex.

3.3 Pressure Measurement

The objective in this stage of the project was to measure the pressure field in the two-dimensional plane, midspan of the slot. In particular, the location and strength of the vortex center as a function of aspect ratio was desired. This task required measuring the static pressure throughout the plane without disturbing the vortex structure. Again we note that the primary vortex is mainly of interest since it was shown by flow visualization to be the strongest vortex whenever more than one vortex is present. Direct pressure measurement was accomplished by passing a thin tube with holes in its circumference

down the third dimension in the model span. The details of the model itself can be found in Chapter 2.

The procedure used to survey the pressure field in the slot was as follows: First the pressure probe was centered in the traverse field and the x and y coordinates relative to the absolute origin (upstream corner of the slot) were recorded. The relative x and y coordinates read from both traverses were also recorded. The software used during the procedure required the three pairs of coordinates for user interaction and storage of the data. This software can be found in Appendix D.

Just prior to the pressure field surveys, the wind tunnel freestream velocity was measured by means of a pitot-static probe placed in the freestream. The dynamic head ($1/2 \rho u_\infty^2$) was later used to nondimensionalize the measured pressure difference between the freestream static pressure (P_∞) and the static pressure inside the slot (P_c). This nondimensionalization provided a negative local pressure coefficient defined as:

$$-C_p = \frac{P_\infty - P_c}{\frac{1}{2} \rho u_\infty^2} .$$

This form was convenient since it is analogous to a cavitation index.

Following the dynamic head measurement the positive side of the pressure transducer was connected to the freestream static pressure tap, and the negative side was connected to the pressure probe inside the

slot. In this manner the pressure coefficient could be measured as defined above. The probe was traveled through a predetermined number of points in a square grid contained within the traverse limits. Each data point was stored in a binary file along with the corresponding absolute x and y coordinates.

The software was written such that either a 7 x 7 point grid with 1/16 inch (1.59 mm) spacing or a 14 x 14 point grid with 1/32 inch (0.79 mm) spacing could be chosen. Obviously the 14 x 14 point grid would allow for higher resolution plots; however, one test run with a 14 x 14 point grid would take about 5 hours compared to only 1 1/2 hours for the 7 x 7 grid. The 14 x 14 grid was used for the aspect ratios of 1.0, 1.5, 2.0 and 3.0, while the 7 x 7 grid was used for all the others (AR = 0.5, 0.6, 0.75, 0.9, 1.25, 1.75, 2.5).

The long periods of time involved in each procedure became a concern in the preliminary tests. Of particular concern was the fact that changes in room temperature could effect the pressure measurement equipment. Therefore, the pressure signal conditioner had to be rezeroed periodically during each test. Specifically, the equipment was zeroed prior to starting a pass in each row in the grid. In other words, the equipment was zeroed every seventh point in a 7 x 7 grid and every fourteenth point in a 14 x 14 point grid. The freestream velocity was readjusted after every seventh or fourteenth point as well.

Despite this extra effort temperature changes in the lab still may have had an effect on the data. The largest observed deviations from the

equipment during these tests were on the order of $\pm 10^{-5}$ mmHg. This represents approximately 6% of the minimum pressure measurements (which were around 0.00018 mmHg).

Early measurements discovered some interesting flow characteristics that required procedure adjustments from those used in the boundary layer measurements. Specifically, the very unsteady nature of the vortex in the slot required longer sampling times. In the final test runs, data were sampled at 100 Hz for 30 seconds. Ten second periods were initially attempted but produced inconsistent results. Secondly, to accurately measure these very low pressure differences, the range selection dial on the pressure signal conditioner had to be adjusted for maximum sensitivity. This adjustment also resulted in more efficient use of the A/D converter voltage range. In particular, for the lowest aspect ratios(0.5 and 0.6) the 0.1x range selection was used, while the 0.01x setting was used for all other aspect ratios.

The pressures for each point in the grid of each test were averaged and the mean values were nondimensionalized by the dynamic head. This produced a square plot of negative pressure coefficients in x-y coordinates which were nondimensionalized by width. Plots of this kind demonstrated that the pressures were lower near the vortex center. In order to bring out this information more clearly a computer code was written to check and interpolate for specific pressure coefficient values along the rows and also the columns of the grid. The computer codes used to average, nondimensionalize, sort, and

interpolate the data can be found in Appendix D. This procedure identified isobars in the grid and the plots can be found in Appendix C.

Due to the wide range of pressure coefficient values most plots representing different aspect ratios had to be treated individually. The deeper aspect ratio tests could be sorted along the same set of isobars but the tests with AR less than 1.5 were processed separately. To avoid confusion each plot contains its own legend.

Quantitative information about the location and relative magnitude of the primary vortex can more easily be seen with the compiled data presented in several new forms. For example, the horizontal location of the vortex center as a function of aspect ratio can be seen in Figure 11. Note the lack of movement of the primary vortex in the x-direction with aspect ratio. This supports earlier observations from the flow visualization. However, the vortex at the aspect ratio of 0.5 did not stay in the same horizontal location as did the higher ones but shifted downstream. Additional tests were done with the aspect ratios of 0.6 and 0.9 to supplement the data in this region and they show the same trend. It should be noted that the lower aspect ratios do push the limits of our model the most. The fact that the pressure probe is taking up a larger percentage of space in the cavity does little for the confidence of these data.

The next two plots on the vortex location are similar to the ones seen earlier from the flow visualization data. Figures 12 and 13 show the change in the vertical vortex location with aspect ratio. Both plots have

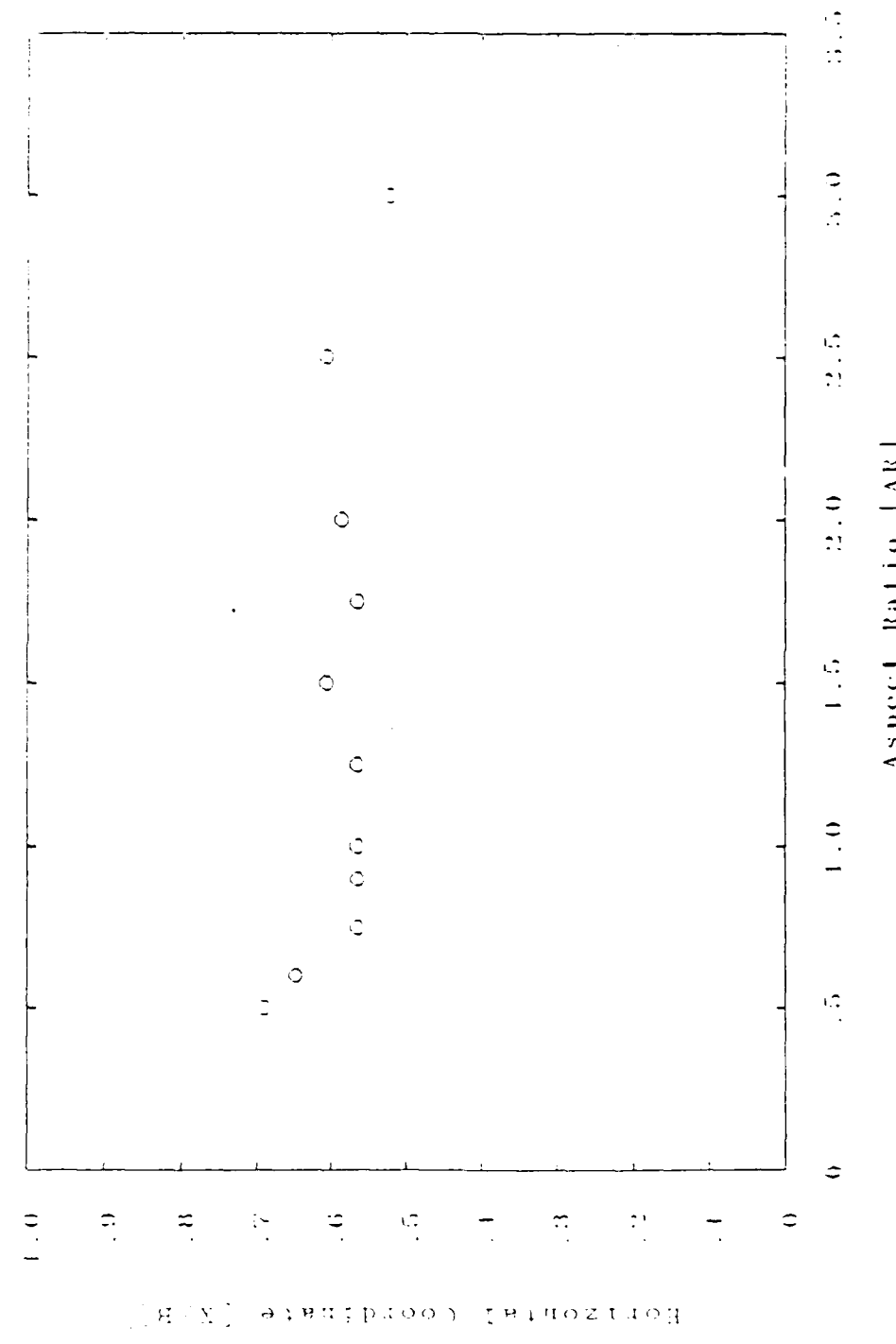


Figure 11. Primary Vortex Horizontal Position.

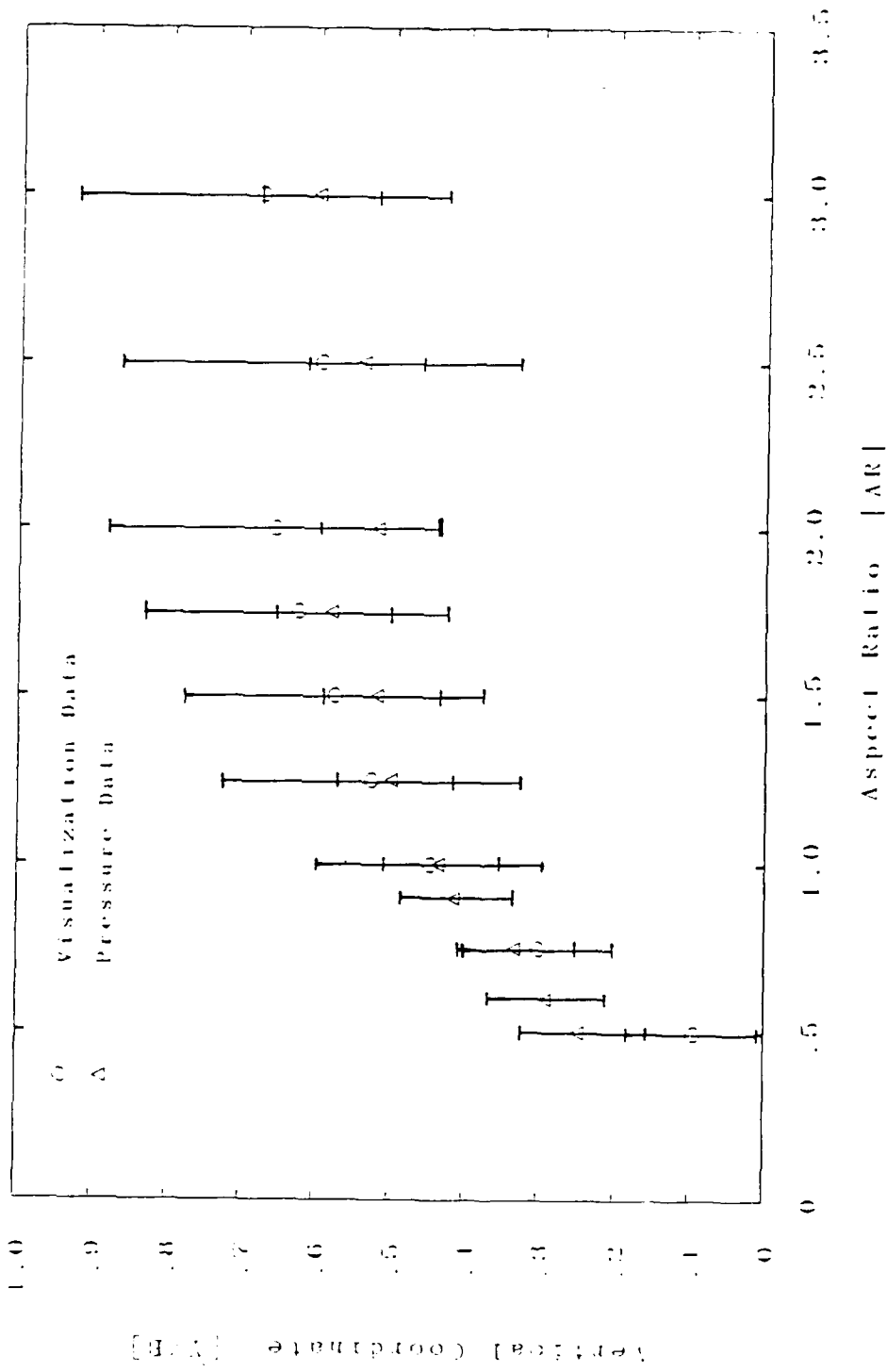


Figure 12. Primary Vortex Vertical Position-Pressure Data.
(nondimensionalized by width)

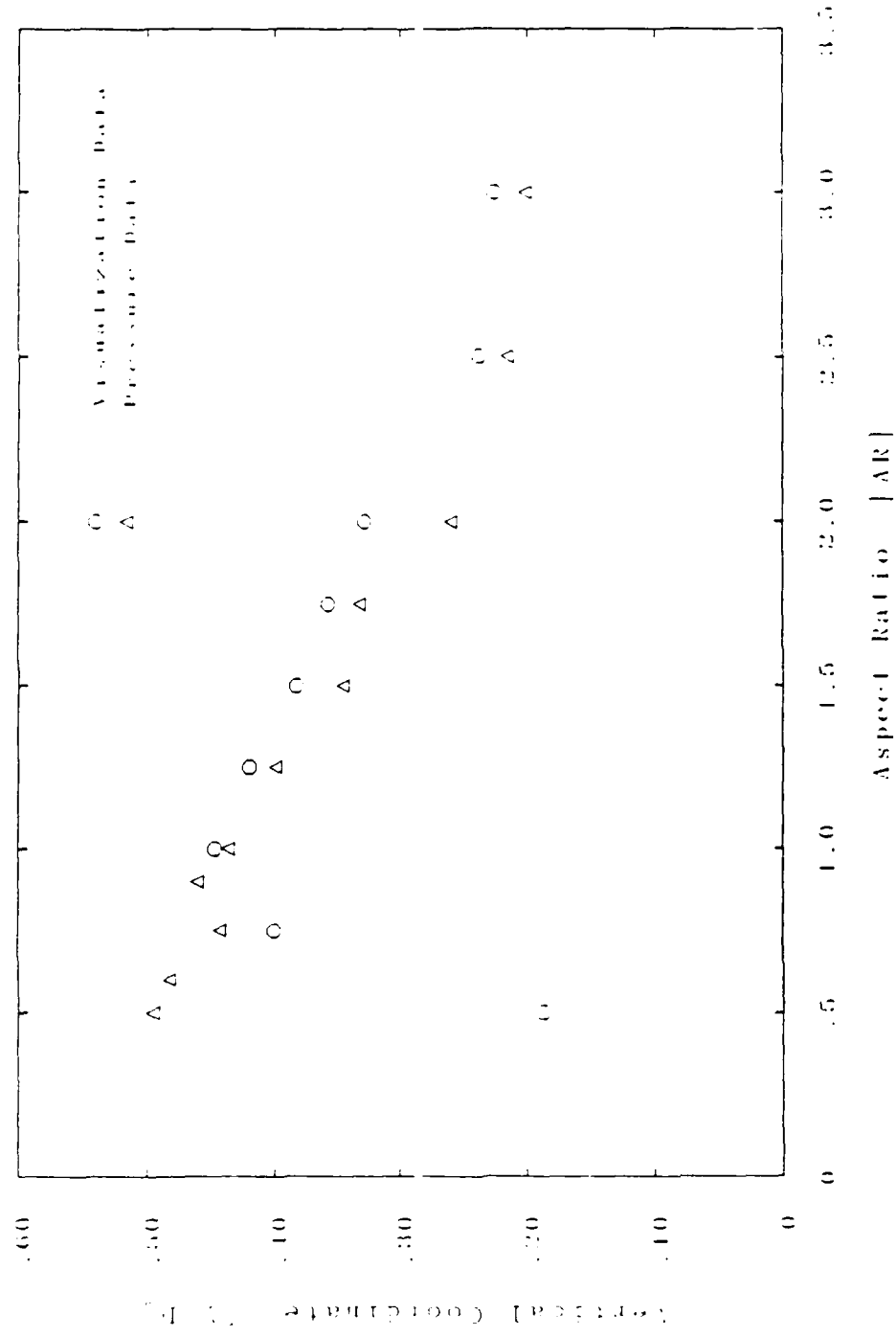


Figure 13. Primary Vortex Vertical Position-Pressure Data.
(nondimensionalized by depth)

the flow visualization data for comparison and Figure 12 contains error bars as seen on the visualization plot earlier. The pressure data error was calculated based on model tolerance and repeatability of the results. This error was ± 0.1 inch (2.5 mm) for all aspect ratios.

The pressure and visualization data are close and consistent within the error limits. The data at aspect ratio of 0.5 indicate that the pressure probe never went low enough to find the true vortex center. For the larger aspect ratios, the visualization data are consistently higher than the pressure data. This may be due in part to buoyancy of the smoke. The effect of the probe on the flow is also a possible cause of error. To test this, a dummy pressure probe (i.e. a 1/16 inch (1.59 mm) O.D. rod) was placed across the entire span at various locations inside the flow visualization model. Photographs with this rod in the model were taken using the smoke wire method. Aspect ratios of 0.5, 1.0 and 2.0 were chosen and these photographs can be seen in Figures 14-18. These all show that the flow is not affected by the added rod.

Finally the strength of the primary vortex is shown in Figure 19 as a function of aspect ratio. This figure shows that the pressure coefficient decays with increasing aspect ratio. Obviously this curve must originate at the origin so it would seem that the tests did not extend to low enough aspect ratios to include both sides of the expected peak. Unfortunately, physical limitations of the model precluded measurements below an aspect ratio of 0.5. The overall error with this pressure data is ± 0.003 in terms of pressure coefficient. This was determined from the error created

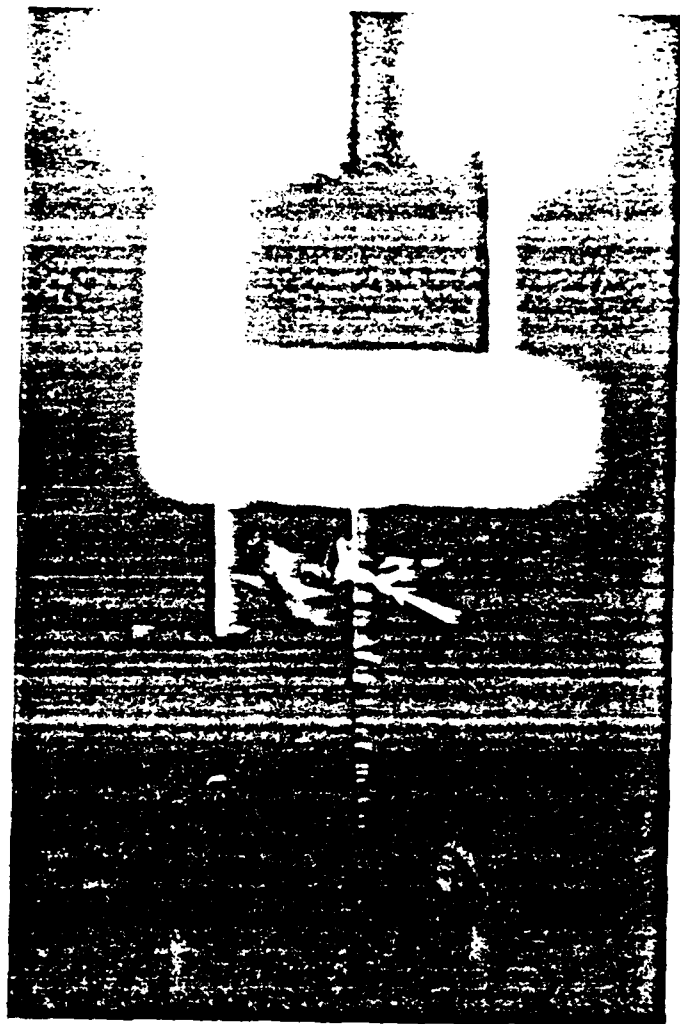


Figure 14. Pressure Probe Visualization AR=0.5.
(downstream probe)

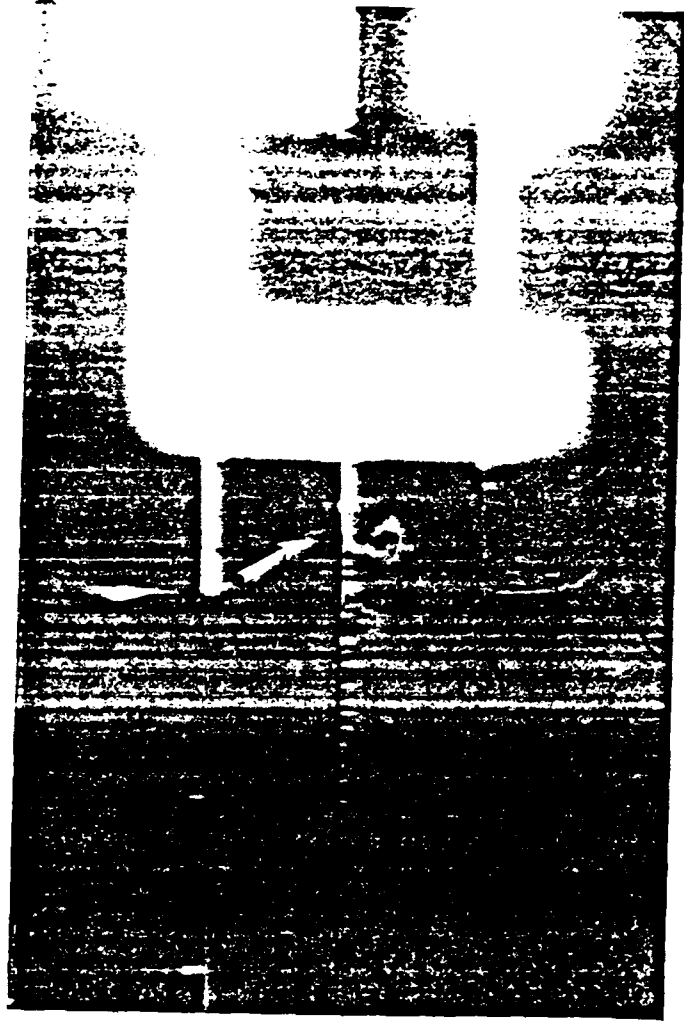


Figure 15. Pressure Probe Visualization AR=0.5.
(upstream probe)

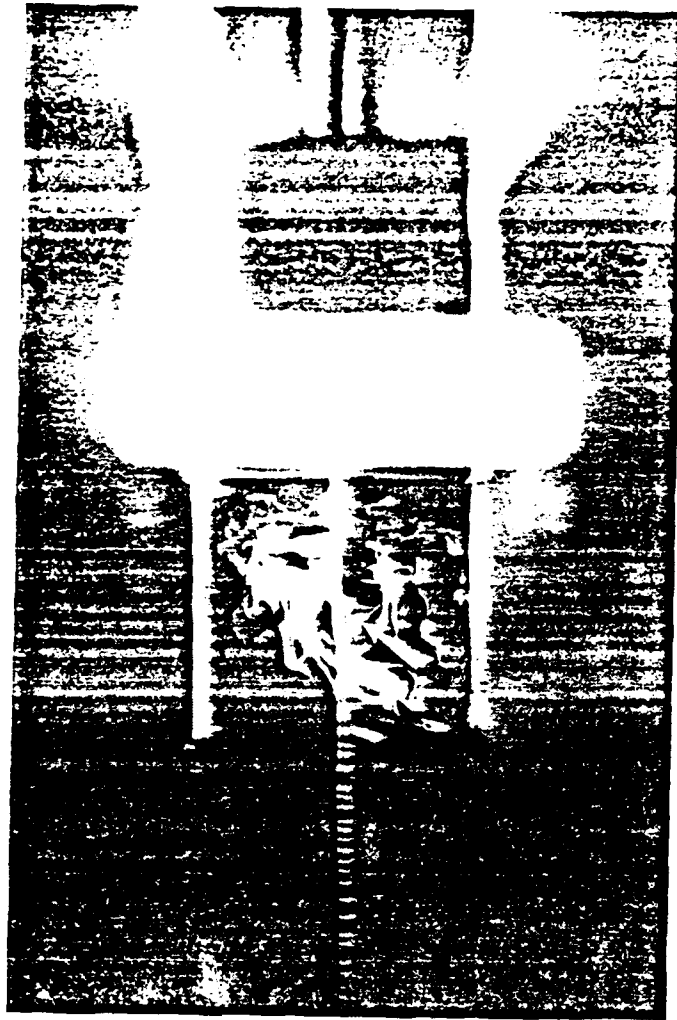


Figure 16. Pressure Probe Visualization AR=1.0.
(downstream probe)

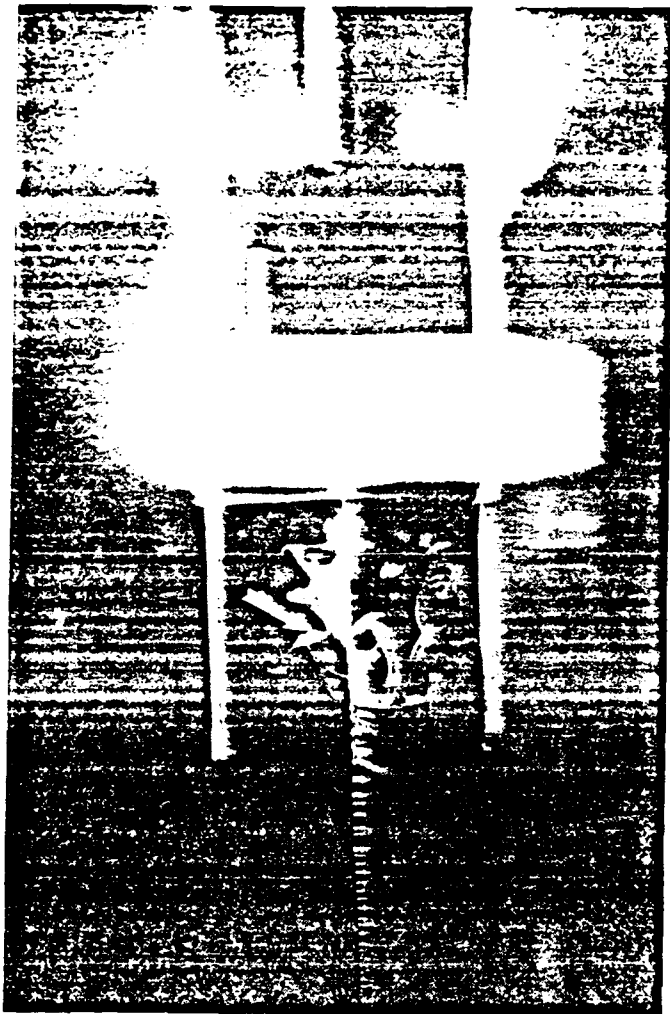


Figure 17. Pressure Probe Visualization AR=1.0.
(upstream probe)

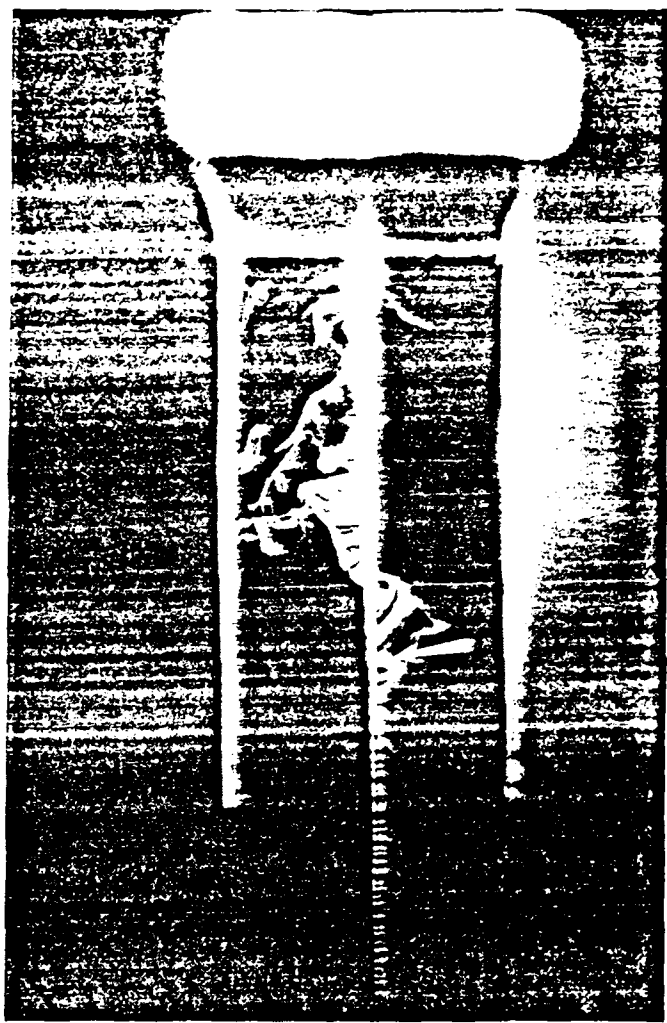


Figure 18. Pressure Probe Visualization AR=2.0.
(downstream probe)

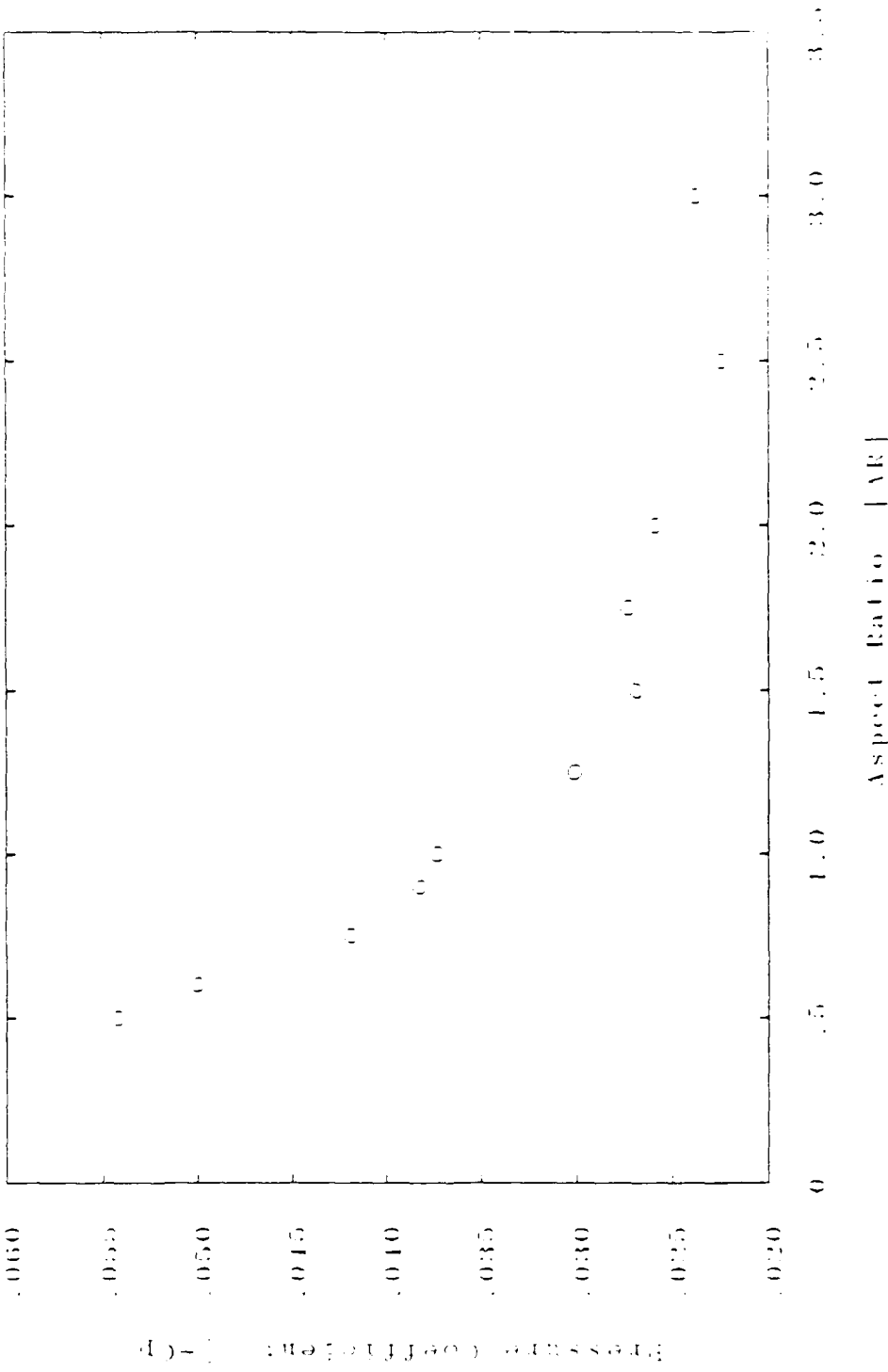


Figure 19. Vortex Strength Data.

by the zero drift of the pressure signal conditioner and from the scatter of the data.

Chapter 4

DISCUSSION AND CONCLUSIONS

The fluid mechanics associated with the flow of a two-dimensional slot in a flat plate has been studied; specifically, the case where a turbulent boundary layer thickness of 1.2 times the slot width has been studied. The flow field macspan of an 8-inch (0.20 m) span slot was visualized by means of the smoke wire method and the flow field was subjected to direct pressure measurement. The flow visualization qualitatively described the flow field and offered the first quantitative data concerning the vortices contained within the field. The pressure measurement of the field produced similar quantitative results concerning the position of the primary vortex with changes in aspect ratio. These measurements also yielded information concerning the flow field pressure distribution with changes in slot aspect ratio.

The boundary layer was maintained at a constant thickness by means of 32 inches (0.81 m) of number 12 rough grain sandpaper and running all the tests at 15.75 ft/s (4.8 m/s). The boundary layer profile was measured at the same location as the upstream corner of the slot. These measurements showed a shift to the right when compared to the Spalding flat plate boundary layer profile. This was attributed to a lack of recovery time the flow had between the sandpaper and the location of boundary layer profile measurement.

An important result from the flow visualization was documentation of the effect of reduction of the slot span. All indications from this investigation show no significant change in primary vortex location or shape when the span was reduced from 38 inches (0.97 m) to 8 inches (0.20 m). These results do not imply that three-dimensional effects don't exist. In fact, three-dimensionality is seen in some photographs where smoke has folded over on itself. Nevertheless, the time-averaged results, and in particular the primary vortex location seem to be unaffected by three-dimensionality. The photographs of the flow structure with various aspect ratios add much clarity to the behavior of this type of flow. For example, the development of a secondary vortex was observed to occur at aspect ratios of 1.75 and 2.0. There was large scatter in the location of the primary vortex as measured from the flow visualization photographs. This scatter is clearly seen by the error bars in Figure 9. The scatter is due to unsteadiness of the flow field, and possibly also to three-dimensionality of the flow. Nevertheless, the trend in Figure 9 is that the vortex center moves deeper into the slot as aspect ratio increases until about $AR = 2.0$, beyond which the location of the primary vortex stays fairly constant.

The pressure measurements inside the slot offer the most enlightening information of all the work described herein. The data shows distinct rings of constant pressure (isobars) that have not been measured previously. The pressure profile at aspect ratio 0.5 shows the vortex center to be very close to the traverse limits and the flow

visualization data indicates that it is much lower and out of range. The lower aspect ratios also place the vortex more downstream than the higher aspect ratio cases. The vortex size seems to scale with the slot minimum dimension, but this does not explain why the vortex moves downstream in the slot. Regarding the vertical location of the vortex center the higher aspect ratio cases (above AR = 0.5) maintain the same trend as the flow visualization location data. Both show the vortex going deeper into the slot with increasing aspect ratio. They both show the leveling off of the primary vortex vertical location at an aspect ratio of about 2.0.

The data on the vortex center pressure coefficient is more meaningful when discussed in terms of previous work. An additional plot was made which superimposes the present wind tunnel pressure coefficient data on Ward's water tunnel cavitation index data (see Figure 20). As discussed earlier, if the observed cavitation by Ward was purely vaporous then

$$\sigma \leq -C_p .$$

This implies that the local pressure is less than or equal to the vapor pressure. Figure 20 shows that an order of magnitude difference exists between the two sets of data. This was the same discrepancy commented on by Hoil and Billet based on their and Ward's cavitation index data compared against their integrated wind tunnel velocity profile data (Hoil and Billet 1986). The suggestion is that the cavitation

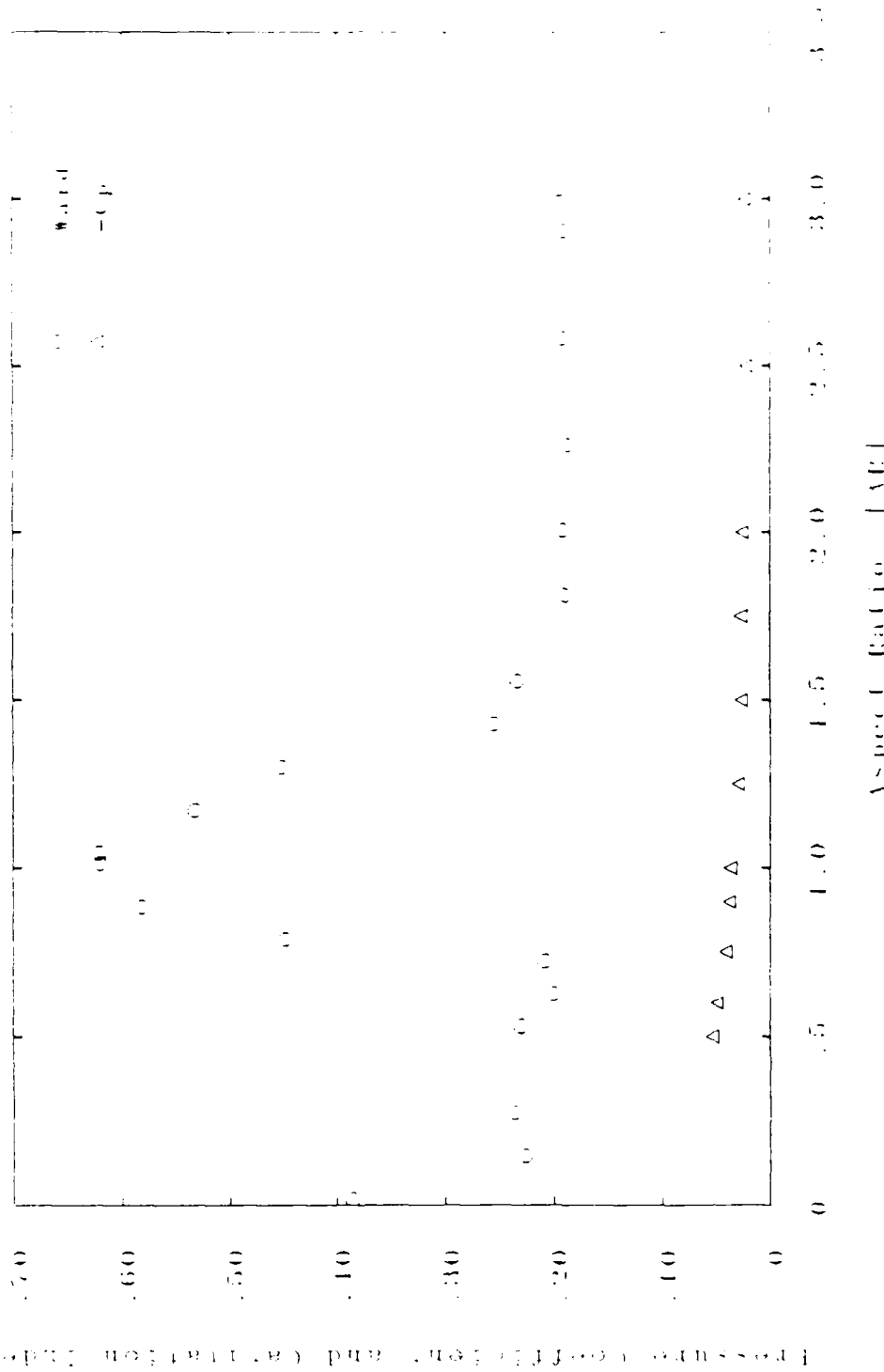


Figure 20. Pressure Coefficient Data Compared to Ward's Cavitation Index Data of 1973.

observed in the vortex center is partially gaseous; which implies that the water tunnel slot local pressure is higher than vapor pressure. The external photographs support this conclusion. Recall that these photographs showed that mass does not pass into the primary vortex despite the mass transfer into the slot through the entrance. By the same argument mass can not leave the primary vortex. Hence, if gaseous bubbles did form inside the vortex by gaseous diffusion they would be trapped. Overall the present data confirms Hoil and Billet's suggestion that the cavitation they and Ward observed was gaseous.

4.1 Summary of Conclusions

An overview of the experiments conducted for the slot fluid mechanics problem is in order. The following is a summary of the significant conclusions reported here:

1. The turbulent boundary layer at the model entrance location was 1.2 times the slot width. The profile shape was similar to Spalding's profile with a slight rightward shift due to a lack of recovery time from the roughness used to trip the boundary layer.
2. Flow visualization showed no change in the two-dimensionality of the slot fluid mechanics where the span was reduced from 38 inches (0.97 m) to 8 inches (0.20 m).

3. Flow visualization demonstrated that the slot vortex location changes with aspect ratio, and showed the formation of a second vortex for aspect ratios of 2.0 and larger.
4. Mass transfer was seen to occur across the slot entrance; however, this mass transfer did not extend into the primary vortex center.
5. Direct pressure measurement showed vortex location to be a function of aspect ratio, similar to the behavior shown by flow visualization.
6. Vortex strength, based on direct pressure measurement, is shown to increase with decreasing aspect ratio. This and the magnitude of the pressure coefficient inside the vortex lead to the conclusion that in previously documented water tunnel experiments, the observed slot cavitation was actually gaseous rather than purely vaporous.
7. Flow visualization showed that the direct pressure measurement did not alter the internal two-dimensional fluid mechanics of the slot.

BIBLIOGRAPHY

- Bennett, H.W. 1949. Flow Past a Slot in a Surface. MS Thesis. The Department of Engineering Mechanics. The Pennsylvania State University.
- Clark, R.L. and L.G. Kauffman. 1980. Aero-Acoustic Measurements for Mach 2.6 to 3.0 Flows Past Rectangular Cavities. AIAA-80-0036. AIAA 18th Aerospace Sciences Meeting.
- Clauser, Francis H. 1956. The Turbulent Boundary Layer. Advances in Applied Mechanics. vol. IV, pp. 1-51.
- Corke, T., D., KOGA, R. Drubka, and H. Nagib. 1977. A New Technique for Introducing Controlled Sheets of Streaklines in Wind Tunnels. IEEE Publication 77-CH. 1251-8 AES.
- Hiwada, M., I. Mabuchi and K. Masaya. 1985. Three Dimensional Flow and Heat Transfer in a Rectangular Cavity. Japanese Research. vol. 14, no. 1: 75-96.
- Holl, J.W. and M.L. Billet. 1986. Limited Cavitation on Isolated Surface Irregularities - Unsolved Problems. Paper Presented at the International Symposium on Cavitation. Sendai, Japan, 16-19, April 1986.
- Kays, William M. and Michael E. Crawford. 1980. Convective Heat and Mass Transfer. 2nd ed. New York: McGraw-Hill Book Company.
- Maull, D.L. and L.F. East. 1963. Three-Dimensional Flow in Cavities. The Journal of Fluid Mechanics. vol. 16, no. 4: 620.
- Metra Byte Corporation. 1986. For-16 Manual. Tauton, MA.
- Metra Byte Corporation. 1986. Dash-16/16F Manual. Tauton, MA.
- Metra Byte Corporation. 1986. Data Acquisition, Industrial Control, and Communications Interfaces for IBM PC/XT/ATs, Compatibles, Apple II's and VME Based Systems. Tauton, MA.
- MKS Instruments, Inc. 1985. Instruction Manual - Type 398/598 Differential High Accuracy Pressure Transducers. Manual 195-109 700-A-3/85. Burlington, MA.

MKS Instruments, Inc. 1984. Instruction Manual - Type 270B High Accuracy Electronic Display Unit. Manual 195-103299-A-9.84. Burlington, MA.

Rockwell, Donald and Charles Knisely. 1979. Unsteady Features of Flow Past a Cavity. Journal of the Hydraulics Division Proceedings of the American Society of Civil Engineers. vol. 105, no. HY8: 869-973.

Rosko, A. 1955. Some Measurements of Flow in a Rectangular Cutout. NACATN 3488. Washington, D.C.: National Advisory Committee for Aeronautics.

Sathianathan, Dhushy. 1986. Constant Temperature Hot-wire Anemometer & Signal Conditioner. Paper in Mechanical Engineering. The Pennsylvania State University.

Sathianathan, Dhushy. 1985. Dual Sequence Controller. MS Thesis. Department of Mechanical Engineering, The Pennsylvania State University.

Sarohia, Virendra. 1977. Experimental Investigation of Oscillations in Flows Over Shallow Cavities. AIAA Journal. vol. 15, no. 7: 984-991.

Ward, T.M. 1973. Slot Cavitation. 1973 Cavitation and Polyphase Flow Forum. p. 24. New York: The American Society of Mechanical Engineers.

White, Frank M. 1974. Viscous Fluid Flow. New York: McGraw-Hill Book Company.

Appendix A: INTERNAL PHOTOGRAPHS

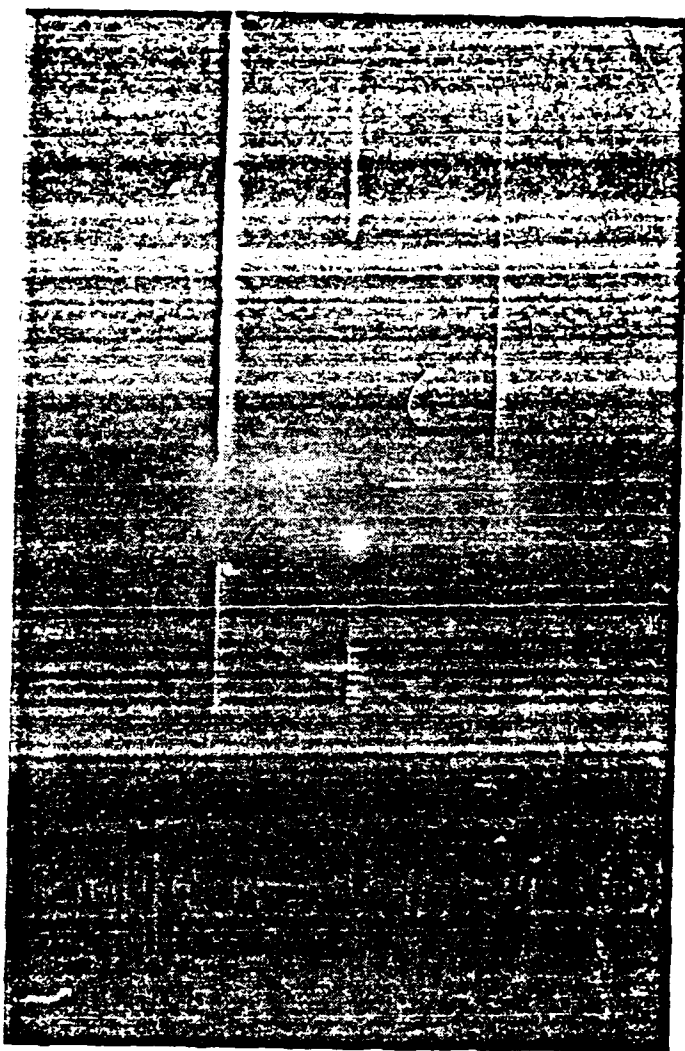


Figure A-1. Cavity Flow Visualization at $AR = 0.5$



Figure A-2. Cavity Flow Visualization at $AR = 0.75$



Figure A-3. Cavity Flow Visualization at AR = 1.0

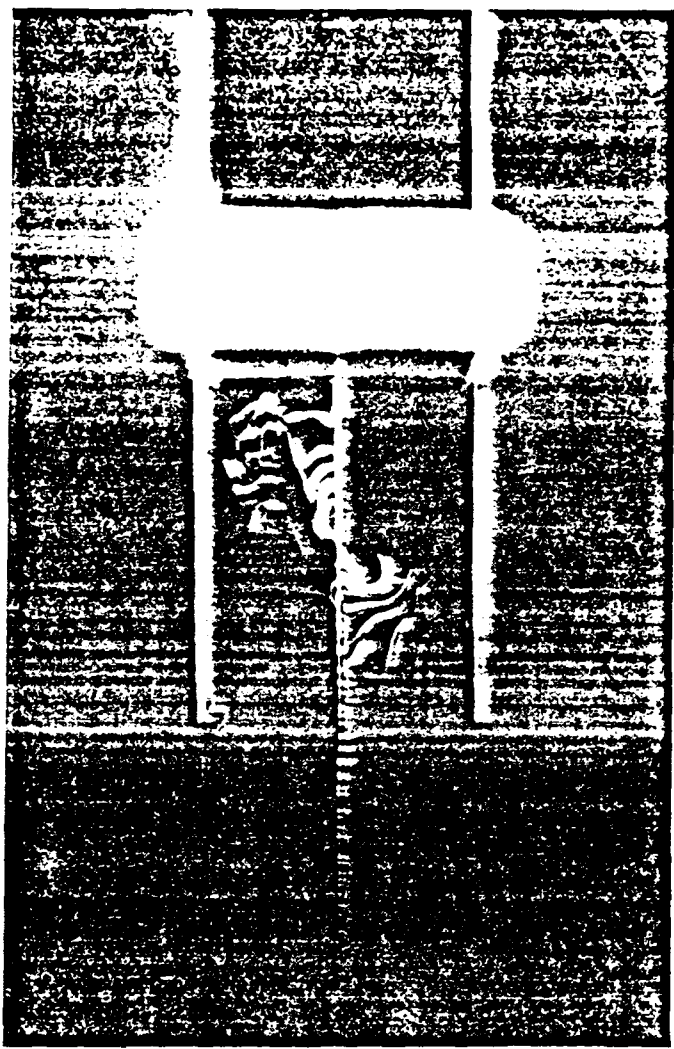


Figure A-4. Cavity Flow Visualization at $AR = 1.25$



Figure A-5. Cavity Flow Visualization at AR = 1.5

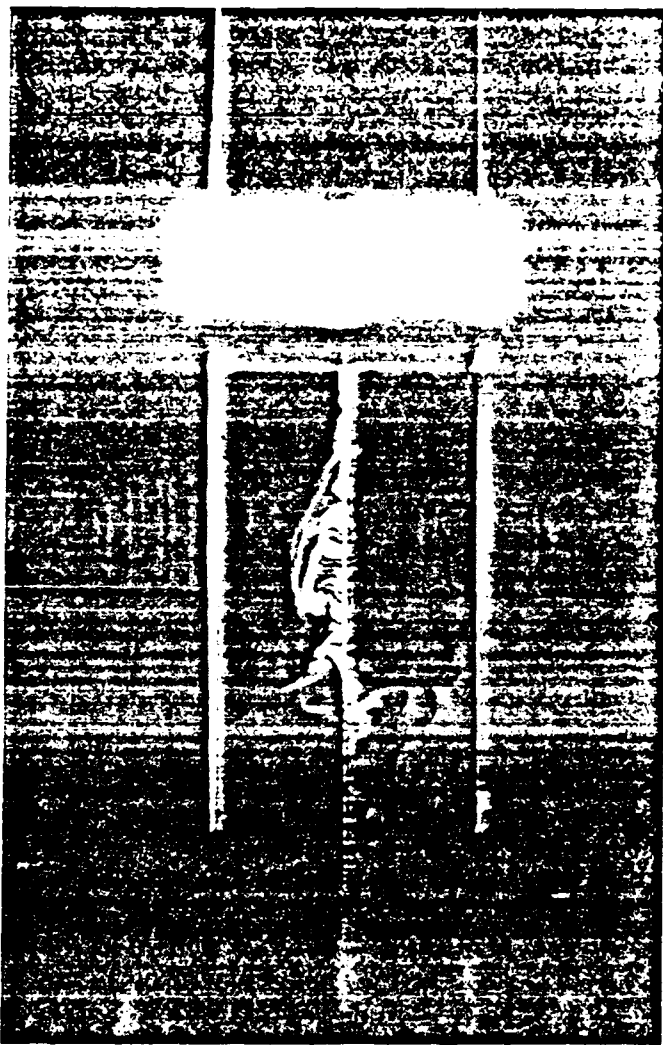


Figure A-6. Cavity Flow Visualization at AR = 1.75



Figure A-7. Cavity Flow Visualization at AR = 2.0



Figure A-8. Cavity Flow Visualization at AR = 2.5

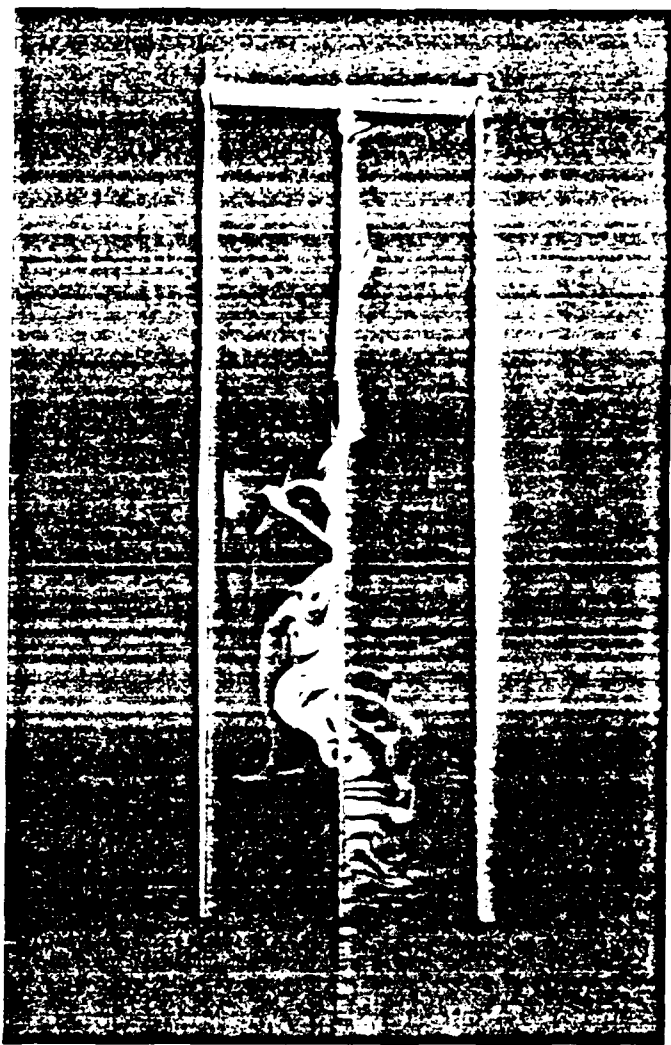


Figure A-9. Cavity Flow Visualization at AR = 3.0

Appendix B: EXTERNAL PHOTOGRAPHS



Figure B-1. External Visualization at $AR = 1.0$ (Smcke)

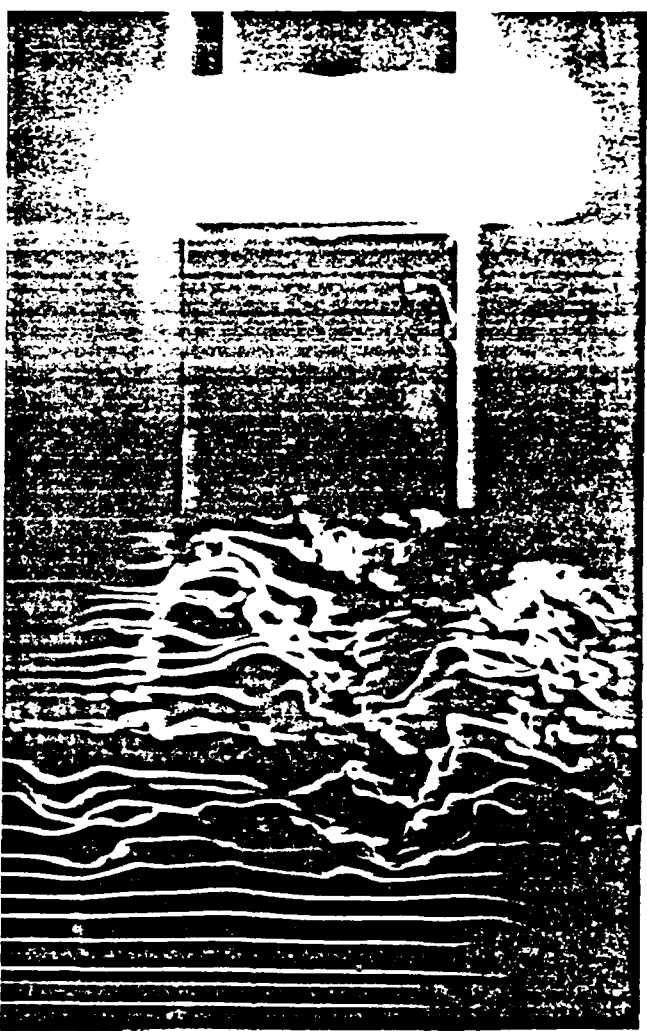


Figure B-2. External Visualization at AR = 1.0 (No Smoke)

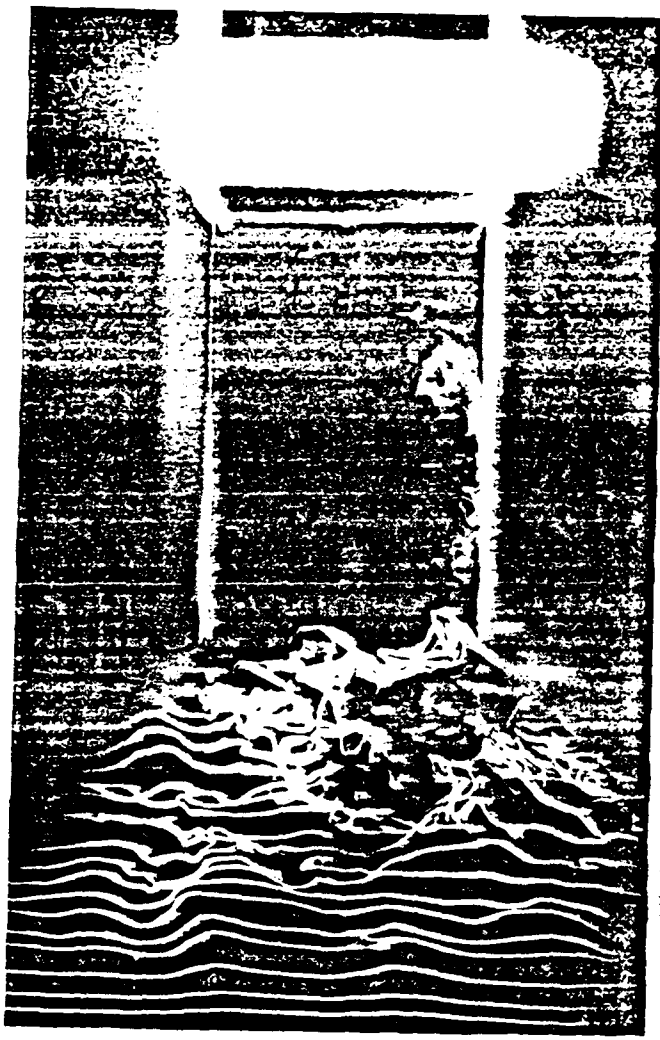


Figure B-3. External Visualization at AR = 1.5 (Smoke)



Figure B-4. External Visualization at AR = 1.5 (No Smoke)

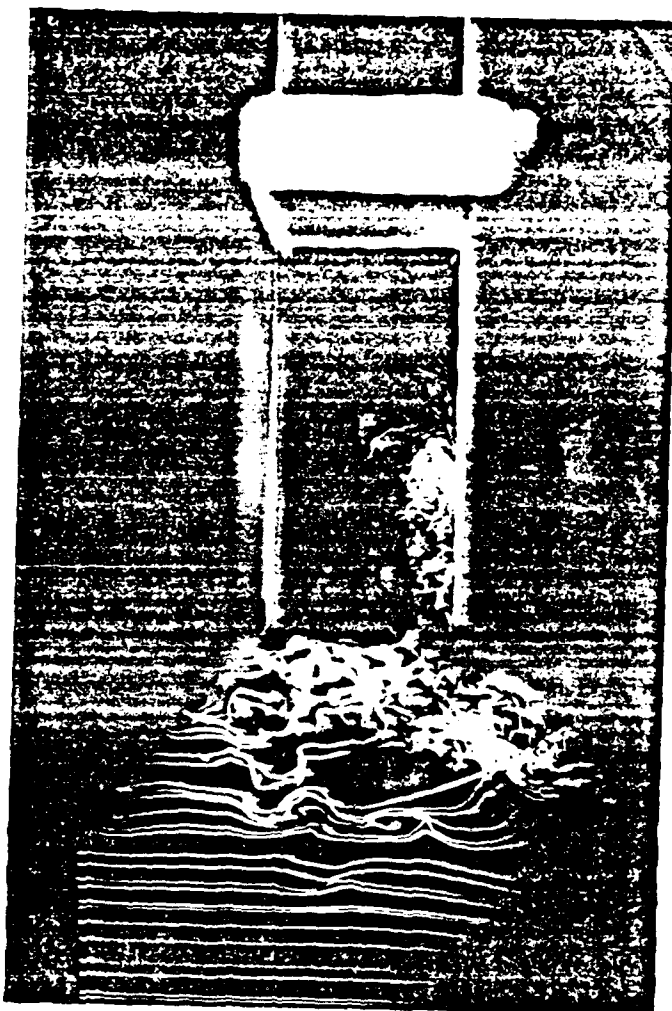


Figure B-5. External Visualization at AR = 2.0 (Smoke)

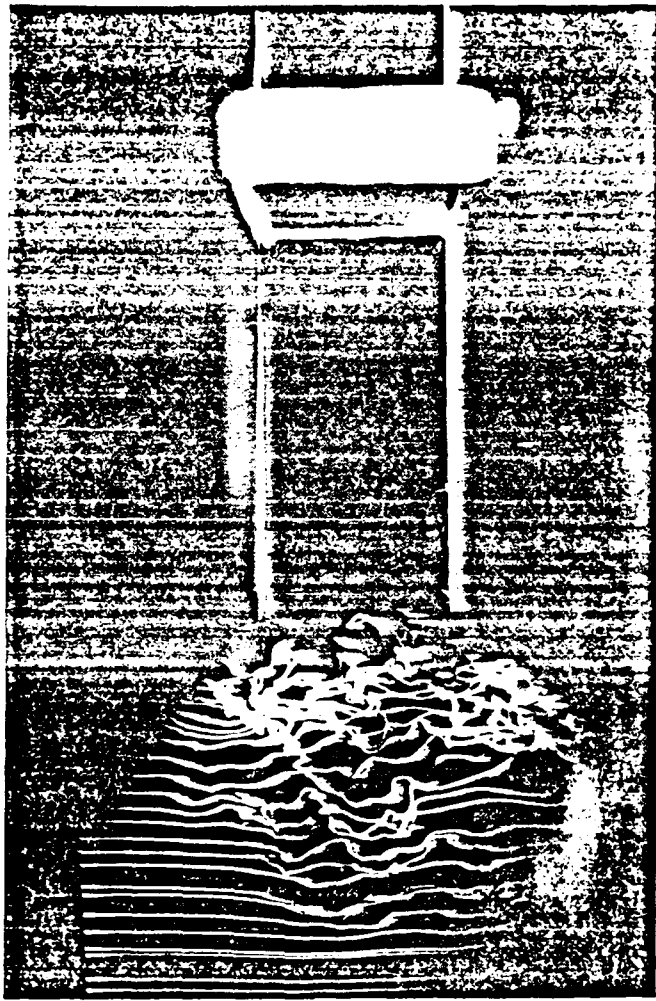


Figure B-6. External Visualization at AR = 2.0 (No Smoke)



Figure B-7. External Visualization at $AR = 3.0$ (Smoke)

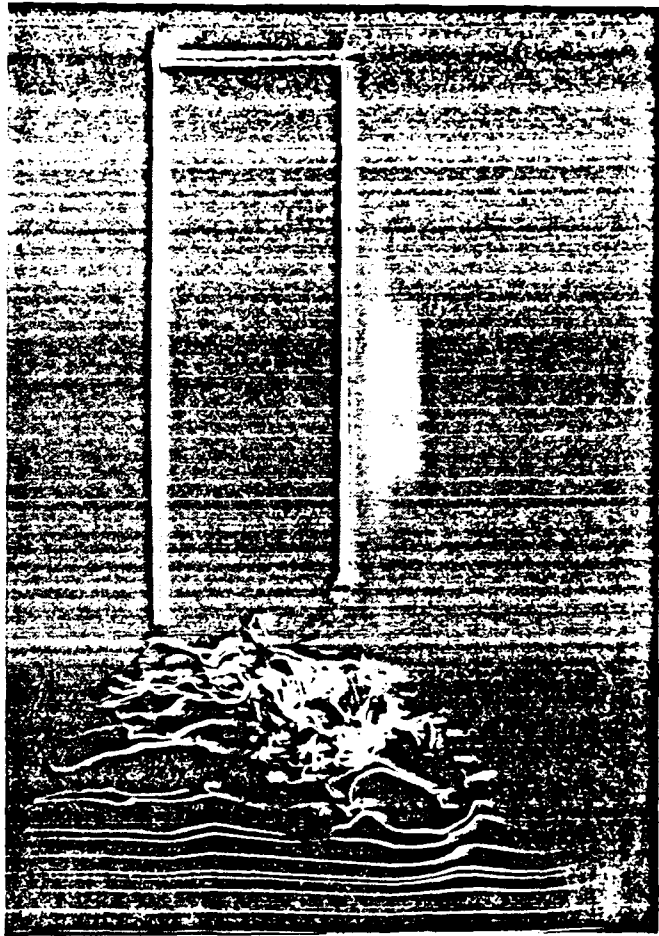


Figure B-8. External Visualization at AR = 3.0 (No Smoke)

Appendix C: PRESSURE COEFFICIENT PROFILES

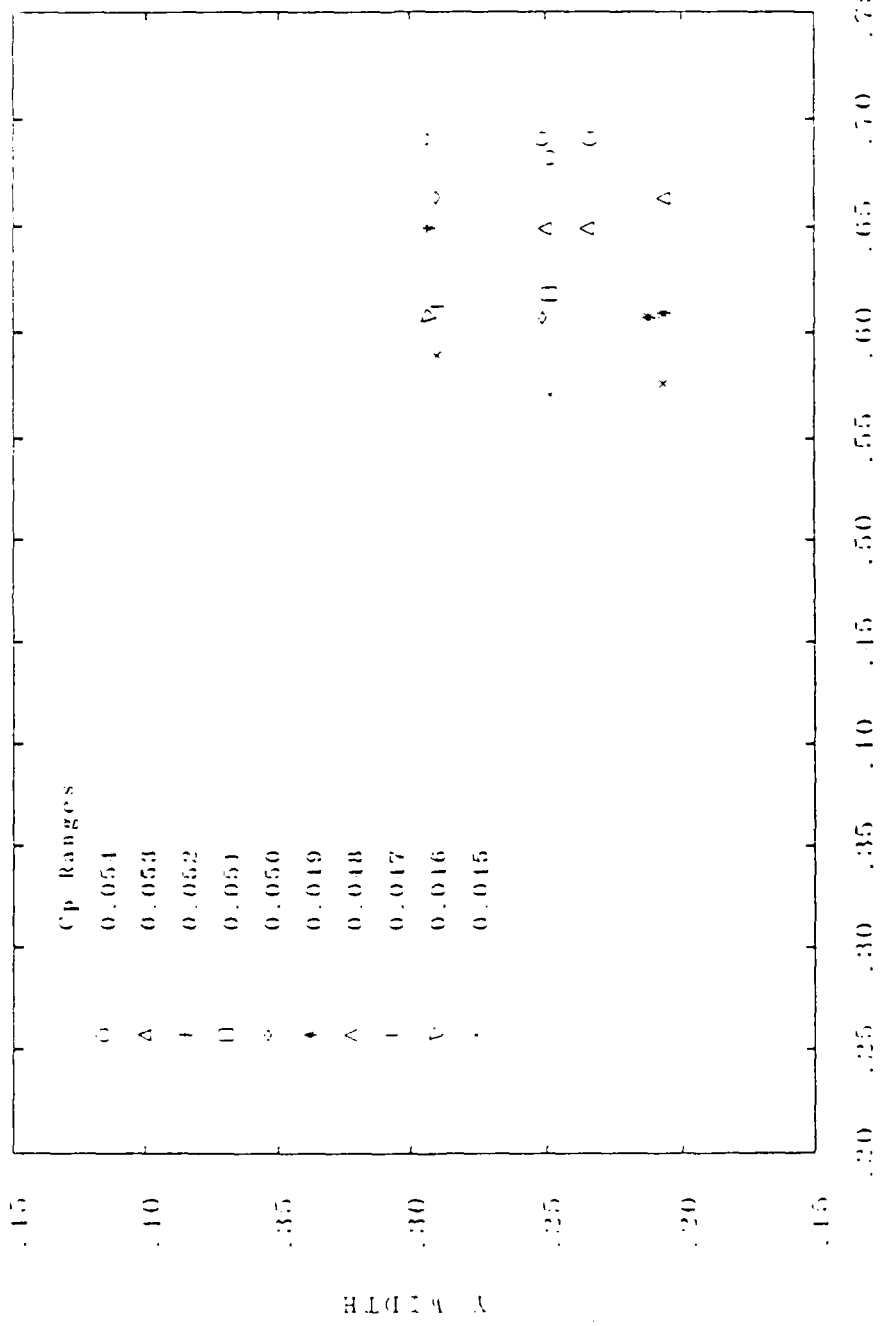


Figure C-1. Pressure Coefficient Profile AR = 0.5

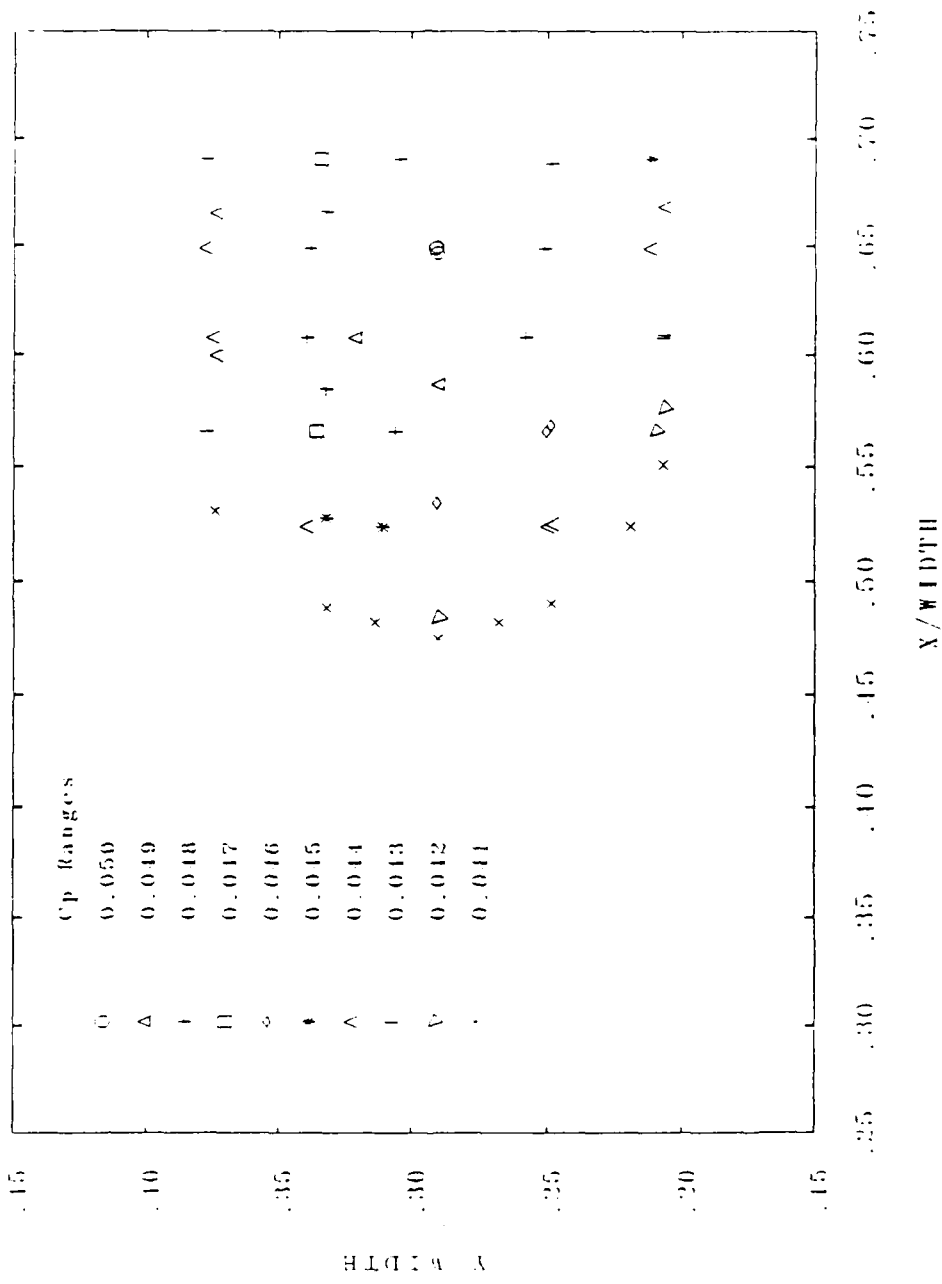


Figure C-2. Pressure Coefficient Profile AR = 0.6

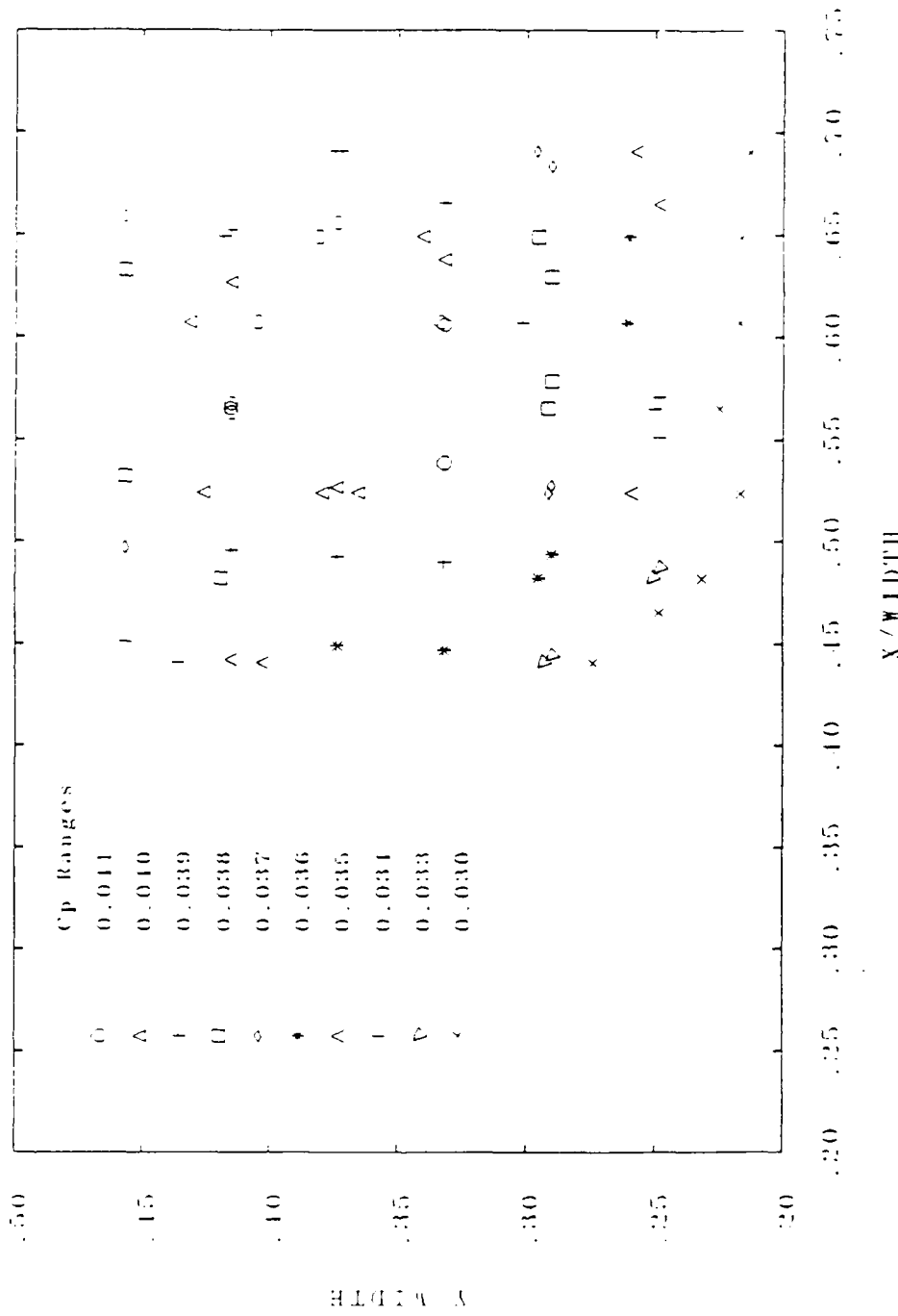


Figure C-3. Pressure Coefficient Profile AR = 0.75

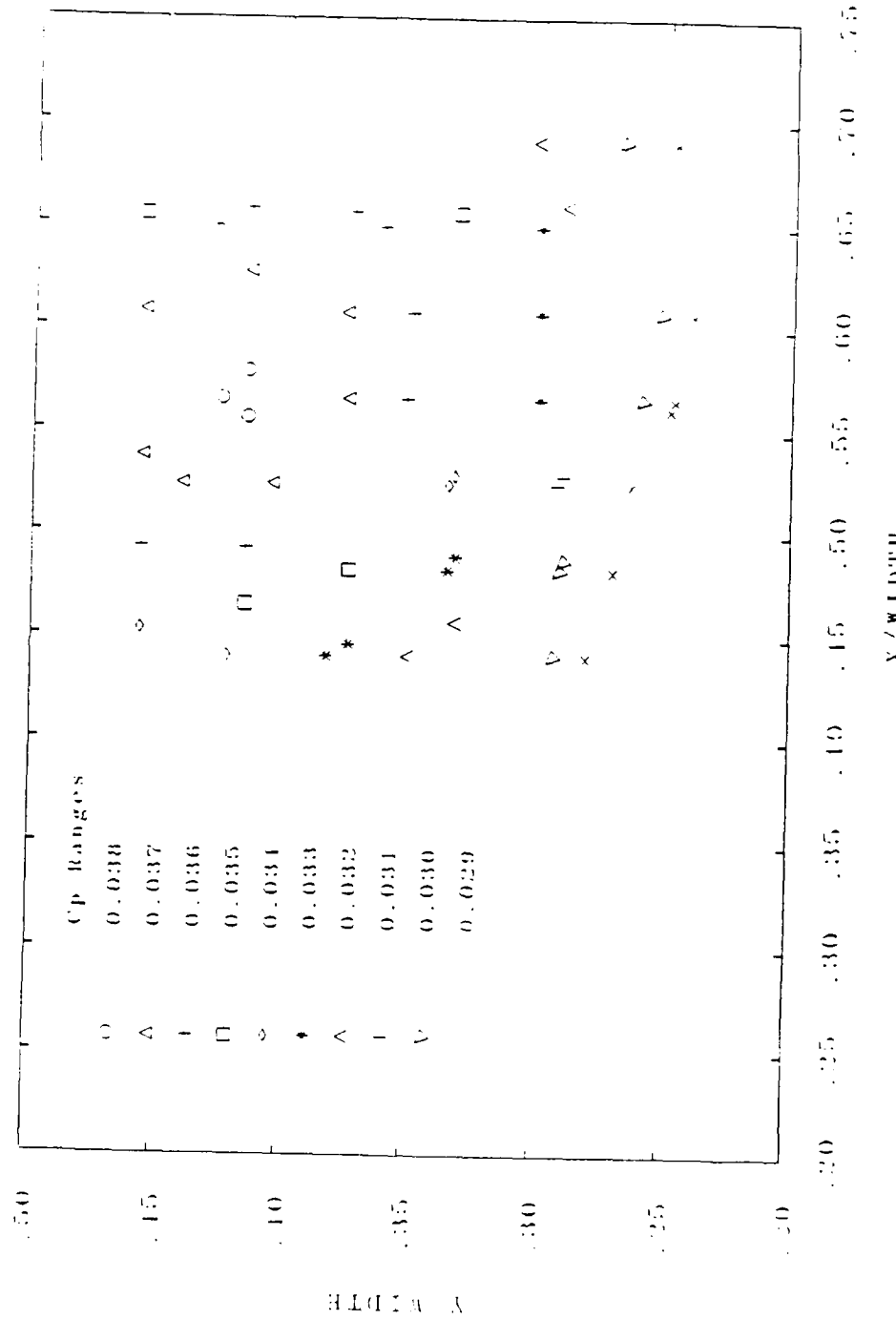


Figure C-4. Pressure Coefficient Profile $\Delta R = 0.9$

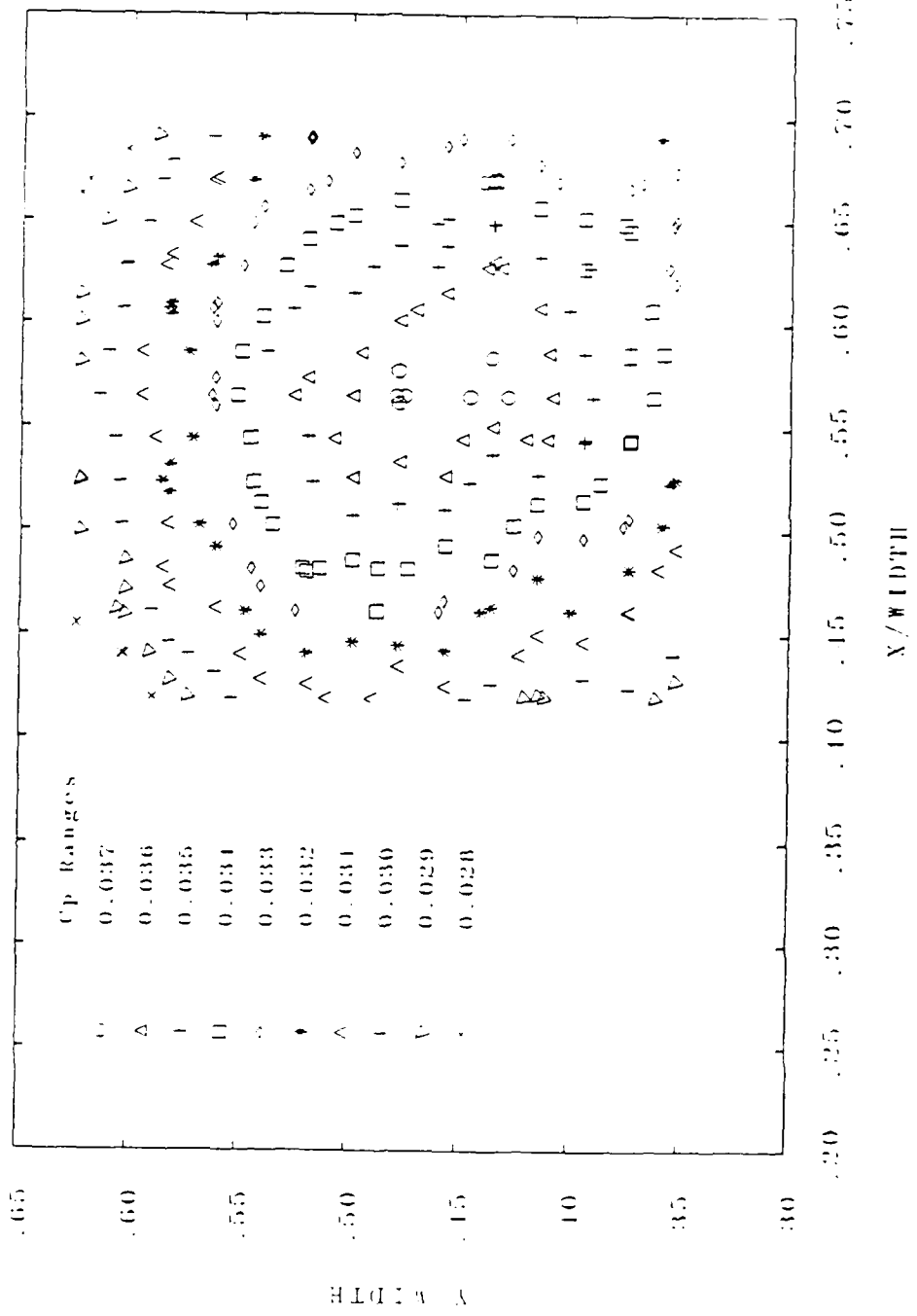


Figure C-5. Pressure Coefficient Profile AR = 1.0

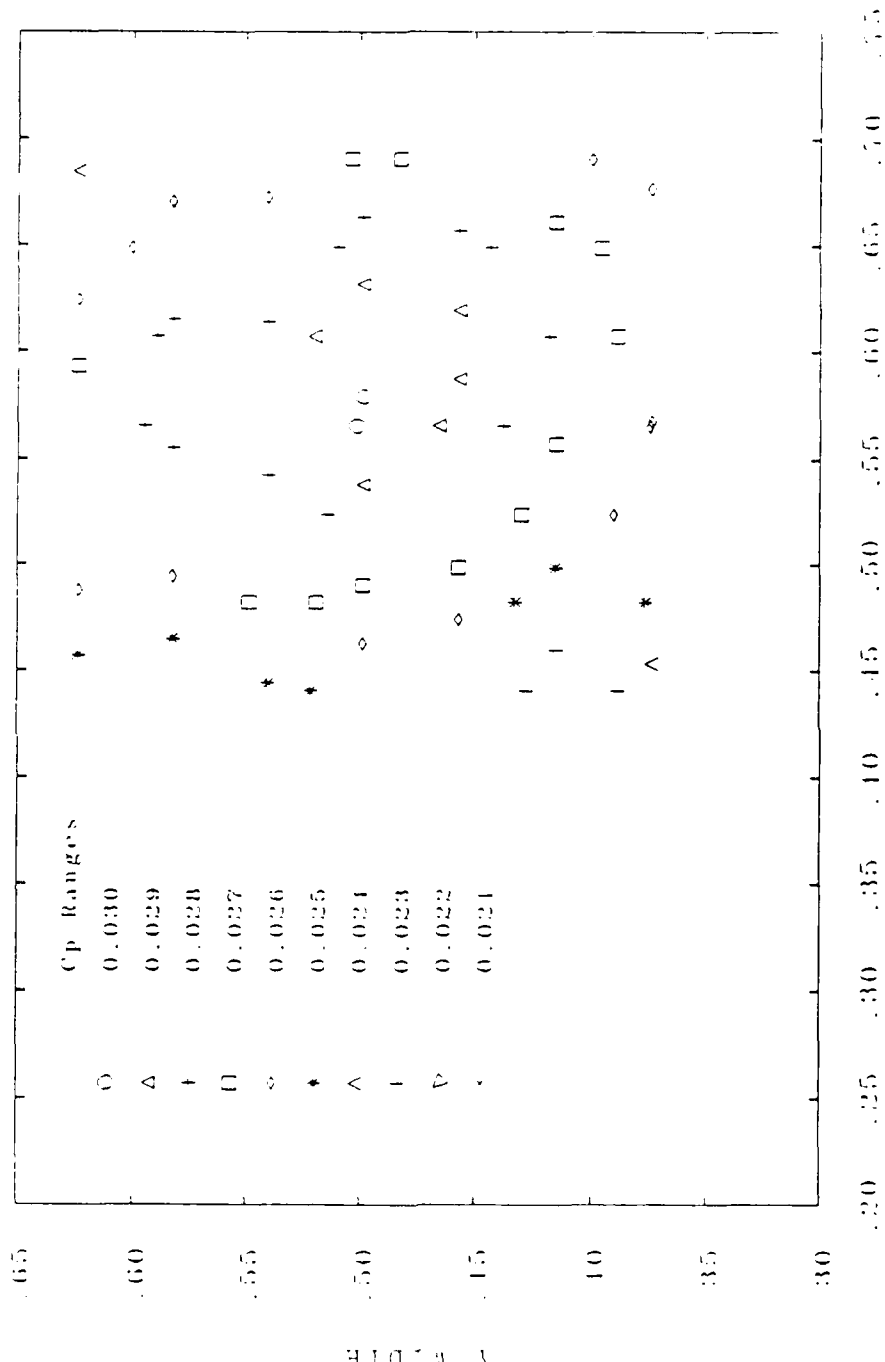


Figure C-6. Pressure Coefficient Profile $AR = 1.25$

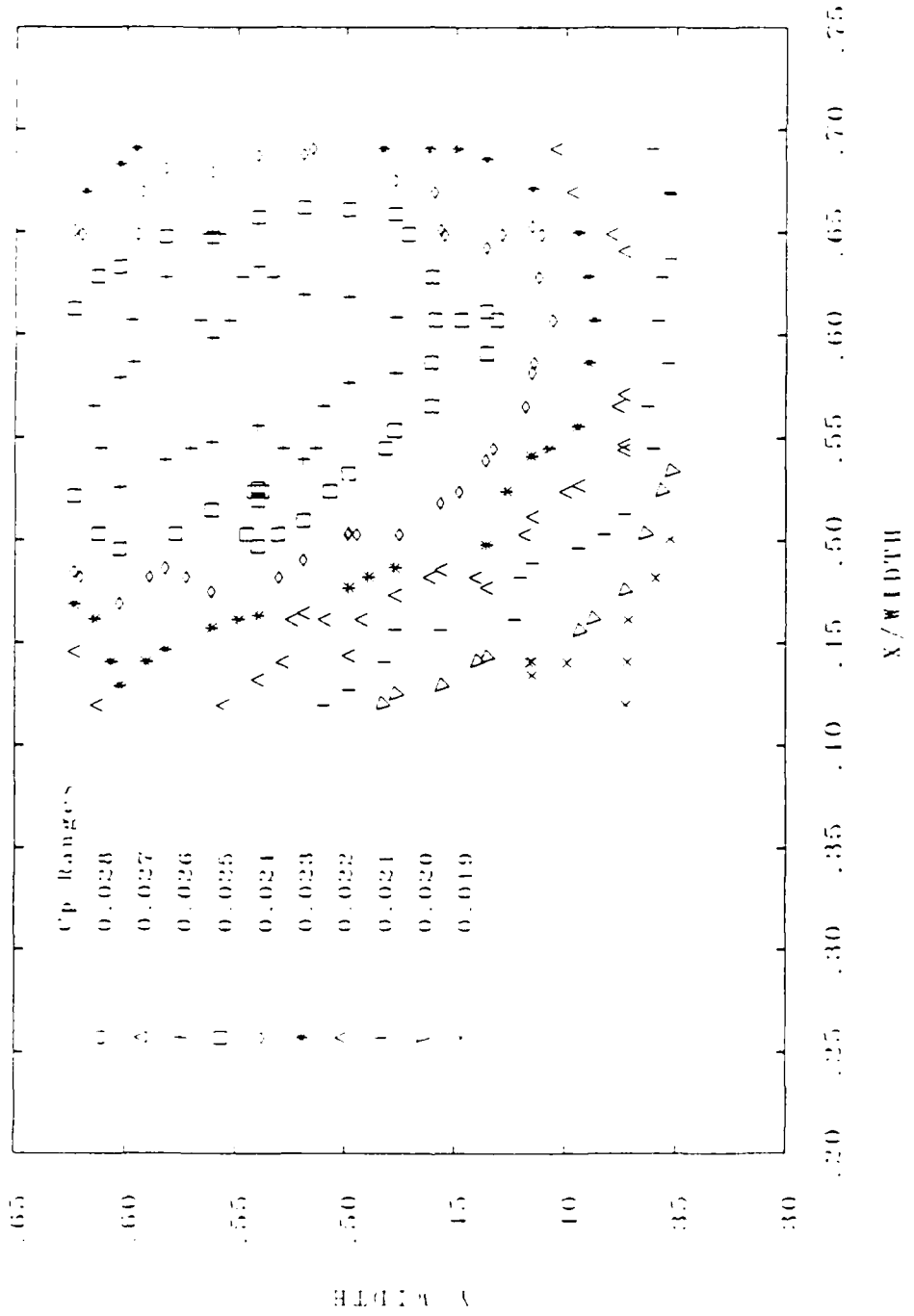


Figure C-7. Pressure Coefficient Profile AR = 1.5

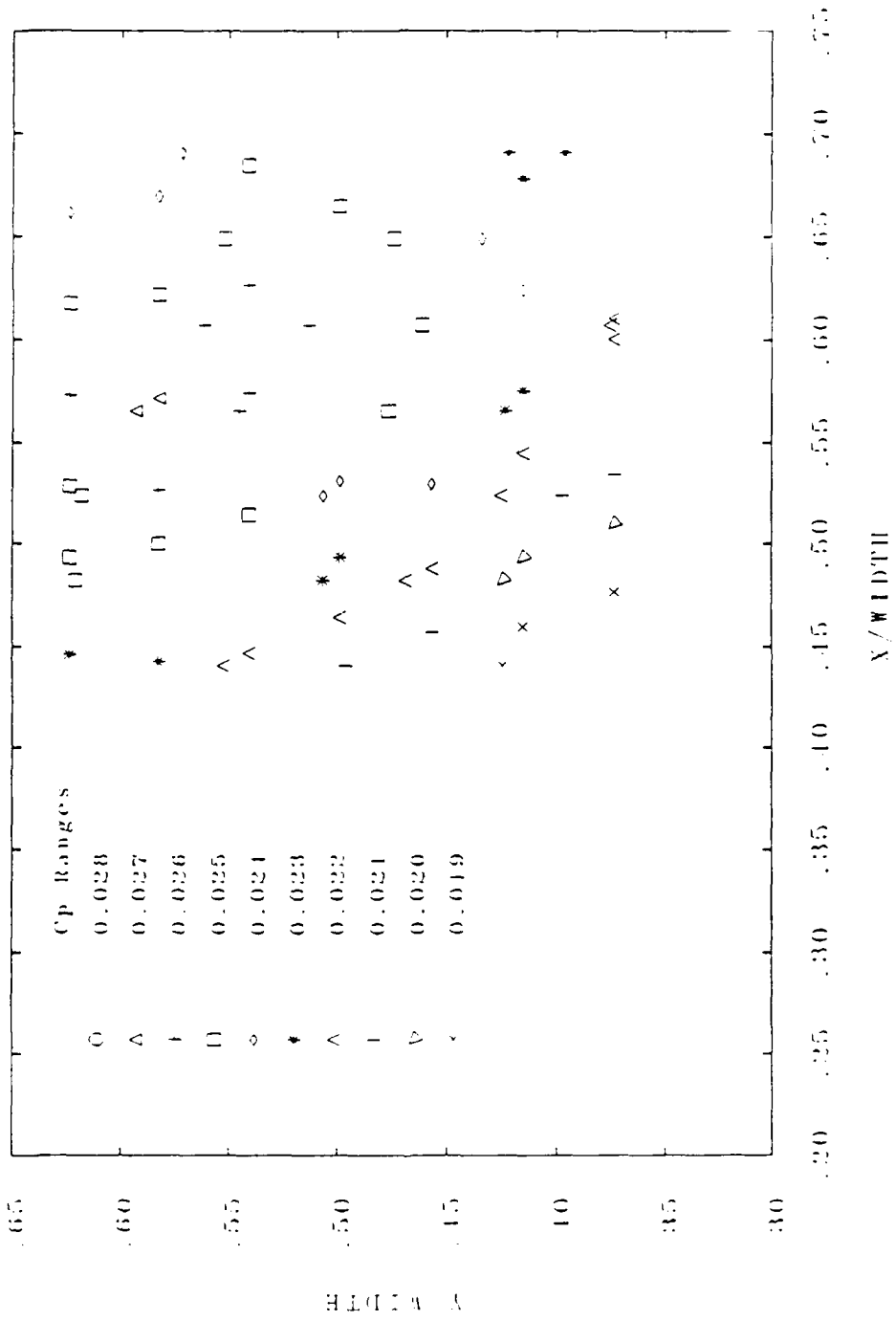


Figure C-8. Pressure Coefficient Profile AR = 1.75

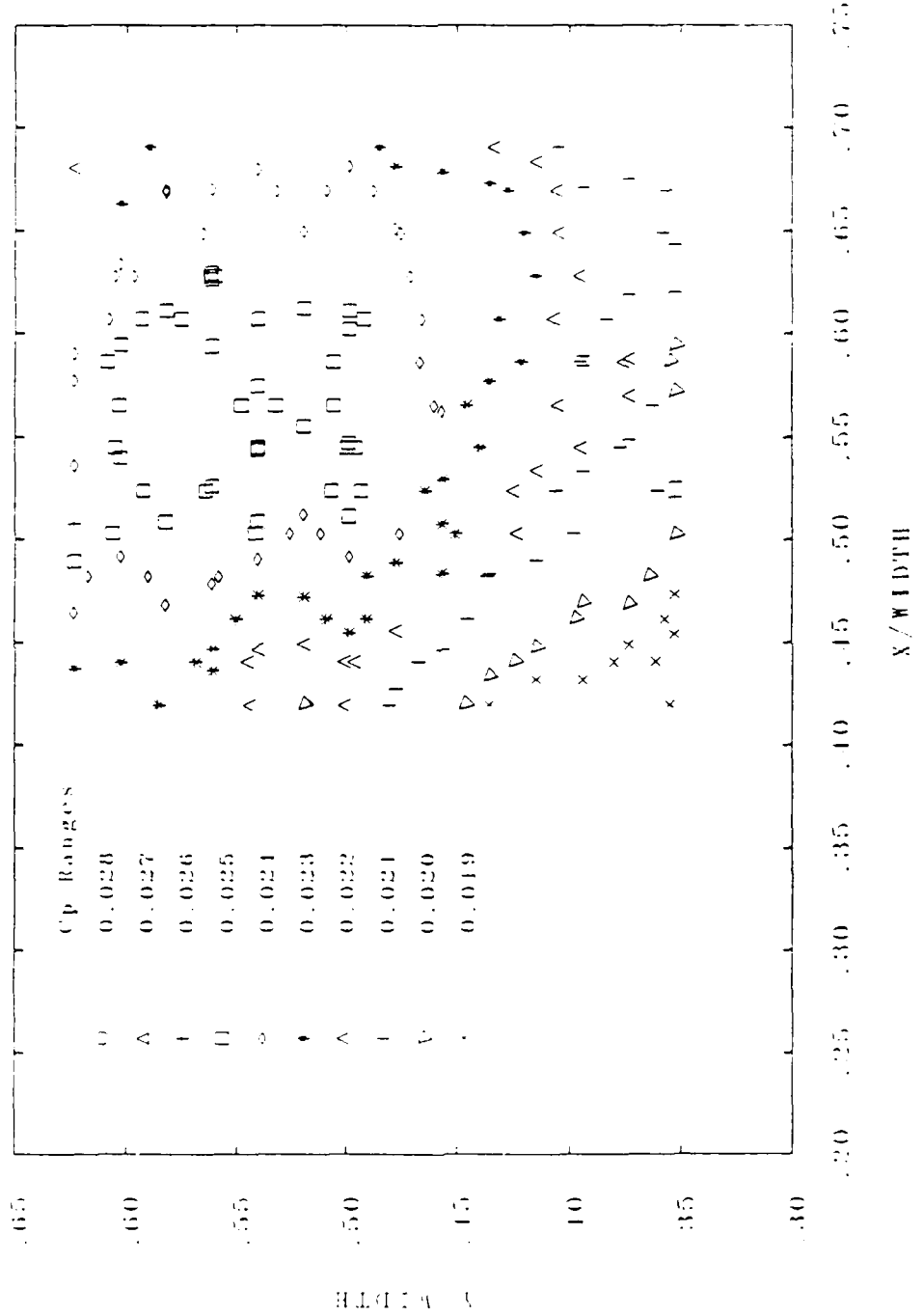


Figure C-9. Pressure Coefficient Profile $AR = 2.0$

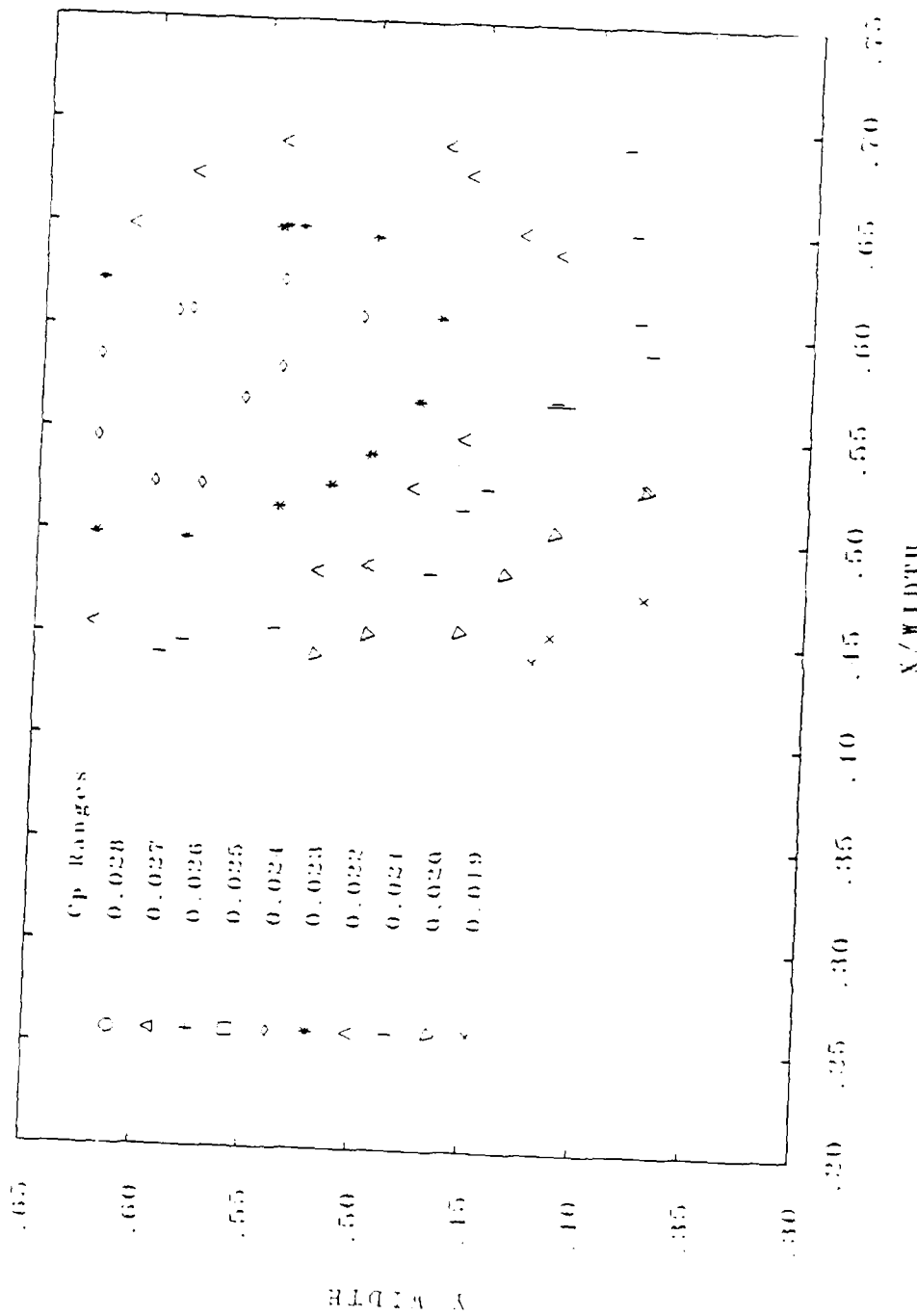


Figure C-10. Pressure Coefficient Profile $AR = 2.5$

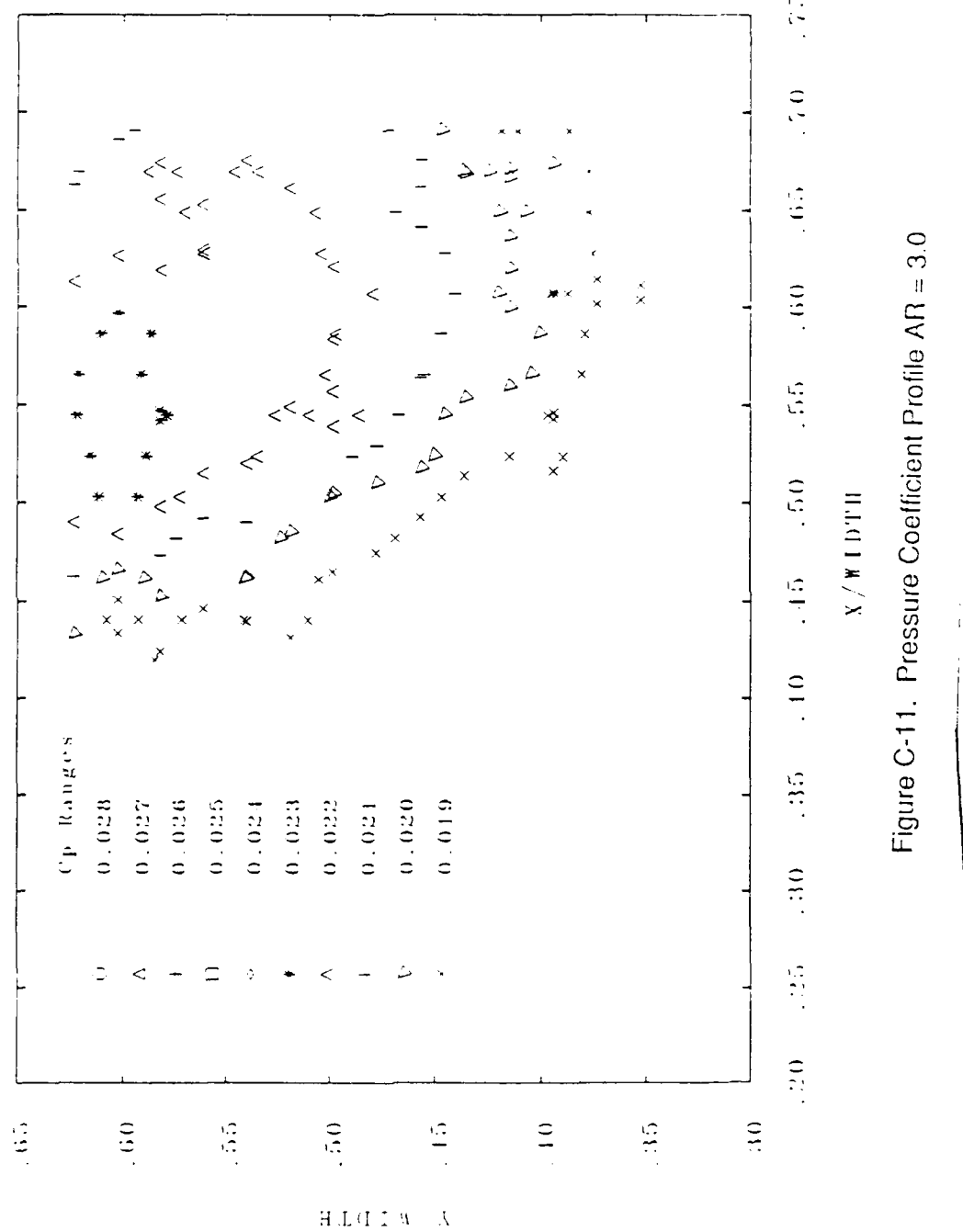


Figure C-11. Pressure Coefficient Profile AR = 3.0

RD-R190 677

CAVITATION INCEPTION IN RECTANGULAR TWO-DIMENSIONAL
SLOTS(U) PENNSYLVANIA STATE UNIV UNIVERSITY PARK
APPLIED RESEARCH LAB W G BLAIR ET AL. DEC 87

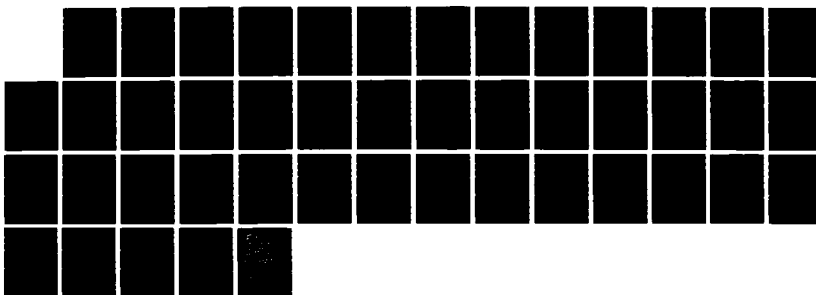
2/2

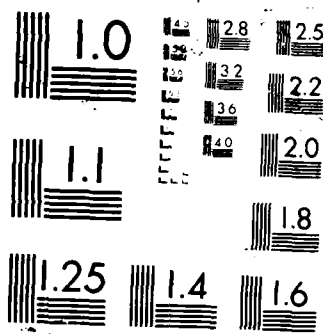
UNCLASSIFIED

ARL/PSU/TR-87-013 N00024-85-C-6041

F/G 28/4

NL





Appendix D: PROGRAMS

PROGRAM PROFILE

C

C

C

BILL BLAIR and MARK KREIN

C

C

NOVEMBER 1986

C

C

C PURPOSE: TO DETERMINE THE VELOCITY PROFILE ACROSS A
C BOUNDARY LAYER AND TO TAKE CALIBRATION DATA IN
C ORDER TO DETERMINE THE RELATIONSHIP OF VOLTAGE
C VS VELOCITY FROM THE HOT WIRE ANEMOMETRY SIGNAL.

C

C

C FUNCTION: The following program performs several tasks
C including:

C

C

- Recording the dynamic head of the wind tunnel
for velocity calculations.
- Recording the voltage signal from the hot wire
circuit.
- Controls the traverse that the hot wire is
mounted on.

C

C

C FORTRAN: The following program was written for use in
C Microsoft Fortran version 3.2.

C

C

C EQUIPMENT: The following equipment and software was used
C in the operation of this program:

C

C

- Metrabyte DASH-16 analog/digital I/O
expansion board
- Metrabyte 24 bit parallel port
- Metrabyte DASH-16 Fortran Library
- MKS high accuracy pressure transducer model
398HD
- MKS signal conditioner type 270B
- Hot wire and bridge circuit
- PSU Mech. Eng. Wind Tunnel
X-Y traverse system

C

C

C OPERATION: The following steps are needed prior to run-
C ning this program:

C

C

C The DASH-16 should be configured as follows:

C

C

- 8 channel differential input
(WARNING note the definition of
Metrabyte 'differential input'.)
- unipolar | This offers a 0-5 volt |
- gain set at 2 | range of measurement. |
- DMA level of 3
- base address set at 768

C

The MKS Signal Conditioner should be set up as follows:

- sensor range set at 1 torr
 - zero the unit according to manual
 - initially set range select at X1

The final set up requirement of the equipment is to have the pressure and hot wire signals placed consecutively in that order on the A/D board. This is for later convenience and is part of the lab procedure.

Following the completion of the above items and noting that the wind tunnel is ready for a test this program can be implemented.

Just prior to running PROFILE the inlet temperatures of the wind tunnel and the atmospheric pressure should be noted for later reference. These will be needed for later calculation of the wind tunnel velocity. This is the time to place the hot wire probe where you want to start the boundary layer measurement. It is easier to place this origin closest to the surface the boundary layer is on and then step away into the freestream. The coordinates of the pitot probe relative to this origin are also required. PROFILE will place the hot wire at that location for the calibration runs.

Now run PROFILE. Extra care should be used when typing in the step size and limit of the measured boundary layer profile. For example when traveling downward in a boundary layer both the y step size and the y limit should be negative or else the program will crash. Care should also be taken so that the computer will not run the hot wire into any thing solid. Finally the user must record the y step size for later use since this is not done by computer.

```

      IMPLICIT INTEGER*2 (A-V)
      REAL FREQ, DX, DY, SPEED
      DIMENSION CALDAT(4,1000), DATA(4,5000)
      CHARACTER*8 CALONE, CALTWO, DATSTOR, DATE, TIME
C
      WRITE(*,'(A)') '*****CALIBRATION INFORMATION*****'
      *****'
      WRITE(*,'(A\')') ' ENTER THE FIRST CALIBRATION FILE NAM
E: '

```

```
      READ(*, '(A)') CALONE
      WRITE(*, '(A\')') ' ENTER THE SECOND CALIBRATION FILE NA
ME: '
      READ(*, '(A)') CALTWO
      WRITE(*, '(A\')') ' ENTER CALIBRATION SAMPLING RATE/CHAN
. IN HZ: '
      READ(*, *) SPEED
      WRITE(*, '(A)') ' ENTER THE FIRST CHANNEL TO BE SCANNED
DURING'
      WRITE(*, '(A\')') ' CALIBRATION: '
      READ(*, *) STRTCAL
      WRITE(*, '(A)') ' ENTER THE LAST CHANNEL TO BE SCANNED
DURING'
      WRITE(*, '(A\')') ' CALIBRATION: '
      READ(*, *) FINCAL
      WRITE(*, '(A\')') ' ENTER THE X CALIBRATION POSITION: '
      READ(*, *) XCAL
      WRITE(*, '(A\')') ' ENTER THE Y CALIBRATION POSITION: '
      READ(*, *) YCAL
      WRITE(*, '(A\')') ' ENTER THE NUMBER OF CALIBRATION SETS
:
      READ(*, *) CALSETS
      XOLD=0.0
      YOLD=0.0
C
C
      WRITE(*, '(A)') '*****SAMPLING INFORMATION*****'
*****'
      WRITE(*, '(A\')') ' ENTER THE DATA FILE NAME: '
      READ(*, '(A)') DATSTOR
      WRITE(*, '(A\')') ' ENTER DATA SAMPLING RATE/CHAN. IN HZ
:
      READ(*, *) FREQ
      WRITE(*, '(A)') ' ENTER THE FIRST CHANNEL TO BE SCANNED
DURING'
      WRITE(*, '(A\')') ' SAMPLING: '
      READ(*, *) SCH
      WRITE(*, '(A)') ' ENTER THE LAST CHANNEL TO BE SCANNED
DURING'
      WRITE(*, '(A\')') ' SAMPLING: '
      READ(*, *) FCH
      WRITE(*, '(A\')') ' ENTER THE Y DIRECTION STEP SIZE: '
      READ(*, *) DY
      WRITE(*, '(A\')') ' ENTER THE MAXIMUM Y VALUE: '
      READ(*, *) YLIM
      WRITE(*, '(A\')') ' ENTER NUMBER OF SAMPLES TAKEN PER PO
SITION: '
      READ(*, *) NCS
C
C CALCULATE THE NUMBER OF CONSECUTIVE CHANNELS TO BE SCANNED
C FOR THE CALIBRATION AND THE SAMPLE ROUNTINES
C
      NUMCAL=NOCHAN(STRTCAL, FINCAL)
      NUMDAT=NOCHAN(SCH, FCH)
```

```
C
C THE FIRST CALIBRATION
C
C     CALL CALIBRATE (XCAL, YCAL, CALSETS, SPEED, CALONE, STRTCAL
,FINCAL,
>     NUMCAL, CALDAT, XOLD, YOLD)
C
C THE BOUNDARY LAYER MEASUREMENT SUBROUTINE
C
C     CALL SAMPLE (SCH, FCH, NOS, FREQ, DY, DATSTOR, NUMDAT, YLIM, D
ATA,
>     XOLD, YOLD)
C
C THE SECOND CALIBRATION
C
C     CALL CALIBRATE (XCAL, YCAL, CALSETS, SPEED, CALTWO, STRTCAL
,FINCAL,
>     NUMCAL, CALDAT, XOLD, YOLD)
STOP
END

C
C
C
C     INTEGER*2 FUNCTION NOCHAN(START, FINISH)
C
C PURPOSE: TO CALCULATE THE NUMBER OF CONSECUTIVE CHANNELS
C           BETWEEN THE STARTING AND FINISHING CHANNELS
C
C     IMPLICIT INTEGER*2(A-V)
IF (START.LT.FINISH) THEN
    NOCHAN=(FINISH-START)+1
ELSEIF (START.GT.FINISH) THEN
    NOCHAN=(8-(START-FINISH))+1
ELSE
    NOCHAN=1
END IF
RETURN
END

C
C
C
C     SUBROUTINE CALIBRATE(XCAL, YCAL, CALSETS, SPEED, CALSTOR, S
TRTCAL,
>     FINCAL, NUMCHN, CALDAT, XOLD, YOLD)
IMPLICIT INTEGER*2 (A-V)
REAL SPEED, DISPLAY
DIMENSION CALDAT(NUMCHN, 1000)
CHARACTER*8 CALSTOR, RESPON
WRITE(*, '(//, /, A)' )  ' ****
***,
****'
WRITE(*, '(A)' )        ' * BEGINNING CALIBRATION PROCEDUR
E *
****'
WRITE(*, '(A, /, /)' )  ' ****
***,
```



```

CHAN=CHAN+1
ELSE
CHAN=0
ENDIF
90      CONTINUE
100    CONTINUE
CLOSE(10)
C
C FINISHED CALIBRATION AND NOW RETURN THE HOT WIRE TO THE
C BOUNDARY LAYER ORIGIN.
C
XOLD=XCAL
YOLD=YCAL
XNEW=0.0
YNEW=0.0
WRITE(*, '(/, /, A, /)') '*****END OF CALIBRATION***'
*****
*      WRITE(*, '(/, A)')      '***RETURNING TO ORIGIN**'
*
CALL TRAVRS (XNEW, YNEW, XOLD, YOLD)
XOLD=0.0
YOLD=0.0
RETURN
END
C
C
C
C
SUBROUTINE SAMPLE (SCH, FCH, NUMPAS, FREQ, DY, DATSTOR, NUM
CHN, YLIM,
    > DATA, XOLD, YOLD)
    IMPLICIT INTEGER*2 (A-V)
    REAL FREQ, DX, DY, DISPLAY
    DIMENSION DATA(NUMCHN, NUMPAS)
    CHARACTER*8 DATSTOR
    DX=0.0
C
C RESET THE A/D BOARD TO THE SAMPLING FREQUENCY
C
    CALL TRIGGER(FREQ, NUMCHN)
    MODE=3+16
    RTNFLG=0
C
C OPEN THE SAMPLING FILE
C
    REC=NUMCHN*2*NUMPAS
    OPEN(11, FILE=DATSTOR, ACCESS='DIRECT', STATUS='NEW', R
ECL=REC)
C
C CALCULATE THE NUMBER OF POINTS TAKEN IN THE BOUNDARY
C LAYER. THE VALUE OF 0.1 IN THE NEXT LINE ALLEVIATES ROUND-
C OFF ERROR.
C
    ISTEPS=IFIX(YLIM/DY)+0.1)-1

```

```
      WRITE(*,'(A,A,A)') '*****  
*****'  
      WRITE(*,'(A)')      ' * DATA ACQUISITION BEGINNING A  
T ORIGIN *'  
      WRITE(*,'(A,A,A)') '*****  
*****'  
      IF (NUMCHN.GT.1) WRITE(*,*) ' //// PROGRAM CHANGE N  
EEDED ////'  
      DO 100 I=1,ISTEPS  
C     DELAY LOOP  
      DO 101 K=1,5000  
101     CONTINUE  
C  
C TAKE A/D MEASUREMENTS FOR THIS BOUNDARY LAYER POINT.  
C  
C     CALL ADCCONV(MODE,SCH,FCH,NUMPAS,DATA(1,1),RTNFLG)  
      WRITE(11,REC=I) ((DATA(J,L),J=1,NUMCHN),L=1,NUMPAS)  
C  
C DISPLAY THE FIRST DATA SAMPLE OF THIS POINT  
C  
      WRITE(*,'(/,A)') ' ***APPROXIMATE DATA VALUES**  
*,  
      CHAN=SCH  
      DO 90 K=1,NUMCHN  
      DISPLAY=(DATA(K,1)/819.0)  
      WRITE(*,80) CHAN,DISPLAY  
80      FORMAT(/,1X,'VALUE (VOLTS) AT CHANNEL ',I1,' = ',F8  
.6)  
      IF (CHAN.LT.7) THEN  
      CHAN=CHAN+1  
      ELSE  
      CHAN=0  
      ENDIF  
90      CONTINUE  
      WRITE(*,70)  
70      FORMAT(/,1X,'*****  
*****  
**',/)  
C  
C CHECK PROGRESS IN MOVING THOURGH THE BOUNDARY LAYER  
C  
      IF(I.EQ.ISTEPS) GOTO 100  
C  
C ITERATE THE TRAVERSE VALUES TO THE NEXT POINT  
C  
      XNEW=XOLD+DX  
      YNEW=YOLD+DY  
      CALL TRAVRS (XNEW, YNEW, XOLD, YOLD)  
      XOLD=XNEW  
      YOLD=YNEW  
100      CONTINUE  
      CLOSE(11)  
      RETURN  
      END  
C
```

```
C
C
C      SUBROUTINE TRIGGER(FREQ, NUM)
C
C      PURPOSE: THIS ROUTINE SETS THE A/D BOARD COUNTERS THAT
C      CONTROL THE FREQUENCY RATE THAT THE BOARD
C      SAMPLES DATA.
C
C      IMPLICIT INTEGER*2 (A-V)
C      REAL FREQ
C      THE VALUE OF 0.1 IN THE NEXT LINE ALLEVIATES ROUND-OFF
C      ERROR
      TRIG=IFIX((500000.0/(FREQ*NUM))-0.1)
      MD=3
      TWO=2
      CALL CNTM01 (MD, TWO)
      CALL CNTMC2 (MD, TRIG)
      RETURN
      END
```

PROGRAM BIDEC

WILLIAM G. BLAIR

10/17/86

PURPOSE: To convert binary files with integer*2 data and write the data to a second formated file.

FORTRAN: The following program was written for use in Microsoft Fortran version 3.2.

```

IMPLICIT INTEGER*2 (A-Z)
CHARACTER*14 BFILE,DFILE
DIMENSION DATA(4,1000)
WRITE(*, '(A\')' ) ' ENTER THE NAME OF UNFORMATED BINARY
FILE----> '
READ(*, '(A\')' ) BFILE
WRITE(*, '(A\')' ) ' ENTER THE NAME OF FORMATED DECIMAL F
ILE----> '
READ(*, '(A\')' ) DFILE
WRITE(*, '(A\')' ) ' ENTER THE NUMBER OF RECORDS IN FILES
----> '
READ(*, * ) NREC
WRITE(*, '(A\')' ) ' ENTER THE NUMBER OF CHANNELS-----
----> '
READ(*, * ) CHAN
WRITE(*, '(A\')' ) ' ENTER THE NUMBER OF POINTS PER CHANN
EL'
WRITE(*, '(A\')' ) ' (IF POINTS .GT. 1000 - ALT PROGRAM)
----> '
READ(*, * ) PNTS
LENGTH=CHAN*PNTS*2
WRITE(*, '(//,/,A\')' ) ' * * * * * * * * * * * * * * * * * * * * *
WRITE(*, '(A\')' ) ' *      THE FIRST POINT OF EACH      *'
WRITE(*, '(A\')' ) ' *      CHANNEL FROM EACH      *'
WRITE(*, '(A\')' ) ' *      RECORD      *'
WRITE(*, '(A\')' ) ' * * * * * * * * * * * * * * * * * * * * * * * '
WRITE(*, '(A\')' ) ' '
WRITE(*, 90)
OPEN(10,FILE=BFILE,ACCESS='DIRECT',STATUS='OLD',RECL=L
ENGTH)
OPEN(20,FILE=DFILE,STATUS='NEW')
DO 10 K=1,NREC
  READ(10,REC=K) ((DATA(I,J),I=1,CHAN),J=1,PNTS)
  WRITE(*,100) (DATA(I,1),I=1,CHAN)
  DO 10 J=1,PNTS
    WRITE(20,100) (DATA(I,J),I=1,CHAN)
10  CONTINUE
WRITE(*, '(A\')' ) ' ***** EOF REACHED *****'

```

```
CLOSE(10)
CLOSE(20)
90  FORMAT(1,5X,'CHANNEL 1',3X,'CHANNEL 2',3X,'CHANNEL 3',
3X,
      3 'CHANNEL 4',
100 FORMAT(4(6X,I6))
STOP
END
```

PROGRAM BLAYER

BILL BLAIR

12/4/86

C PURPOSE: To calculate the least square curve fits of the
C calibration data or produce a new file made up
C of the boundary layer profile points.

C FUNCTION: The following program performs several tasks
C including:

- Reads and averages each record of the given file. The new mean value(s) is either a calibration velocity pair or a boundary layer point.
- For calibration data the mean values of the dynamic head in the first column of the array are used to calculate the wind tunnel velocity for that point.
- For calibration data a least-squares curve fit of order 5 is performed on the velocity vs voltage data. Both the polynomial coefficients and the velocity vs voltage data are stored in a new file.
- For boundary layer data the mean hot wire voltages are mapped onto their velocity counterparts with the calibration data curves. The calibration curve used is a linearly time weighted combination of the first and second calibration sets.
- For boundary layer data the position vs velocity curve is stored in a new file.

C FORTRAN: The following program was written for use in
C Microsoft Fortran version 3.2.

C OPERATION: This program does not do all of its functions
C in one session. The calibration files need to
C be curve fit prior to processing the boundary
C layer points. This requires BLAYER to be
run three separate times for each boundary
layer test.

C The actual operation of this program is self-
C explanatory provided its purpose and function

C are understood by the user and little attention is payed to the prompts for computer-user interaction.

C The final caution is in the interpretation of the output data. The calibration data units are in meters/sec and volts. The boundary layer data is in inches and meters/sec. English and Metric units were mixed for convenience since our wind tunnel velocities are often found in m/s and the traverse used for hot wire movement has a 1/4000 inch resolution. Nondimensionalization of the data is done with other software.

```

    C
    C IMPLICIT INTEGER*2 (A-H,O-Z)
    C INTEGER WAVE
    C REAL MEAN, VAR, A, ANS, X, Y, PROFIL, RHO, CONST, PRES, TEMP, YOU
    T, DY, YY
    C
    C $ ,C1,C2
    C CHARACTER*20 FILE1,FILE2,FILE3,FILE4
    C DIMENSION DATA(1000,8),MEAN(8),PROFIL(50,3),A(100),VAR
    (100)
    C $ ,ANS(20),C1(10),C2(10)
    C COMMON X(100),Y(100)
    C
    C
    C FIT=0
    C WRITE(*,'(A\')') ' ENTER THE NAME OF THE DECIMAL DATA FILE----->
    C
    C READ(*,'(A')') FILE1
    C WRITE(*,'(A\')') ' ENTER THE NUMBER OF CHANNELS IN THE FILE----->
    C
    C READ(*,*) CHAN
    C WRITE(*,'(A\')') ' ENTER THE NUMBER OF POINTS PER CHANNEL----->
    C
    C READ(*,*) PNTS
    C WRITE(*,'(A\')') ' ENTER THE NUMBER OF RECORDS IN THE FILE----->
    C
    C READ(*,*) WAVE
    C WRITE(*,'(A')') ' DO YOU WANT LEAST SQUARE FIT OF THE 1st CHANNEL'
    C
    C WRITE(*,'(A\')') ' vs 2nd CHANNEL (1/0) ----->
    C
    C READ(*,*) FIT
    C WRITE(*,'(A')') ' ENTER THE NEW DATA FILE NAME----->
    C
    C WRITE(*,'(A\')') ' (HOLDS COEFS OF LEAST SQUARE FIT OR AVERAGES)----->
    C
    C READ(*,'(A')') FILE2
    C
    C
    C OPEN(11,FILE=FILE1,STATUS='OLD')
    C OPEN(12,FILE=FILE2,STATUS='NEW')
  
```

```
C READ THE DATA IN FROM A FORMATED FILE
C
      DO 10 I=1,WAVE
      DO 9 K=1,PNTS
        READ(11,100) (DATA(K,J),J=1,CHAN)
      9    CONTINUE
C
C AVERAGE EACH RECORD FOR THE MEAN SAMPLED POINT
C
      CALL STAT (DATA,CHAN,PNTS,MEAN)
      DO 10 J=1,CHAN
C
C PROFIL IS AN AVERAGE VOLTAGE BASED ON AN A/D RANGE OF 0-5
C VOLTS USING THE 12 BIT BOARD.
C
      PROFIL(I,J)=MEAN(J)*5.0/4095.0
      10    CONTINUE
C
C DISPLAY THE AVERAGE VALUES ON THE SCREEN
C
      DO 17 I=1,WAVE
        WRITE(*,98) I,(J,J=1,4)
        WRITE(*,99) (PROFIL(I,J),J=1,CHAN)
      17    CONTINUE
C
C CHECK TO SEE IF A LEAST-SQUARE CURVE FIT IS DESIRED
C
      IF (FIT.EQ.1) THEN
        WRITE(*,'(A\')' ) ' ENTER CURRENT LOCAL PRESSURE (cmHg
)----->
        READ(*,*) PRES
        WRITE(*,'(A\')' ) ' ENTER THE CURRENT ROOM TEMPERATURE
(deg C)--->
        READ(*,*) TEMP
C
C CONST CONVERTS VOLTS TO PRESSURE UNITS
C CONST = (Pa/mmHg)*(mmHg/Volts)
C
        CONST=133.323
C
C RHO IS DENSITY kg/m**3
C GAS CONSTANT FOR AIR R=286.9 J/(kg*K)
C
        RHO=(PRES*10.0*CONST)/((TEMP+273.16)*286.9)
        WRITE(*,*) 'AIR DENSITY = ',RHO
C
C 1ST CHANNEL OF PRESSURE IS CONVERTED TO VELOCITY
C
        DO 13 I=1,WAVE
          PROFIL(I,1)=SQRT(2.0*PROFIL(I,1)*(CONST/10.0)/RHO
)
      13    CONTINUE
C
```

```

C NPOL=5 MEANS A FIFTH ORDER POLYNOMIAL WILL BE PERFORMED ON
C THE CALIBRATION DATA.
C
C      NPOL=5
C      KS=0
C
C MOVE DATA TO COMMON SINGLE COLUMN FOR CURVE FIT
C
C      DO 14 I =1, WAVE
C      X(I)=PRCFIL(I,2)
C      Y(I)=PRCFIL(I,1)
C      14      WRITE(*,*) Y(I),X(I)
C
C CALL CURVE FIT SUBROUTINE
C
C      CALL LSFIT (WAVE, X, Y, NPOL, A, VAR, ANS, KS)
C      IF (KS.EQ.1) THEN
C          WRITE(*,'(A\')') ' SINGULAR SOLUTION ---RESULTS I
NVALID'
C          WRITE(*,'(A\')') ' *****PROGRAM STOP REACHED**'
C          *****'
C          STOP
C          END IF
C
C STORE THE CALIBRATION COEFFICIENTS IN A FILE
C WITH THE ORIGINAL DATA
C
C      WRITE (*,'(A\')') ' COEFFICIENTS: '
C      DO 50 I=1,NPOL+1
C          WRITE(12,'(10X,E15.8)') ANS(I)
C      50      WRITE(*,'(10X,E15.8)') ANS(I)
C          WRITE(12,103)
C          DO 51 I=1,WAVE
C              WRITE(12,99) PROFIL(I,2),PROFIL(I,1)
C      51      CONTINUE
C          ELSE
C
C IF NO CURVE FIT THEN THE DATA MUST BE FROM PROFILE
C
C      WRITE(*,'(A\')') ' ENTER THE FIRST COEF FILE NAME -
C----->
C      READ(*,'(A\')') FILE3
C      WRITE(*,'(A\')') ' ENTER THE SECOND COEF FILE NAME-
C----->
C      READ(*,'(A\')') FILE4
C      WRITE(*,'(A\')') ' ENTER THE Y STEP SIZE (in)-----
C----->
C      READ(*,*) DY
C      OPEN(13,FILE=FILE3,STATUS='OLD')
C      OPEN(14,FILE=FILE4,STATUS='OLD')
C
C OPEN COEFFICIENT FILES FOR VOLTAGE TO VELOCITY MAPPING OF
C THE BOUNDARY LAYER HOT WIRE DATA
C

```

```

C NPOL =5 FOR FIFTH ORDER POLYNOMIAL
C
C
C NPOL=5
C DO 30 I=1,NPOL+1
C     READ(13, '(10X,E15.8)') C1,I
C     READ(14, '(10X,E15.8)') C2,I
C     WRITE(*,110)
C     WRITE(12,110)
C     YY=C1,I
C
C TIME WEIGHTING OF THE FIRST AND SECOND CALIBRATIONS OF THE
C HOT WIRE
C
C
C DO 25 I=1,WAVE
C     G=I-1
C     DO 33 J=1,NPOL+1
C         ANS(J)=(FLOAT(G)*C2(J)+FLOAT(WAVE-I+G)*C1,J)/WAVE
C     AVE-1)
C         WRITE(*,*) I,G,J,ANS(J)
C     33     CONTINUE
C
C CALL LSGET TO MAP A VOLTAGE POINT TO A VELOCITY
C
C     CALL LSGET(NPOL,ANS,PROFIL(I,1),YOUT)
C
C WRITE THE BOUNDARY LAYER COORDINATE AND VELOCITY
C TO A NEW FILE
C
C
C     PROFIL(I,1)=YOUT
C     WRITE(12,99) YY,(PROFIL(I,J),J=1,CHAN)
C     WRITE(*,99) YY,(PROFIL(I,J),J=1,CHAN)
C     YY=YY+DY
C     25     CONTINUE
C     CLOSE(13)
C     CLOSE(14)
C     END IF
C
C
C     CLOSE(11)
C     CLOSE(12)
C
C
C     90     FORMAT(10X,'ORDER: ',I1,10X,E15.8)
C     91     FORMAT(30X,'COEFFICIENTS: ')
C     92     FORMAT(/10X,'RECORD: ',I2//10X,4('CHAN ',I1,5X))
C     93     FORMAT(4(5X,E13.6))
C     100    FORMAT(I12,I12)
C     103    FORMAT(/7X,'VOLTAGE',5X,'VELOCITY')
C     110    FORMAT(10X,'***** BOUNDARY LAYER PROFILE *****')
C             & 3X,'Y-AXIS',3X,'VELOCITY')
C     STOP
C     END
C
C

```

```
C      SUBROUTINE STAT (DATA,CHAN,PNTS,MEAN)
C
C      THIS ROUTINE ONLY DOES THE FOLLOWING:
C
C      - FINDS THE MEAN VALUE FOR THE POINTS IN EACH CHAN
C        OF EVERY RECORD
C
C
C      IMPLICIT INTEGER*2 (A-H,O-Z)
C      REAL MEAN
C      DIMENSION DATA(1000,3),MEAN(3)
C
C
      DO 10 I=1,CHAN
         MEAN(I)=0.0
         DO 5 J=1,PNTS
            MEAN(I)=MEAN(I)+FLOAT(DATA(J,I))
5          CONTINUE
         MEAN(I)=MEAN(I)/FLOAT(PNTS)
10        CONTINUE
         RETURN
         END
```

PROGRAM MCMEM

WILLIAM G. BLAIR

JANUARY 1987

C PURPOSE: TO PERFORM THE NECESSARY INTEGRATION IN ORDER
 C TO CALCULATE THE MOMENTUM THICKNESS OF A GIVEN
 C BOUNDARY LAYER.

C FORTRAN: The following program was written for use in
 C Microsoft Fortran version 3.2.

C OPERATION: The only needed information on the boundary
 C layer is the freestream velocity and the number
 C of points in the file. Otherwise, this program
 C is self-explanatory.

```

IMPLICIT REAL*8(A-H,O-Z)
INTEGER*4 PNTS
REAL*8 NU
CHARACTER*14 FILE1
DIMENSION U(100),Y(100)
DATA NU/1.508D-05/
WRITE(*,'(A\')' ) ' ENTER THE MEAN VELOCITY (m/s)-----
----->
      READ(*,*) UFREE
      WRITE(*,'(A\')' ) ' ENTER THE BOUNDARY LAYER FILE NAME--
----->
      READ(*,'(A\')' )FILE1
      WRITE(*,'(A\')' ) ' ENTER THE NUMBER OF POINTS IN THE FI
LE----->
      READ(*,*) PNTS
      OPEN(10,FILE=FILE1,STATUS='OLD')
      DO 10 I=1,PNTS
         READ(10,*) Y(I),U(I)

C ALL Y'S HAVE 0.1 INCH ADDED TO SHIFT DATA TO THE ACTUAL
C OBJECT SURFACE THE BOUNDARY LAYER IS FOLLOWING. THEN
C CONVERT Y'S TO METERS FROM INCHES.
C
      Y(I)=(Y(I)+0.1)*0.0254
10      CONTINUE
      CLOSE(10)

C AREA UNDER CURVE IS INITIALLY ZERO
C
      SUM=0.0
C
C CALL INTEGRAL FUNCTION FOR FIRST POINT
C

```

```
      CALL F(UFREE,U,1,FX1)
C
C START THE TRAPEZOIDAL INTEGRATION LOOP
C
DO 20 I=1,PNTS-1
      H=(Y(I+1)-Y(I))
      CALL F(UFREE,U,I+1,FX2)
      SUM=SUM+(FX2+FX1)*H/2.0D0
      FX1=FX2
20      CONTINUE
C
C PRINT OUT MOMENTUM THICKNESS AND THE WALL-FRICTION
C VELOCITY .
C
      WRITE(*,*) ' MOMENTUM THICKNESS IS = ',SUM
      REY=UFREE*SUM/NU
      CF=0.0125D0/(REY**(0.25))
      V=UFREE*SQRT(CF)
      WRITE(*,*) ' THE VALUE V* (m/s) = ',V
      STOP
      END
C
C
C
      SUBROUTINE F(UFREE,U,I,FX)
C
C THE FUNCTION TO BE INTEGRATED
C
      IMPLICIT REAL*8 (A-H,O-Z)
      DIMENSION U(100)
      FX=(U(I)/UFREE)*(1.0D0-U(I)/UFREE)
      RETURN
      END
```

PROGRAM NONDIM

C
C
C
C
C WILLIAM G. BLAIR
C
C 1.80 87C PURPOSE: To convert the velocity profile numbers into the
C nondimensionalized form of $\gamma = \gamma^*$ "Viscosity" and
C $U = U^*/V^*$.
CC FORTRAN: The following program was written for use in
C Microsoft Fortran version 3.2.
CC OPERATION: Before running this program the wall-friction
C velocity is required. This is found by run-
C ning MCMEN specifically made for that purpose.
C Once this information is available then the
C operation of NONDIM is self-explainatory.
C

```

C IMPLICIT REAL*8 (A-H,O-Z)
C REAL*8 NU
C CHARACTER*20 FILE1,FILE2
C DATA NU/1.508E-05/
C
C V IS THE WALL-FRICTION VELOCITY PREVIOUSLY CALCULATED
C
C      WRITE(*, '(A\')') ' ENTER V* -----
C----->
C      READ(*,*) V
C      WRITE(*, '(A\')') ' ENTER THE BOUNDARY LAYER FILE NAME--
C----->
C      READ(*, '(A\')') FILE1
C      WRITE(*, '(A\')') ' ENTER THE NUMBER OF POINTS IN THE FI
C LE----->
C      READ(*,*) NUM
C      WRITE(*, '(A\')') ' ENTER THE NONDIMENSIONALIZED BLAYER
C FILE ----->
C      READ(*, '(A\')') FILE2
C      OPEN(10,FILE=FILE1,STATUS='OLD')
C      OPEN(20,FILE=FILE2,STATUS='NEW')
C      DO 10 I=1,NUM
C          READ(10,09) Y,U
C
C 0.1 INCHES ARE ADDED TO Y COORDINATE THEN Y IS CONVERTED
C TO METERS PRIOR TO BEING NONDIMENSIONALIZED
C
C      Y=(Y+0.1)*0.0254DC*V/NU
C
C THE BOUNDARY LAYER VELOCITIES ARE NONDIMENSIONALIZED BY TH
C E

```

```
C WALL- FRICTION VELOCITY
C
C      U=U/V
C
C  WRITE THE NONDIMENSIONALIZED DATA TO A NEW FILE
C
      WRITE(*,*) Y,U
      WRITE(20,99) Y,U
10    CONTINUE
      CLOSE(10)
      CLOSE(20)
99    FORMAT(2(5X,E13.6))
      END
```

PROGRAM PRESSURE

BILL BLAIR

MAY 1987

PURPOSE: THIS PROGRAM IS TO RECORD THE PRESSURE DIFFERENCE BETWEEN STATIC PRESSURE OF THE FREE STREAM AND THE LOCAL PRESSURE IN A 2-D SLOT OF VARYING AR.

FUNCTION: The following program performs several tasks including:

- Recording the dynamic head of the wind tunnel for velocity calculations and nondimensionalization of the pressure difference.
- Recording the pressure difference between the pressure at the center of slot base and the static pressure of the free stream.
- Records the pressure difference between the static pressure of the free stream and the pressure of the slot probe.
- Calculates the absolute X and Y coordinates relative to the up stream corner at the slot entrance and records the calculated location with each pressure data set.
- Calculates the relative X and Y coordinates for interactive use between the user and terminal. These coordinates tell the user the X and Y values for the traverses; since they need to be set by hand.

FORTRAN: The following program was written for use in Microsoft Fortran version 3.2.

EQUIPMENT: The following equipment and software was used in the operation of this program:

- Metrabyte DASH-16 analog/digital I/O expansion board
- Metrabyte 24 bit parallel port
- Metrabyte DASH-16 Fortran Library
- MKS high accuracy differential pressure transducer model 398HD
- MKS signal conditioner type 270B

OPERATION: The following steps are needed prior to running this program:

- The DASH-16 should be configured as follows:
 - 3 channel differential input

- WARNING note the definition of Metrabyte 'differential input':
 - unipolar This offers a 0-5 volt range of measurement.
 - gain set at 8
 - IMA level of 0
 - base address set at 768
- The MKG Signal Conditioner should be set up as follows:
 - sensor range set at 1 torr
 - zero the unit according to manual
 - initially set range select at X1
- Configure the model accordingly for the new test. This includes the following:
 - mounting the correct side walls for the test
 - centering the slot pressure probe in the middle of the 2-D grid to be scanned (use calipers)
 - record the absolute and relative coordinates from the model and the traverses respectively

Following the completion of the above items and noting that the model is correctly configured for a test this program can be implemented.

Just prior to running PRESSure the inlet temperatures of the wind tunnel and the atmospheric pressure should be noted for later reference. These will be needed for later calculation of the wind tunnel velocity.

The use of the relative and absolute coordinate systems needs some explanation. The absolute coordinates are the recorded positions of the slot pressure probe with reference to the up stream corner at the slot opening.

The relative coordinates are only for user benefit. They refer to the two manual traverses and their coordinates. Note that the user must input the X and Y for both of the two traverses since they will not necessarily be the same. Once the inputs have been typed into the computer no further interaction is needed other than two hit the return key for each pressure point once the traverses are set. However, the user will be busy connecting and disconnecting the tubing on the pitot tube, base pressure tap and the slot pressure

Manual examination that the MNC signal conditioner is cased is suggested so that changing room temperature effects are avoided.

The program's basic traverse step size is 1/16" for a usual grid of 7x7 for 49 points. When a higher resolution grid is used (i.e. 14x14 point grid) the basic step of 1/16 [in] is divided accordingly. This program will only cover a 6/16" x 6/16" area in the slot.

```
IMPLICIT INTEGER*2 (A-V)
REAL FREQ
DIMENSION DATA(4,3000)
CHARACTER*20 DATSTOR
COMMON XFACE, XCEFF, XCENN, YFACE, YCENN, YCEFF

WRITE(*, '(A)') '*****SAMPLING INFORMATION*****'
****'
WRITE(*, '(A\')') ' ENTER THE DATA FILE NAME: '
READ(*, '(A)') DATSTOR
WRITE(*, '(A\')') ' ENTER DATA SAMPLING RATE/CHAN. IN HZ
READ(*, *) FREQ
WRITE(*, '(A)') ' ENTER THE CHANNEL TO BE SCANNED DURIN
WRITE(*, '(A\')') ' SAMPLING: '
READ(*, *) SCH
WRITE(*, '(A\')') ' ENTER THE NUMBER OF GRID POINTS: '
READ(*, *) NPNTS
WRITE(*, '(A\')') ' ENTER THE ABSOLUTE FACE CENTER X (in
READ(*, *) XFACE
WRITE(*, '(A\')') ' ENTER THE ABSOLUTE FACE CENTER Y (in
READ(*, *) YFACE
WRITE(*, '(A\')') ' ENTER THE RELATIVE NEAR CENTER X (in
READ(*, *) XCENN
WRITE(*, '(A\')') ' ENTER THE RELATIVE FAR CENTER X (in
READ(*, *) XCEFF
WRITE(*, '(A\')') ' ENTER THE RELATIVE NEAR CENTER Y (in
READ(*, *) YCENN
WRITE(*, '(A\')') ' ENTER THE RELATIVE FAR CENTER Y (in
READ(*, *) YCEFF
```

```
FCH=SCH
C
C MAIN PROGRAM
C
C NCS=3000 PNTS PER SAMPLE OF PRESSURE
C
C      NCS=3000
C      NUMDAT=FCH-SCH-1
C      CALL SAMPLE (NPNTS, SCH, FCH, NCS, FREQ, DATSTOR, NUMDAT, DAT
A)
C      STOP
C      END
C
C
C      SUBROUTINE SAMPLE (NPNTS, SCH, FCH, NUMPAS, FREQ, DATSTOR, N
UMCHN, DATA)
C          IMPLICIT INTEGER*2 (A-V)
C          REAL FREQ, DISPLAY, X, Y
C          DIMENSION DATA(NUMCHN, NUMPAS)
C          CHARACTER*8 DATSTOR, JUNK
C          COMMON XFACE, XCEFF, XCENN, YFACE, YCENN, YCEFF
C
C      JUMP TO X=-1/16 AND Y=-1/16 PRIOR TO FIRST ITERATION
C
C          XJUMP=0.25225
C
C      CALCULATE GRID SIZE (i.e. 7x7 or 14x14)
C
C          NUMK=INT(SQRT(FLOAT(NPNTS)))
C
C      SET STEP SIZE AND JUMP TO START X AND Y
C
C          XD=0.0625*7.0/(FLOAT(NUMX))
C          X=XFACE-XJUMP
C          Y=YFACE-XJUMP
C          XCEN=XCENN-XJUMP
C          XCEP=XCEFF+XJUMP
C          YCEN=YCENN-XJUMP
C          YCEP=YCEFF-XJUMP
C
C      INITALIZE THE A/D BOARD
C
C          DASHBS=763
C          DMALEV=1
C          INTLEV=2
C          RTNFLG=0
C          CALL ADINIT(DASHBS, DMALEV, INTLEV, RTNFLG)
C          CALL TRIGGER(FREQ, NUMCHN)
C          MODE=8-16
C          RTNFLG=0
C
C      OPEN FILES
C
```

```

REC=NUMCHN*2+NUMPAS+6
OPEN(11,FILE=DAT3TOR,ACCESS='DIRECT',STATUS='NEW',R
ECL=REC)
C
C MEASURE THE PITOT PROBE PRESSURE FOR VELOCITY
C
      WRITE(*,70)
      WRITE(*,'(A)') ' RETURN TO STORE THE PITOT PRESS. '
      READ(*,'(A)') JUNK
      CALL ADCCONV(MODE,SCH,FCH,NUMPAS,DATA(1,1),RTNFLG)
      WRITE(11,REC=1) ((DATA(J,L),J=1,NUMCHN),L=1,NUMPAS)
      WRITE(*,'(/,A)') ' ***AN APPROXIMATE DATA VALUE***'
C
C DISPLAY AN FIRST SAMPLED VOLTAGE ON THE SCREEN
C
      CHAN=SCH
      DO 91 K=1,NUMCHN
        DISPLAY=(DATA(K,1)/819.0)
        WRITE(*,80) CHAN,DISPLAY
        IF (CHAN.LT.7) THEN
          CHAN=CHAN+1
        ELSE
          CHAN=0
        ENDIF
91      CONTINUE
C
C USER WARNING TO MODIFY THE RANGE SELECT ON THE
C PRESSURE SIGNAL CONDITIONER TO TAKE ADVANTAGE
C OF THE FULL VOLTAGE RANGE MEASURED BY THE COMPUTER
C
      WRITE(*,70)
      WRITE(*,'(A)') ' ***** CHANGE RANGE SELECT *****'
*****'
      WRITE(*,70)
C
C MEASURE THE BASE PRESSURE TAP
C
      WRITE(*,70)
      WRITE(*,'(A)') ' RETURN TO STORE THE BASE TAP PRESS. '
      READ(*,'(A)') JUNK
      CALL ADCCONV(MODE,SCH,FCH,NUMPAS,DATA(1,1),RTNFLG)
      WRITE(11,REC=2) ((DATA(J,L),J=1,NUMCHN),L=1,NUMPAS)
C
C DISPLAY AN FIRST SAMPLED VOLTAGE ON THE SCREEN
C
      WRITE(*,'(/,A)') ' ***AN APPROXIMATE DATA VALUE***'
      CHAN=SCH
      DO 92 K=1,NUMCHN
        DISPLAY=(DATA(K,1)/819.0)
        WRITE(*,80) CHAN,DISPLAY
        IF (CHAN.LT.7) THEN

```

```

CHAN=CHAN+1
ELSE
CHAN=0
ENDIF
END CONTINUE
WRITE(*,70)
C
C SET POINT COUNTER
C
COUNT=0
WRITE(*,'(//,A)') ' ****
*****'
*****'
WRITE(*,'(A)')      ' *      DATA ACQUISITION BEGINN
ING
'*'
WRITE(*,'(A,/,/)') ' ****
*****'
*****'
C
C START NUMX x NUMX GRID PATTERN
C
DO 201 II=1,NUMX
C
C SET ALL Y COORDINATES
C
Y=Y+XD
YCEF=YCEF+XD
YCEN=YCEN+XD
C
C TELL USER RELATIVE Y COORDINATES
C
WRITE(*,'(A,F5.3/)') ' THE RELATIVE NEAR Y = ',YCE
N
WRITE(*,'(A,F5.3/)') ' THE RELATIVE FAR Y = ',YCEF
WRITE(*,'(A\\)') ' HIT RETURN TO CONTINUE'
READ(*,'(A)') JUNK
DO 202 JJ=1,NUMX
C
C SET ALL X COORDINATES
C
X=X+XD
XCEN=XCEN+XD
XCEF=XCEF+XD
COUNT=COUNT+1
WRITE(*,'(A,I6)') ' THIS DATA POINT IS NUMBER : ',COUNT
WRITE(*,'(/)')
C
C TELL USER RELATIVE X COORDINATES
C
WRITE(*,'(A,F5.3/)') ' THE RELATIVE NEAR X = ',XCE
N
WRITE(*,'(A,F5.3/)') ' THE RELATIVE FAR X = ',XCEF
WRITE(*,'(A\\)') ' HIT RETURN TO START A/D'
READ(*,'(A)') JUNK
C

```

```

C PERFORM A D ON FREESTREAM STATIC PRESSURE LESS THE
C CAVITY STATIC PRESSURE
C
      CALL ADCONV(MODE, SCH, FCH, NUMPAS, DATA(1,1), RENFL)
      WRITE(11, REC=1, COUNT=3) K, T, (DATA(J,L), L=1, NUMCHN,
      L=1, NUMPAS)
C
C DISPLAY AN FIRST SAMPLED VOLTAGE ON THE SCREEN
C
      WRITE(*, '(/,A)') '      ***AN APPROXIMATE DATA VALU
E***'
      CHAN=SCH
      DO 90 K=1, NUMCHN
      DISPLAY=(DATA(K, 1)/819.0)
      WRITE(*, 80) CHAN, DISPLAY
      80      FORMAT(/, 1X, 'VALUE (VOLTS) AT CHANNEL ', I1, ' = ',
      F6.6)
      IF (CHAN.LT.7) THEN
      CHAN=CHAN+1
      ELSE
      CHAN=0
      ENDIF
      90      CONTINUE
      WRITE(*, 70)
      202      CONTINUE
C
C RESET THE X COORDINATES FOR A PASS ON A NEW ROW
C
      X=XFACE-XJUMP
      XCEN=XCENN-XJUMP
      XCEF=XCEFF+XJUMP
      201      CONTINUE
      WRITE(*, 70)
      70      FORMAT(/, 1X, '*****')
      ,/
      CLOSE(11)
      RETURN
      END
C
C
C
      SUBROUTINE TRIGGER(FREQ, NUM)
C
C THIS SUBROUTINE IS USED TO SET THE COUNTERS ON THE
C A/D BOARD AT THE DESIRED SAMPLING FREQUENCY
C
      IMPLICIT INTEGER*2 (A-V)
      REAL FREQ
      THE VALUE OF 0.1 IN THE NEXT LINE ALLEVIATES ROUND-OFF
      F ERROR
      TRIG=IFIX((500000.0/(FREQ*NUM))+0.1)
      MD=3
      TWO=2
      CALL CNTMC1 (MD, TWO)

```

```
CALL CNTMOS (MD, TRIG)  
RETURN  
END
```

PROGRAM CAVITATION

WILLIAM BLAIR

8.10.86

PURPOSE: THIS PROGRAM COMPILES THE DATA OF THE SLOT PRESSURE MEASUREMENTS BY CALCULATING THE MEAN OF THE DATA IN EACH RECORD, NONDIMENSIONALIZING WHEN NECESSARY, THEN WRITING IT INTO A NEW FORMATED FILE.

FUNCTION: The following program performs several tasks including:

- Convert the binary file data into the voltages they represent from the 12 bit integer to the 0-5 volt range the computer was configured for during the pressure tests (i.e. $x5.0/4095$).
- Reading the first record with the dynamic head data of the given data set then calculate the velocity from the user input room temperatures.
- Reading the base pressure data averaging it convert it to pascals then storing it in the new formated data file.
- Read the data on the pressure difference between the static pressure of the free stream and the pressure of the slot probe then averaging and nondimensionalizing it prior to storing the data in the formated file.

FORTRAN: The following program was written for use in Microsoft Fortran version 3.2.

OPERATION: The following steps are needed prior to running this program:

- The room starting and ending temperatures for the test need to be available.
- The barometric pressure during the test must be available.

The operation of CAVITATION is straightforward. The program was written so that the user can follow the data through the process and confirm that the correct coefficients are in use for correct interpretation of the data. The only warning required is to emphasize that the user must understand the use of the conversion factors in the code.

IMPLICIT INTEGER*2 (A-H,O-Z)

```

INTEGER WAVE
REAL MEAN, X, Y, PROFIL, RHO, CONST, PRES, TEMP, TEMP1, TEMP2, V
PREC 8.16E, BOTTOM, BOTM, IP
CHARACTER*20 FILE1, FILE2
DIMENSION DATA(4,3000), MEAN(3), PROFIL, 50
WRITE(*, '(A\*)') ' ENTER THE NAME OF THE BINARY DATA FILE-----'
READ(*, '(A\*)') FILE1
C
C SET THE NUMBER OF CHANNELS (COLUMNS) TO 1 AND THE NUMBER
C OF POINTS PER CHANNEL TO 3000
C
CHAN=1
PNTS=3000
WRITE(*, '(A\*)') ' ENTER THE NUMBER OF LOCATIONS IN THE
FILE-----'
READ(*, *) WAVE
WRITE(*, '(A\*)') ' ENTER THE NEW DATA FILE NAME-----'
-----'
READ(*, '(A\*)') FILE2
WRITE(*, '(A\*)') ' ENTER CURRENT LOCAL PRESSURE (cmHg)
-----'
READ(*, *) PRES
WRITE(*, '(A\*)') ' ENTER THE STARTING ROOM TEMPERATURE
E (deg F)->'
READ(*, *) TEMP1
WRITE(*, '(A\*)') ' ENTER THE ENDING ROOM TEMPERATURE
(deg F)->'
READ(*, *) TEMP2
C
C CONST CONVERTS VOLTS TO PRESSURE UNITS
C (Pa/mmHg)*(mmHg/Volts)
C
CONST=133.323
C
C CONVERT TEMPERATURES TO METRIC UNITS
C
TEMP1=(TEMP1-32.0)*5.0/9.0
TEMP2=(TEMP2-32.0)*5.0/9.0
TEMP=(TEMP1+TEMP2)/2.0
C
C CALCULATE THE DENSITY OF AIR
C
RHO=(PRES*10.0*CONST)/((TEMP+273.16)*286.9)
C
C CALCULATE THE SIZE OF THE OLD FILE RECORDS
C
HLONG=CHAN*2*PNTS-8
OPEN(11,FILE=FILE1,ACCESS='DIRECT',STATUS='OLD',RECL=H
LONG)
OPEN(12,FILE=FILE2,STATUS='NEW')
C
C READ IN THE DATA THEN AVERAGE THE POINTS IN EACH RECORD

```

```

C
C      READ(11,REC=1)  DATA(J,L),J=1,CHAN,L=1,PNTS
C      CALL STAT(DATA,CHAN,PNTS,MEAN)
C
C      1ST RECORD OF PRESSURE IS THE DYNAMIC HEAD AND IS
C      CONVERTED TO VELOCITY
C
C      THE RANGE SELECT ON THE PRESSURE SIGNAL CONDITIONER WAS
C      SET AT 1K SO DIVIDE BY A FACTOR OF 10 [VOLT/mmHg]
C
C      VPRES=MEAN(CHAN)*5.0*CONST/4095.0/10.0
C      VEL=SQRT(2.0*VPRES/RHO)
C      WRITE(*,70)
C      WRITE(*,'(A,F6.3)')  ' AFFROK FREESTREAM VELOCITY = '
C      ,VEL
C      WRITE(*,'(A,F6.3)')  ' FREESTREAM DYNAMIC HEAD (Pa) = '
C      ,VPRES
C      WRITE(12,99) VEL
C      WRITE(*,70)
C
C      READ THE DATA FOR THE PASE PRESSURE RECORD THEN AVERAGE
C
C      READ(11,REC=2)  ((DATA(J,L),J=1,CHAN),L=1,PNTS)
C      CALL STAT(DATA,CHAN,PNTS,MEAN)
C
C      RANGE SELECT ON THE SIGNAL PRESSURE CONDITIONER WAS SET AT
C      0.01K SO DIVIDE BY A FACTOR OF 1000 [VOLT/mmHg]
C
C      BOTTCM=MEAN(CHAN)*5.0/4095.0/1000.0
C      BOTK=BOTTCM*CONST
C      WRITE(*,70)
C      WRITE(*,'(A,F9.6)')  ' THE BASE PRESSURE IS (mmHg) = '
C      ,BOTTCM
C      WRITE(*,'(/A,F9.6)')  ' THE BASE PRESSURE IS (Pa) = '
C      ,BOTK
C      WRITE(12,99) BOTK
C      WRITE(*,70)
C      WRITE(*,'(A/)')  ' THE PRESSURE DISTRIBUTION :'
C      WRITE(*,71)
C
C      READ THE DATA FOR THE SLOT 2-D PROFILE THEN AVERAGE EACH
C      RECORD
C
C      DO 10 I=1,NAVE
C      READ(11,REC=I+2) X,Y,((DATA(J,K),J=1,CHAN),K=1,PNTS)
C      CALL STAT (DATA,CHAN,PNTS,MEAN)
C
C      RANGE SELECT ON THE PRESSURE SIGNAL CONDITIONER WAS SET AT
C      1.01K SO DIVIDE BY A FACTOR OF 1000 [VOLT/mmHg]
C
C      PROFILE(CHAN)=MEAN(CHAN)*5.0*CONST/4095.0/1000.0
C
C      NONDIMENSIONALIZE EVERY PRESSURE POINT BY THE DYNAMIC HEAD
C      AND EVERY LENGTH BY THE MODEL WIDTH OF 1.5 INCH

```

```

C P=PROFIL,CHAN, WREC
C X=X(1,5
C Y=Y(1,5
C
C WRITE THE COMPILED DATA INTO A NEW FILE
C
C      WRITE(*,38) X,Y,PROFIL,CHAN, CP
C      WRITE(10,39) X,Y,PROFIL,CHAN,, CP
10      CONTINUE
      CLOSE(11)
      CLOSE(10)
C
C
C      FORMAT(7,1X,'*****')
C
C      FORMAT(10X,'X',10X,'Y',10X,'PRESSURE (Pa)',15X,'Ca',1)
C      FORMAT(4(4X,E18.6))
100     FORMAT(112,112)
      STOP
      END
C
C
C      SUBROUTINE STAT (DATA,CHAN,PNTS,MEAN)
C
C      THIS ROUTINE ONLY DOES THE FOLLOWING:
C
C      - FINDS THE MEAN VALUE FOR THE PNTS IN EACH CHAN OF EVERY
C        RECORD
C
C
C      IMPLICIT INTEGER*2 (A-H,O-Z)
C      REAL MEAN
C      DIMENSION DATA(4,2000),MEAN(8)
C
C
C      DO 10 I=1,CHAN
C          MEAN(I)=0.0
C          DO 5 J=1,PNTS
C              MEAN(I)=MEAN(I)+FLOAT(DATA(I,J))
C          CONTINUE
C          MEAN(I)=MEAN(I)/FLOAT(PNTS)
10      CONTINUE
      RETURN
      END

```

PROGRAM ISOCBAR

WILLIAM J. BLAIRE

7.9.87

PURPOSE: To convert the pressure coefficient values from the pressure measurements into groups of constant pressure for plotting.

FUNCTION: The following program performs several tasks including:

- calculating the group set parameters which represent isobars in the cavity vortex
- reading in the data
- check each data point with the next point in both the positive x and y directions for each grouping defined by the calculated parameters
- interpolate between the neighboring points that straddle a group parameter
- store the data by group in a new file that will be ready for the available plotting routine

FORTRAN: The following program was written for use in Microsoft Fortran version 3.2.

OPERATION: The following steps are needed prior to running this program:

- know the number of points in the file
- know the value of the highest pressure coefficient

The actual use of this program is very simple, however, understanding its purpose is critical toward its proper use. One final warning is that the group arrays are presently dimensioned 70. If more than 70 addresses were ever required this program would have to be modified accordingly.

```
IMPLICIT REAL*8 (A-I,O-S)
CHARACTER*20 FILE1,FILE2
INTEGER*2 I,TWO,S,SEVEN
```

```
C DIMENSION THE 10 GROUP ARRAYS
```



```

C START THE X COORDINATE GROUPING CHECK
      DO 10 I=1,NUM-1
      C
      C CHECK TO SEE IF THIS IS THE LAST POINT IN THE ROW
      C
      C IF I.NE.SEVEN THEN
      C
      C IF NOT THE LAST POINT THEN START MATCHING THE DATA TO A
      C GROUPING
      C
      C CHECK TO SEE IF I POINT AND I-1 POINT STRADDLE A GROUP
      C INITIATION INDEX
      C
      C FIRST CHECK IF THE I POINT IS GREATER THAN ISCI
      C
      C IF (CA(I).GE.ISCI) THEN
      C
      C CHECK IF THE I-1 POINT IS LESS THAN ISCI
      C
      C IF (CA(I-1).LT.ISCI) THEN
      C
      C COUNT THE NUMBER OF POINTS IN THE ISCI GROUPING
      C
      C K1=K1-1
      C
      C INTERPOLATE BETWEEN I AND I-1 FOR ISCI LOCATION IN THE X
      C COORDINATE
      C
      C      ISCK1(K1)=X(I)+(ISCI-CA(I))*(X(I-1)-X(I))/(CA(I-
      C      -1)-CA(I))
      C
      C Y LOCATION DOES NOT CHANGE
      C
      C      ISCY1(K1)=Y(I)
      C      END IF
      C      END IF
      C
      C REPEAT THE SORTING PROCEDURE FOR THE REST OF THE GROUPINGS
      C IN THE X DIRECTION
      C
      C IF ((CA(I).GE.ISCC).AND.(CA(I).LT.ISCI)) THEN
      C      IF (CA(I-1).GE.ISCI) THEN
      C          K1=K1+1
      C          ISCK1(K1)=X(I)+(ISCI-CA(I))*(X(I-1)-X(I))/(CA(I-
      C          -1)-CA(I))
      C          ISCY1(K1)=Y(I)
      C      ELSE IF (CA(I-1).LE.ISCC) THEN
      C          KC=KC+1
      C          ISCK2(KC)=X(I)+(ISCC-CA(I))*(X(I-1)-X(I))/(CA(I-
      C          -1)-CA(I))
      C          ISCY2(KC)=Y(I)
      C      END IF
      C      END IF

```

```

IF((CA(I)).GE.ISC0) .AND. (CA(I).LT.ISC0)) THEN
  IF((CA(I+1)).GE.ISC0) THEN
    KC=KC+1
    ISOCX(KC)=X(I)+ISC0-CA(I)*(X(I+1)-X(I))/CA(I-
1)-CA(I))
    ISOCY(KC)=Y(I)
  ELSE IF((CA(I+1)).LE.ISC0) THEN
    KC=KC+1
    ISOCX(KC)=X(I)+ISC0-CA(I)*(X(I+1)-X(I))/CA(I-
1)-CA(I))
    ISOCY(KC)=Y(I)
  END IF
END IF
IF((CA(I)).GE.ISC1) .AND. (CA(I).LT.ISC1)) THEN
  IF((CA(I+1)).GE.ISC1) THEN
    KC=KC+1
    ISOCX(KC)=X(I)+(ISC1-CA(I))*(X(I+1)-X(I))/CA(I-
1)-CA(I))
    ISOCY(KC)=Y(I)
  ELSE IF((CA(I+1)).LE.ISC1) THEN
    KC=KC+1
    ISOCX(KC)=X(I)+(ISC1-CA(I))*(X(I+1)-X(I))/CA(I-
1)-CA(I))
    ISOCY(KC)=Y(I)
  END IF
END IF
IF((CA(I)).GE.ISC2) .AND. (CA(I).LT.ISC2)) THEN
  IF((CA(I+1)).GE.ISC2) THEN
    KC=KC+1
    ISOCX(KC)=X(I)+(ISC2-CA(I))*(X(I+1)-X(I))/CA(I-
1)-CA(I))
    ISOCY(KC)=Y(I)
  ELSE IF((CA(I+1)).LE.ISC2) THEN
    KC=KC+1
    ISOCX(KC)=X(I)+(ISC2-CA(I))*(X(I+1)-X(I))/CA(I-
1)-CA(I))
    ISOCY(KC)=Y(I)
  END IF
END IF
IF((CA(I)).GE.ISC3) .AND. (CA(I).LT.ISC3)) THEN
  IF((CA(I+1)).GE.ISC3) THEN
    KC=KC+1
    ISOCX(KC)=X(I)+(ISC3-CA(I))*(X(I+1)-X(I))/CA(I-
1)-CA(I))
    ISOCY(KC)=Y(I)
  ELSE IF((CA(I+1)).LE.ISC3) THEN
    KC=KC+1
    ISOCX(KC)=X(I)+(ISC3-CA(I))*(X(I+1)-X(I))/CA(I-
1)-CA(I))
    ISOCY(KC)=Y(I)
  END IF
END IF
IF((CA(I)).GE.ISC4) .AND. (CA(I).LT.ISC4)) THEN
  IF((CA(I+1)).GE.ISC4) THEN
    KC=KC+1
    ISOCX(KC)=X(I)+(ISC4-CA(I))*(X(I+1)-X(I))/CA(I-
1)-CA(I))
    ISOCY(KC)=Y(I)
  ELSE IF((CA(I+1)).LE.ISC4) THEN
    KC=KC+1
    ISOCX(KC)=X(I)+(ISC4-CA(I))*(X(I+1)-X(I))/CA(I-
1)-CA(I))
    ISOCY(KC)=Y(I)
  END IF
END IF
IF((CA(I)).GE.ISC5) .AND. (CA(I).LT.ISC5)) THEN
  IF((CA(I+1)).GE.ISC5) THEN
    KC=KC+1
    ISOCX(KC)=X(I)+(ISC5-CA(I))*(X(I+1)-X(I))/CA(I-
1)-CA(I))
    ISOCY(KC)=Y(I)
  ELSE IF((CA(I+1)).LE.ISC5) THEN
    KC=KC+1
    ISOCX(KC)=X(I)+(ISC5-CA(I))*(X(I+1)-X(I))/CA(I-
1)-CA(I))
    ISOCY(KC)=Y(I)
  END IF
END IF
IF((CA(I)).GE.ISC6) .AND. (CA(I).LT.ISC6)) THEN
  IF((CA(I+1)).GE.ISC6) THEN
    KC=KC+1
    ISOCX(KC)=X(I)+(ISC6-CA(I))*(X(I+1)-X(I))/CA(I-
1)-CA(I))
    ISOCY(KC)=Y(I)
  ELSE IF((CA(I+1)).LE.ISC6) THEN
    KC=KC+1
    ISOCX(KC)=X(I)+(ISC6-CA(I))*(X(I+1)-X(I))/CA(I-
1)-CA(I))
    ISOCY(KC)=Y(I)
  END IF
END IF
IF((CA(I)).GE.ISC7) .AND. (CA(I).LT.ISC7)) THEN
  IF((CA(I+1)).GE.ISC7) THEN
    KC=KC+1
    ISOCX(KC)=X(I)+(ISC7-CA(I))*(X(I+1)-X(I))/CA(I-
1)-CA(I))
    ISOCY(KC)=Y(I)
  ELSE IF((CA(I+1)).LE.ISC7) THEN
    KC=KC+1
    ISOCX(KC)=X(I)+(ISC7-CA(I))*(X(I+1)-X(I))/CA(I-
1)-CA(I))
    ISOCY(KC)=Y(I)
  END IF
END IF

```

```

      K6=K6+1
      ISCK6(K6)=X(I)+ISCB-CA(I)*(X(I+1)-X(I))/CA(I+1)
      11=CA(I+1)
      ISCY6(K6)=Y(I)
      ELSE IF (CA(I+1).LE.ISC7) THEN
      K7=K7+1
      ISCK7(K7)=X(I)+(ISCB-CA(I))*(X(I+1)-X(I))/CA(I+1)
      11=CA(I+1)
      ISCY7(K7)=Y(I)
      END IF
      END IF
      IF ((CA(I).GE.ISC8).AND.(CA(I).LT.ISC7)) THEN
      IF (CA(I+1).GE.ISC7) THEN
      K7=K7+1
      ISCK7(K7)=X(I)+(ISCB-CA(I))*(X(I+1)-X(I))/CA(I+1)
      11=CA(I+1)
      ISCY7(K7)=Y(I)
      ELSE IF (CA(I+1).LE.ISC8) THEN
      K8=K8+1
      ISCK8(K8)=X(I)+(ISCB-CA(I))*(X(I+1)-X(I))/CA(I+1)
      11=CA(I+1)
      ISCY8(K8)=Y(I)
      END IF
      END IF
      IF ((CA(I).GE.ISC9).AND.(CA(I).LT.ISC8)) THEN
      IF (CA(I+1).GE.ISC8) THEN
      K8=K8+1
      ISCK8(K8)=X(I)+(ISCB-CA(I))*(X(I+1)-X(I))/CA(I+1)
      11=CA(I+1)
      ISCY8(K8)=Y(I)
      ELSE IF (CA(I+1).LE.ISC9) THEN
      K9=K9+1
      ISCK9(K9)=X(I)+(ISCB-CA(I))*(X(I+1)-X(I))/CA(I+1)
      11=CA(I+1)
      ISCY9(K9)=Y(I)
      END IF
      END IF
      IF ((CA(I).GE.ISC10).AND.(CA(I).LT.ISC9)) THEN
      IF (CA(I+1).GE.ISC9) THEN
      K9=K9+1
      ISCK9(K9)=X(I)+(ISCB-CA(I))*(X(I+1)-X(I))/CA(I+1)
      11=CA(I+1)
      ISCY9(K9)=Y(I)
      ELSE IF (CA(I+1).LE.ISC10) THEN
      K10=K10+1
      ISCK10(K10)=X(I)+(ISCB-CA(I))*(X(I+1)-X(I))/CA(I+1)
      11=CA(I+1)
      ISCY10(K10)=Y(I)
      END IF
      END IF
      IF (CA(I).LT.ISC10) THEN
      IF (CA(I+1).GE.ISC10) THEN
      K10=K10+1
      ISCK10(K10)=X(I)+(ISCB-CA(I))*(X(I+1)-X(I))/CA(I+1)
      11=CA(I+1)
      ISCY10(K10)=Y(I)
      END IF
      END IF
      END IF

```

```

I+1)-CA(I))
    ISOCY1(K1)=Y(I)
    END IF
END IF
ELSE
    SEVEN=SEVEN+8
END IF

C
C START Y OR COLUMN GROUP CHECKING
C
C FIRST CHECK TO MAKE SURE THAT I IS NOT THE LAST POINT
C IN THE Y DIRECTION (i.e. THE TOP OF ANY COLUMN IN THE
C GRID)
C
    IF(I.LT.(NUM-8)) THEN
C
C CHECK IF I IS GREATER THAN ISCI WHICH DEFINES THE FIRST
C GROUPING
C
    IF (CA(I).GE.ISCI) THEN
C
C CHECK IF I+8 (THE POINT IN THE ROW DIRECTLY ABOVE IN THE
C GRID) IS LESS THAN ISCI
C
    IF(CA(I+8).LT.ISCI) THEN
C
C ADD TO THE NUMBER OF POINTS IN THE FIRST GROUP THEN
C INTERPOLATE IN THE Y DIRECTION THE X COORDINATE DOES NOT
C CHANGE
C
        K1=K1+1
        ISOCX1(K1)=X(I)
        ISOCY1(K1)=Y(I)+(ISCI-CA(I))*(Y(I+8)-Y(I))/(CA(I+8)-CA(I))
    END IF
    END IF
C
C REPEAT THE SORTING PROCEDURE FOR THE I'TH POINT IN THE
C Y DIRECTION
C
    IF((CA(I).GE.ISC2).AND.(CA(I).LT.ISC1)) THEN
        IF(CA(I+8).GE.ISC1) THEN
            K1=K1+1
            ISOCX1(K1)=X(I)
            ISOCY1(K1)=Y(I)+(ISCI-CA(I))*(Y(I+8)-Y(I))/(CA(I+8)-CA(I))
        ELSE IF(CA(I+8).LE.ISC2) THEN
            K2=K2+1
            ISOCX2(K2)=X(I)
            ISOCY2(K2)=Y(I)+(ISCI-CA(I))*(Y(I+8)-Y(I))/(CA(I+8)-CA(I))
        END IF
    END IF
    IF((CA(I).GE.ISC3).AND.(CA(I).LT.ISC2)) THEN

```

```

      IF (CA(I-S).GE.ISC2) THEN
        K2=K2+1
        ISCX2(K2)=X(I)
        ISCY2(K2)=Y(I)+(ISC2-CA(I))*Y(I-S)-Y(I)/(CA(I-S)-CA(I))
      ELSE IF (CA(I-S).LE.ISC2) THEN
        K2=K2+1
        ISCX2(K2)=X(I)
        ISCY2(K2)=Y(I)+(ISC2-CA(I))*Y(I-S)-Y(I)/(CA(I-S)-CA(I))
      END IF
    END IF
    IF ((CA(I).GE.ISC3).AND.(CA(I).LT.ISC3)) THEN
      IF (CA(I+S).GE.ISC3) THEN
        K3=K3+1
        ISCX3(K3)=X(I)
        ISCY3(K3)=Y(I)+(ISC3-CA(I))*Y(I+S)-Y(I)/(CA(I+S)-CA(I))
      ELSE IF (CA(I+S).LE.ISC3) THEN
        K3=K3+1
        ISCX3(K3)=X(I)
        ISCY3(K3)=Y(I)+(ISC3-CA(I))*Y(I+S)-Y(I)/(CA(I+S)-CA(I))
      END IF
    END IF
    IF ((CA(I).GE.ISC4).AND.(CA(I).LT.ISC4)) THEN
      IF (CA(I+S).GE.ISC4) THEN
        K4=K4+1
        ISCX4(K4)=X(I)
        ISCY4(K4)=Y(I)+(ISC4-CA(I))*Y(I+S)-Y(I)/(CA(I+S)-CA(I))
      ELSE IF (CA(I+S).LE.ISC4) THEN
        K4=K4+1
        ISCX4(K4)=X(I)
        ISCY4(K4)=Y(I)+(ISC4-CA(I))*Y(I+S)-Y(I)/(CA(I+S)-CA(I))
      END IF
    END IF
    IF ((CA(I).GE.ISC5).AND.(CA(I).LT.ISC5)) THEN
      IF (CA(I+S).GE.ISC5) THEN
        K5=K5+1
        ISCX5(K5)=X(I)
        ISCY5(K5)=Y(I)+(ISC5-CA(I))*Y(I+S)-Y(I)/(CA(I+S)-CA(I))
      ELSE IF (CA(I+S).LE.ISC5) THEN
        K5=K5+1
        ISCX5(K5)=X(I)
        ISCY5(K5)=Y(I)+(ISC5-CA(I))*Y(I+S)-Y(I)/(CA(I+S)-CA(I))
      END IF
    END IF
    IF ((CA(I).GE.ISC6).AND.(CA(I).LT.ISC6)) THEN
      IF (CA(I+S).GE.ISC6) THEN
        K6=K6+1
        ISCX6(K6)=X(I)
        ISCY6(K6)=Y(I)+(ISC6-CA(I))*Y(I+S)-Y(I)/(CA(I+S)-CA(I))
      ELSE IF (CA(I+S).LE.ISC6) THEN
        K6=K6+1
        ISCX6(K6)=X(I)
        ISCY6(K6)=Y(I)+(ISC6-CA(I))*Y(I+S)-Y(I)/(CA(I+S)-CA(I))
      END IF
    END IF
    IF ((CA(I).GE.ISC7).AND.(CA(I).LT.ISC7)) THEN
      IF (CA(I+S).GE.ISC7) THEN
        K7=K7+1
        ISCX7(K7)=X(I)
        ISCY7(K7)=Y(I)+(ISC7-CA(I))*Y(I+S)-Y(I)/(CA(I+S)-CA(I))
      ELSE IF (CA(I+S).LE.ISC7) THEN
        K7=K7+1
        ISCX7(K7)=X(I)
        ISCY7(K7)=Y(I)+(ISC7-CA(I))*Y(I+S)-Y(I)/(CA(I+S)-CA(I))
      END IF
    END IF
  END IF

```

```

      ISOX6(K6)=X(I)
      ISOY6(K6)=Y(I)+(ISC6-CA(I))*(Y(I+S)-Y(I))/(CA(I+S)-CA(I))

      S)-CA(I))
      ELSE IF(CA(I+S).LE.ISC7) THEN
      K7=K7+1
      ISOX7(K7)=X(I)
      ISOY7(K7)=Y(I)+(ISC7-CA(I))*(Y(I+S)-Y(I))/(CA(I+S)-CA(I))

      S)-CA(I))
      END IF
      END IF
      IF((CA(I).GE.ISC8).AND.(CA(I).LT.ISC7)) THEN
      IF(CA(I+S).GE.ISC7) THEN
      K7=K7+1
      ISOX7(K7)=X(I)
      ISOY7(K7)=Y(I)+(ISC7-CA(I))*(Y(I+S)-Y(I))/(CA(I+S)-CA(I))

      S)-CA(I))
      ELSE IF(CA(I+S).LE.ISC8) THEN
      K8=K8+1
      ISOX8(K8)=X(I)
      ISOY8(K8)=Y(I)+(ISC8-CA(I))*(Y(I+S)-Y(I))/(CA(I+S)-CA(I))

      S)-CA(I))
      END IF
      END IF
      IF((CA(I).GE.ISC9).AND.(CA(I).LT.ISC8)) THEN
      IF(CA(I+S).GE.ISC8) THEN
      K8=K8+1
      ISOX8(K8)=X(I)
      ISOY8(K8)=Y(I)+(ISC8-CA(I))*(Y(I+S)-Y(I))/(CA(I+S)-CA(I))

      S)-CA(I))
      ELSE IF(CA(I+S).LE.ISC9) THEN
      K9=K9+1
      ISOX9(K9)=X(I)
      ISOY9(K9)=Y(I)+(ISC9-CA(I))*(Y(I+S)-Y(I))/(CA(I+S)-CA(I))

      S)-CA(I))
      END IF
      END IF
      IF((CA(I).GE.ISC10).AND.(CA(I).LT.ISC9)) THEN
      IF(CA(I+S).GE.ISC9) THEN
      K9=K9+1
      ISOX9(K9)=X(I)
      ISOY9(K9)=Y(I)+(ISC9-CA(I))*(Y(I+S)-Y(I))/(CA(I+S)-CA(I))

      S)-CA(I))
      ELSE IF(CA(I+S).LE.ISC10) THEN
      K10=K10+1
      ISOX10(K10)=X(I)
      ISOY10(K10)=Y(I)+(ISC10-CA(I))*(Y(I+S)-Y(I))/(CA(I+S)-CA(I))

      S)-CA(I))
      END IF
      END IF
      IF(CA(I).LT.ISC10) THEN
      IF(CA(I+S).GE.ISC10) THEN
      K10=K10+1
      ISOX10(K10)=X(I)
      ISOY10(K10)=Y(I)+(ISC10-CA(I))*(Y(I+S)-Y(I))/(CA(I+S)-CA(I))

```

```

1-3)-CONT)
      END IF
      END IF
      END IF
10  CONTINUE
C
C DONE ALL SORTING AND INTERPOLATING
C
C START WRITING THE DATA IN THE ORDER OF EACH GROUPING INTO
C A NEW FILE READY FOR PLOTING
C
C
      TWO=2
      ZERO=1.0
      WRITE(80, '(A11)') FILE2
C
C CHECK TO SEE IF ANY POINTS ARE IN THE GROUPING
C
C
      IF(K1.EQ.0) THEN
C
C SINCE NO POINTS ARE IN THIS GROUP WRITE THE POINT AT
C (1.0,1.0) TO THE FILE WHICH WILL PLACE A POINT OUT OF
C RANGE OF THE ACTUAL PLOT BUT WILL NOT IGNORE THE LEGEND
C
      K1=1
      WRITE(20,98) K1
      WRITE(20,98) TWO
      WRITE(20,99) ZERO,ZERO
      ELSE
C
C WRITE THE NUMBER OF POINTS, FILE TYPE AND GROUP
C COORDINATES INTO THE FILE
C
      WRITE(20,98) K1
      WRITE(20,98) TWO
      DO 21 I=1,K1
         WRITE(20,99) ISOX1(I),ISOY1(I)
21  CONTINUE
      END IF
C
C REPEAT THE WRITING PROCEDURE FOR EACH GROUP
C
      IF(K2.EQ.0) THEN
      K2=1
      WRITE(20,98) K2
      WRITE(20,98) TWO
      WRITE(20,99) ZERO,ZERO
      ELSE
      WRITE(20,98) K2
      WRITE(20,98) TWO
      DO 22 I=1,K2
         WRITE(20,99) ISOX2(I),ISOY2(I)
22  CONTINUE
      END IF
      IF(K3.EQ.0) THEN

```

```
K3=1
  WRITE(20,98) K3
  WRITE(20,98) TWO
  WRITE(20,99) ZERO,ZERO
ELSE
  WRITE(20,98) K3
  WRITE(20,98) TWO
  DO 23 I=1,K3
    WRITE(20,99) ISOX3(I),ISOY3(I)
  CONTINUE
END IF
IF(K4.EQ.0) THEN
  K4=1
  WRITE(20,98) K4
  WRITE(20,98) TWO
  WRITE(20,99) ZERO,ZERO
ELSE
  WRITE(20,98) K4
  WRITE(20,98) TWO
  DO 24 I=1,K4
    WRITE(20,99) ISOX4(I),ISOY4(I)
  CONTINUE
END IF
IF(K5.EQ.0) THEN
  K5=1
  WRITE(20,98) K5
  WRITE(20,98) TWO
  WRITE(20,99) ZERO,ZERO
ELSE
  WRITE(20,98) K5
  WRITE(20,98) TWO
  DO 25 I=1,K5
    WRITE(20,99) ISOX5(I),ISOY5(I)
  CONTINUE
END IF
IF(K6.EQ.0) THEN
  K6=1
  WRITE(20,98) K6
  WRITE(20,98) TWO
  WRITE(20,99) ZERO,ZERO
ELSE
  WRITE(20,98) K6
  WRITE(20,98) TWO
  DO 26 I=1,K6
    WRITE(20,99) ISOX6(I),ISOY6(I)
  CONTINUE
END IF
IF(K7.EQ.0) THEN
  K7=1
  WRITE(20,98) K7
  WRITE(20,98) TWO
  WRITE(20,99) ZERO,ZERO
ELSE
  WRITE(20,98) K7
```

```
      WRITE(20,98) TWO
      DO 27 I=1,K7
         WRITE(20,99) ISCX7(I), ISCY7(I)
      CONTINUE
   END IF
   IF(K8.EQ.0) THEN
      K8=1
      WRITE(20,98) K8
      WRITE(20,98) TWO
      WRITE(20,99) ZERO,ZERO
   ELSE
      WRITE(20,98) K8
      WRITE(20,98) TWO
      DO 28 I=1,K8
         WRITE(20,99) ISCX8(I), ISCY8(I)
      CONTINUE
   END IF
   IF(K9.EQ.0) THEN
      K9=1
      WRITE(20,98) K9
      WRITE(20,98) TWO
      WRITE(20,99) ZERO,ZERO
   ELSE
      WRITE(20,98) K9
      WRITE(20,98) TWO
      DO 29 I=1,K9
         WRITE(20,99) ISCX9(I), ISCY9(I)
      CONTINUE
   END IF
   IF(K10.EQ.0) THEN
      K10=1
      WRITE(20,98) K10
      WRITE(20,98) TWO
      WRITE(20,99) ZERO,ZERO
   ELSE
      WRITE(20,98) K10
      WRITE(20,98) TWO
      DO 30 I=1,K10
         WRITE(20,99) ISCX10(I), ISCY10(I)
      CONTINUE
   END IF
   CLOSE(10)
   CLOSE(20)
 93  FORMAT(5(4X,13))
 93  FORMAT(5(4X,E13.6))
 END
```

END
DATE
FILED

4-88

DTIC